Aus dem Pathologischen Institut der Ludwig-Maximilians-Universität München

Direktor: Prof. Dr. med. Thomas Kirchner

In der Arbeitsgruppe Experimentelle und Molekulare Pathologie

Leiter: Prof. Dr. rer. nat. Heiko Hermeking

Characterization of ZNF281 and its Role in Colorectal Carcinogenesis

---

Dissertation zum Erwerb des Doktorgrades der Naturwissenschaften (Dr. rer. nat.) an der Medizinischen Fakultät der Ludwig-Maximilians-Universität München

vorgelegt von

Stefanie Hahn

aus Weimar

2014

Gedruckt mit der Genehmigung der Medizinischen Fakultät

der Ludwig-Maximilians-Universität München

Erstgutachter: Prof. Dr. rer. nat. Heiko Hermeking

Zweitgutachter: Prof. Dr. rer. nat. Peter Nelson

Dekan: Prof. Dr. med. Dr. h. c. Maximilian Reiser, FACR, FRCR

Tag der mündlichen Prüfung: 06.11.2014

Meiner Familie.

EIDESSTATTLICHE VERSICHERUNG

Stefanie Hahn

Ich erkläre hiermit an Eides statt, dass ich die vorliegende Dissertation mit dem Thema

„Characterization of ZNF281 and its Role in Colorectal Carcinogenesis"

selbständig verfasst, mich außer der angegebenen keiner weiteren Hilfsmittel bedient und alle Erkenntnisse, die aus dem Schrifttum ganz oder annähernd übernommen sind, als solche kenntlich gemacht und nach ihrer Herkunft unter Bezeichnung der Fundstelle einzeln nachgewiesen habe.
Ich erkläre des Weiteren, dass die hier vorgelegte Dissertation nicht in gleicher oder in ähnlicher Form bei einer anderen Stelle zur Erlangung eines akademischen Grades eingereicht wurde.

Ort, Datum:_____ Unterschrift:_____

PUBLICATIONS

Parts of this thesis have been published in:

Original article:

- **Hahn S**, Jackstadt R, Siemens H, Huenten S, Hermeking H (2013) SNAIL and miR-34a feed-forward regulation of ZNF281/ZBP99 promotes epithelial-mesenchymal transition. *EMBO J* **32:** 3079-3095

  Impact factor 2012 (ISI, Thomson Reuters): 9.8

Review article:

- **Hahn S** and Hermeking H (2014) ZNF281/ZBP-99: a new player in epithelial-mesenchymal-transition, stemness and cancer. *Journal of Molecular Medicine*, *revised version submitted*

  Impact factor 2012 (ISI, Thomson Reuters): 4.8

ABBREVIATIONS

Ago	argonaute protein
APC	adenomatous polyposis coli
APS	ammonium peroxodisulfate
ATM	ataxia telangiectasia mutated
ATR	ATM and Rad3-related kinases
bHLH-(LZ)	basic helix-loop-helix (leucine zipper)
bp	base pair(s)
CCSC	colorectal cancer stem cell
CD133	prominin 1
CDK	cyclin-dependent kinase
cDNA	complementary DNA
(q)ChIP	(quantitative) chromatin immunoprecipitation
c-MYC	v-MYC avian myelocytomatosis viral oncogene homologue
CpG	cytidine-phosphate-guanidin
CRC	colorectal cancer
CSC	cancer stem cell
Cy3	cyanine 3
DAPI	2-(4-Amidinophenyl)-6-indolecarbamidine dihydrochloride
DMEM	Dulbecco`s modified Eagles medium
DMSO	dimethyl-sulfoxide
DNA	deoxyribonucleic acid
DNMT	DNA-methyltransferase
DOX	doxycycline
E.coli	*Escherichia coli*
E-box	enhancer box
EGF	epidermal growth factor
eGFP	enhanced green fluorescent protein
EMT	epithelial-mesenchymal transition
EMT-TF	epithelial-mesenchymal transition transcription factor
ESC	embryonic stem cell
FACS	fluorescence-activated cell sorting
FCS	fetal calf serum
FGF	fibroblast growth factor
FOXO3	forkhead box O3
GAPDH	glyceraldehyde 3-phosphate dehydrogenase
gDNA	genomic DNA
GSK3β	glycogen synthase kinase-3β
GZP1	GC-box-binding zinc-finger protein (ZNF281)
HBSS	Hank’s balanced salt solution
HDAC	histone deacetylase
HIF-1α	hypoxia-inducible factor-1α
HDF	human diploid fibroblast
HGF	hepatocyte growth factor
hMSC	human multiple stem cell
HRP	horseradish peroxidase

IF	immunofluorescence
IgG	immunoglobulin
INR	initiator region
IP	immunoprecipitation
kbp	kilo base pairs
LB	lysogeny broth
LEF1	lymphoid enhancer-binding factor 1
LGR5	leucine-rich repeat containing G protein-coupled receptor 5
LOX	lysyl oxidase
MAPK	mitogen-activated protein kinase
MAX	MYC associated factor X
MB	MYC homology box
MDCK cell	Madin-Darby canine kidney cell
MET	mesenchymal-epithelial transition
miR(NA)	microRNA
MIZ1	MYC-interacting zinc finger protein-1
mRNA	messenger RNA
mRFP	monomer red fluorescent protein
NICD	Notch-intracellular domain
ODC	ornithine decaboxylase
ORF	open reading frame
PAGE	polyacrylamide gel electrophoresis
P/C	phase constrast
PBS	phosphate buffered saline
(q)PCR	(quantitative) polymerase chain reaction
PDGF-β	platelet-derived growth factor-β
PDGFR	platelet-derived growth factor receptor
PI3K	phosphoinositide-3-kinase
PI	propidium iodide
polyHEMA	poly(2-hydroxyethyl methacrylate)
PP2A	protein phosphatase 2A
pri-miR(NA)	primary microRNA
RISC	RNA induced silencing complex
RNA	ribonucleic acid
RNAPol II	RNA polymerase II
ROS	reactive oxygen species
RT	room temperature
RTK	receptor tyrosine kinase
SD	standard deviation
SDS	sodium dodecyl sulfate
siRNA	small interfering RNA
TCF4	T-cell factor 4
temed	tetramethylethylenediamine
TF	transcription factor
TGF-β	transforming growth factor-β
TIC	tumor initiating cell
TRIS	tris(hydroxymethyl)-aminomethan
TSS	transcription start site

TWIST	twist family bHLH transcription factor 1
UTR	untranslated region
VSV	vesicular stomatitis virus (tag)
WB	Western blot
WNT	wingless-related integration site
ZEB	zinc finger E-box-binding homeobox protein
ZNF281	zinc finger protein 281

TABLE OF CONTENTS

1. INTRODUCTION

1.1 The c-MYC oncogene

The *MYC* gene family consists of several members (*c-MYC, N-MYC, L-MYC, B-MYC* and *S-MYC*) and was discovered by studying oncogenic retroviruses causing chicken tumors. MYC is named after the myelocytomatosis disease that results from infection with a retrovirus encoding a viral MYC (*v-MYC*) gene (Duesberg & Vogt, 1979; Hu et al, 1979; Sheiness & Bishop, 1979).

The human *c-MYC* (cellular MYC) gene is located on chromosome 8q24.21 and contains three exons. The c-MYC protein belongs to the family of basic helix-loop-helix leucine zipper (bHLH-LZ) transcription factors. c-MYC dimerizes with the bHLH-LZ protein MYC associated factor X (MAX) via its C-terminal region (reviewed in (Dang et al, 1999)). The heterodimer formation is necessary for the binding to enhancer box (E-Box) motifs CA(C/T)GTG via the basic region (Eilers & Eisenman, 2008). The N-terminal region contains two highly conserved c-MYC homology boxes (MBI and MBII) which mediate cellular transformation and are responsible for transactivation (reviewed in (Meyer & Penn, 2008)). The c-MYC-induced transcriptional program includes promotion of cell cycle progression, cell growth as well as the regulation of telomerase activity, cell motility, metabolism and vascularization (reviewed in (Jung & Hermeking, 2009)). The regulation of target genes occurs mainly via binding of c-MYC/MAX heterodimers to E-boxes and regulation of gene transcription by various mechanisms. Recruitment of different co-factors supports the effects on gene expression by various mechanisms, among them chromatin modification, chromatin remodeling, histone phosphorylation and promoter clearance (Cowling & Cole, 2006; Dang et al, 1999; Jung & Hermeking, 2009; Meyer & Penn, 2008). Repressive functions of c-MYC are, at least in part, mediated by a c-MYC/MAX/ MYC-interacting zinc finger protein-1 (MIZ1) (or SP1/NFY) complex binding to initiator region (INR) elements in the DNA and the replacement of co-activators or co-repressors by this multi-protein complex (Meyer & Penn, 2008).

1.1.1 c-MYC and cancer

In normal cells the c-MYC proto-oncogene is stringently regulated by multiple upstream effectors such as different signaling pathways as for example WNT (wingless-related integration site), Hedgehog, Notch, transforming growth factor-β (TGF-β) and many receptor tyrosine kinases (RTKs) (Dang, 2012). In the vast majority of tumors the MYC family members are deregulated by various mechanisms such as translocations, amplifications and transcriptional deregulation by mutations in upstream regulators (Beroukhim et al, 2010; Eilers & Eisenman, 2008; Vervoorts et al, 2006). Enhanced activity of c-MYC has been observed in a variety of tumor types including hematological malignancies such as Burkitt's lymphoma (91%) and solid tumors originating from the prostate (70%), colon (67%) and breast (45%) (Bubendorf et al, 1999; Buttyan et al, 1987; Fleming et al, 1986; Frost et al, 2004; Naidu et al, 2002). Besides deregulation of cell proliferation and growth c-MYC influences additional aspects of tumor biology such as vascularization, metastasis, genomic instability, proteolysis and alterations in the tumor microenvironment (Baudino et al, 2002; Felsher & Bishop, 1999; Gavioli et al, 2001; Pelengaris et al, 2002; Shchors et al, 2006).

In colorectal cancer (CRC) the loss of the adenomatous polyposis coli (APC) protein, which is part of the β-catenin destruction complex of the WNT pathway, is the major initiating event. Loss of *Apc* in the mouse small intestine results in constitutively active Wnt signaling, which is characterized by nuclear β-catenin and induction of c-*MYC* as a WNT target gene (He et al, 1998; Sansom et al, 2004). Furthermore, stabilization of the c-MYC protein upon *Apc* loss is mediated by ERK signaling (Lee et al, 2010). Moreover, it has been shown that phosphatase 2A (PP2A, also CIP2A), itself being over-expressed in a number of malignancies such as e.g. colon, gastric and breast cancer, can stabilize the c-MYC protein during colorectal cancer progression (summarized in (Myant & Sansom, 2011)). The induction of c-MYC leads to an increase in reactive oxygen species (ROS), which is presumably caused by enhanced mitochondrial biogenesis and metabolic functions and has been implicated in genomic instability (Dang, 2012). Normal cells with normal regulated c-MYC have appropriate compensatory mechanisms to detoxify free oxygen radicals. However, highly activated c-MYC induces a sustained ROS insult on the genome, which causes genomic instability. Additionally, c-MYC can directly induce telomerase activity and thereby promote immortalization (reviewed in (Dang, 2012)).

1.2 ZNF281/ZBP-99

The ZNF281/ZBP-99 protein has first been identified less than fifteen years ago in a yeast one-hybrid screen for proteins that bind to GC-rich sequences and was therefore first named GC-box-binding zinc-finger protein (GZP1) (Lisowsky et al, 1999). The *ZNF281* gene is phylogenetically conserved among mammals and is located on chromosome 1q32.1 (Law et al, 1999). The ZNF281 protein displays characteristics of a transcription factor since it contains four C_2H_2 zinc-finger domains (residues 263 to 368) separated by the $S^TG^REK^RPF^Y$ consensus motif typical for the Krüppel zinc finger family (see also Figure 1). Further features are poly-glycine, poly-proline and poly-histidine stretches, a basic region as well as a bipartite nuclear localization signal (Law et al, 1999; Lisowsky et al, 1999). ZNF281 shares substantial sequence homology with the ubiquitously expressed ZBP-89/ZFP148 protein (28% identity and additionally 30% similarity), which is especially pronounced in the zinc finger domains with 79% identity and 91% sequence similarity (Lisowsky et al, 1999). The ZBP-89 protein has been implicated in the regulation of cell proliferation (Bai & Merchant, 2001), apoptosis (Bai et al, 2004), differentiation (Li et al, 2006) and tumorigenesis (Law et al, 2006b). Elevated levels of ZNF281 have been detected in placenta, kidney, brain, heart, liver and lymphocytes, whereas most other tissues display detectable albeit low ZNF281 expression (Fidalgo et al, 2011; Law et al, 1999).

Recently, a direct interaction between ZNF281 and c-MYC has been detected (Koch et al, 2007). Moreover, it has been shown that ZNF281 mediates transcriptional repression and activation (Wang et al, 2008). For example, ZNF281 directly regulates the expression of *gastrin* and *HIS3* and represses *ornithine decarboxylase (ODC)* by binding to GC-rich sequences in their promoters and activates the expression of a *HIS3* reporter gene (Law et al, 1999; Lisowsky et al, 1999). Similar to ZNF281 other transcription factors, such as Sp1 and Sp3, which belong to the Sp/Krüppel-like factor (KLF) family of transcription factors, have been shown to bind to GC-rich regions (Griffin et al, 2003; Nagaoka et al, 2001). Therefore, overlapping DNA-binding specificities of those Sp/KLF family members with ZNF281 may result in competition for binding to regulatory sequences and establishes a complex network of gene regulation (Black et al, 2001; Griffin et al, 2003).

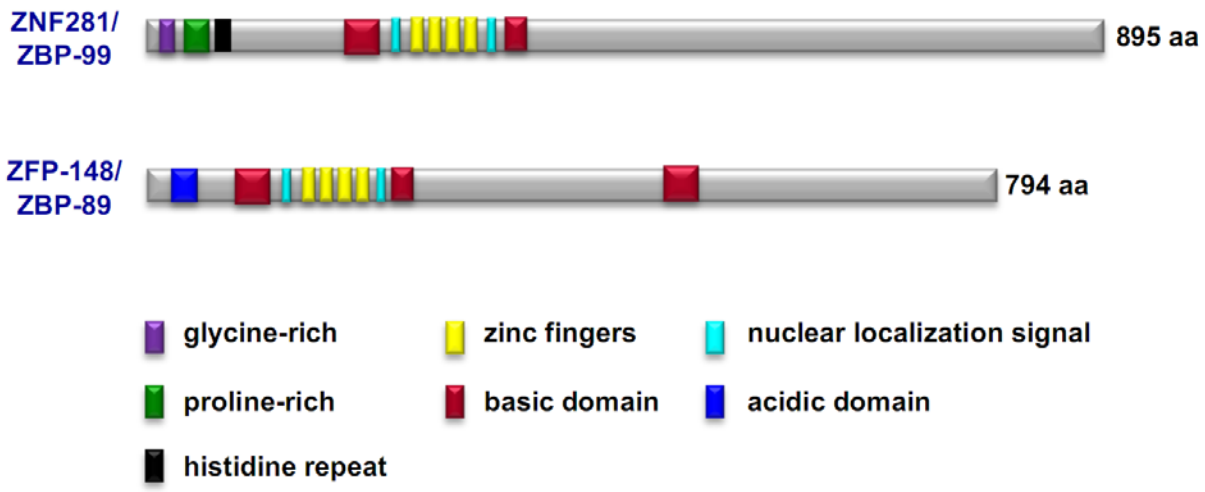

Figure 1: Structural comparison between ZNF281/ZBP-99 and ZFP-148/ZBP-89. Numbers represent amino acids (aa). Colored boxes represent the indicated domains. Modified from (Hahn & Hermeking, 2014, *revised version submitted)*

A chromatin immunoprecipitation (ChIP) analysis in mouse embryonic stem cells (ESCs) ectopically expressing ZNF281 revealed more than 2,000 direct ZNF281 targets including several known regulators of pluripotency (Wang et al, 2008). Moreover, ZNF281 seems to be required for the regulation and maintenance of pluripotency by interacting with the core transcriptional regulatory network factors controlling the stem cell state such as NANOG, OCT4 and SOX2 (Wang et al, 2006; Wang et al, 2008). Additionally, ZNF281 directly regulates NANOG expression and contributes to its auto-regulation by recruiting the NuRD complex in mouse ESCs (Fidalgo et al, 2012; Fidalgo et al, 2011). A microarray analysis revealed activated and repressed genes upon ZNF281 knock-down, indicating bifunctional roles of ZNF281 in the regulation of gene expression within different networks (Wang et al, 2008).

Several different knock-out and knock-down studies of *ZNF281* and *ZBP-89* have been performed in order to delineate the function of these genes (summarized in Table 1). The importance of ZNF281 for development was first demonstrated by Fidalgo et al., who showed that homozygous deletion of ZNF281 results in embryonic lethality between day 7.5 and 8.5 (E7.5-8.5), whereas mice with deletion of one allele showed no obvious phenotype (Fidalgo et al, 2011). The underlying cause of lethality has so far not been determined. Furthermore, loss of *ZNF281* inhibited differentiation of ESCs into embryoid bodies (Fidalgo et al, 2011). The first studies of mice deficient for the ZNF281 paralog *ZBP-89* revealed that loss of one *ZBP-89* allele blocks germ cell

gene	experimental strategy	species	type of analysis	observed phenotype	underlying mechanism	reference
ZNF281	RNA-interference	*Mus musculus*	*in vitro* (embryonic stem cell (ESC) clones from E14 cell line)	differentiation of ESCs		(Wang et al, 2008)
ZNF281	germ-line knock-out (null allele)	*Mus musculus*; C57BL/6 background	*in vivo*	homozygous: embryonic lethality (E7.5-E8.5) heterozygous: phenotypically normal	unknown	(Fidalgo et al, 2011)
			in vitro (ESCs)	differentiation inhibition of embryoid bodies, enhanced self-renewal capacity		
ZNF281	shRNA-mediated knock-down	*Homo sapiens*	*in vitro* (multipotent stem cells)	decrease in proliferation, inhibition of adipogenic differentiation, enhanced osteogenic potential, decreased β-catenin expression		(Seo et al, 2013)
ZNF281	shRNA-mediated knock-down	*Mus musculus*	*in vitro* (neural stem cells)	enhanced reprogramming of pre-iPSCs to iPSCs		(Wang et al, 2006)
ZBP-89	germ-line knock-out of exon 9 (>60% of coding region deleted)	*Mus musculus*; C57BL/6J background	*in vivo*	failure to generate homozygous KO offspring and infertility of the heterozygous KO males, smaller testes of heterozygous males	aberrant spermatogenesis, blocked germ cell differentiation, absence of gametes	(Takeuchi et al, 2003)
			in vitro (ESCs)	impaired p53 phosphorylation, loss of cell cycle arrest of heterozygous KO ESCs		
ZBP-89	germ-line knock-out of exon 4 (loss of N-terminal acidic domain and p300 interaction domain)	*Mus musculus*; 129Sv/J background	*in vivo*	postnatal lethality of homozygous KO mice, increased intestinal inflammation and colitis upon DSS treatment		(Law et al, 2006a; Law et al, 2006b)
ZBP-89	Villin-Cre-mediated conditional intestinal epithelial cell specific knock-out of exon 8 and 9 (>60% of coding region deleted)	*Mus musculus*; C57BL/6J background	*in vivo*	increased susceptibility to colitis and sepsis after infection with *Salmonella typhimurium*	in part due to reduced 5-hydroxytryptamine (5HT) production in response to butyrate and diminished secretion of antimicrobial peptides	(Essien et al, 2013)
ZBP-89	insertion of a *LacZ* reporter gene into intron 4 (behind ZBP-89 residue 111; >85% of coding region deleted)	*Mus musculus*; C57BL/6 background	*in vivo*	embryonic lethality around E9.5, growth retardation	anemia and neural tube defects	(Woo et al, 2008)
ZBP-89	insertion of a *LacZ* reporter gene into intron 4 (behind ZBP-89 residue 111; >85% of coding region deleted)	*Mus musculus*; 129P2/OlaHsd and C57BL76 mixed genetic background	*in vivo*	newborn lethality, reduced lifespan, growth retardation	respiratory distress due to prevention of lung maturation and disrupted cell proliferation	(Sayin et al, 2013)
			in vitro (mouse embryonic fibroblasts)	decreased cell proliferation	premature senescence	

Table 1: Summary of *ZNF281/ZBP-99* and *ZBP-89* inactivation studies. ESCs = embryonic stem cells, pre-iPSCs = pre-induced pluripotent stem cells, KO = knock-out, DSS = dextran sulphate sodium, 5HT = 5-hydroxytryptamine (Hahn & Hermeking, 2014, *revised version submitted*).

differentiation (Takeuchi et al, 2003) and homozygous targeting of *ZBP-89* exon 4 resulted in postnatal lethality (Law et al, 2006a). In addition, treatment with dextran sulphate sodium (DSS) led to increased intestinal inflammation and colitis in mice with deletion of *ZBP-89* exon 4 (Law et al, 2006a). Tissue-specific deletion of *ZBP-89* in intestinal epithelial cells increased the susceptibility to colitis and sepsis after infection with *Salmonella typhimurium,* which was, at least in part, due to decreased secretion of antimicrobial peptides and reduced 5-hydroxytryptamine (5-HT) production in response to butyrate (Essien et al, 2013). In another study *ZBP-89* deficiency caused embryonic lethality at around E9.5 due to anemia and neural tube defects (Woo et al, 2008). In a different study *ZBP-89* deficiency resulted in newborn lethality at a high frequency (postnatal day 1 (P1) ~50%, P21 ~70%) due to respiratory distress caused by incomplete maturation of the prenatal lung (Sayin et al, 2013).

SOX4 directly induces *ZNF281* transcription (Scharer et al, 2009). The SOX4 transcription factor is critical for vertebrate development since it coordinates differentiation and proliferation of various tissue types. SOX4 has been implicated in the regulation of epithelial-mesenchymal transition (EMT) and shows increased expression in many human cancers besides its regulatory functions during differentiation and proliferation (Tiwari et al, 2013; Zhang et al, 2012b). Moreover, after DNA damage the ZNF281 protein is phosphorylated by ataxia telangiectasia mutated (ATM) and ATM and Rad3-related (ATR) kinases (Matsuoka et al, 2007) (Figure 2). Interestingly, it has been demonstrated that the ZNF281 paralog ZBP-89 interacts with ATM and mediates recruitment of ATM to GC-rich elements in the $p21^{waf1}$ promoter (Bai et al, 2006). ZBP-89 is phosphorylated at serine 202 within its zinc finger domain (Bai & Merchant, 2007), which is highly conserved between ZNF281 and ZBP-89 (Law et al, 1999). Therefore, ZNF281 is presumably also phosphorylated by the ATM kinase within its zinc finger domain.

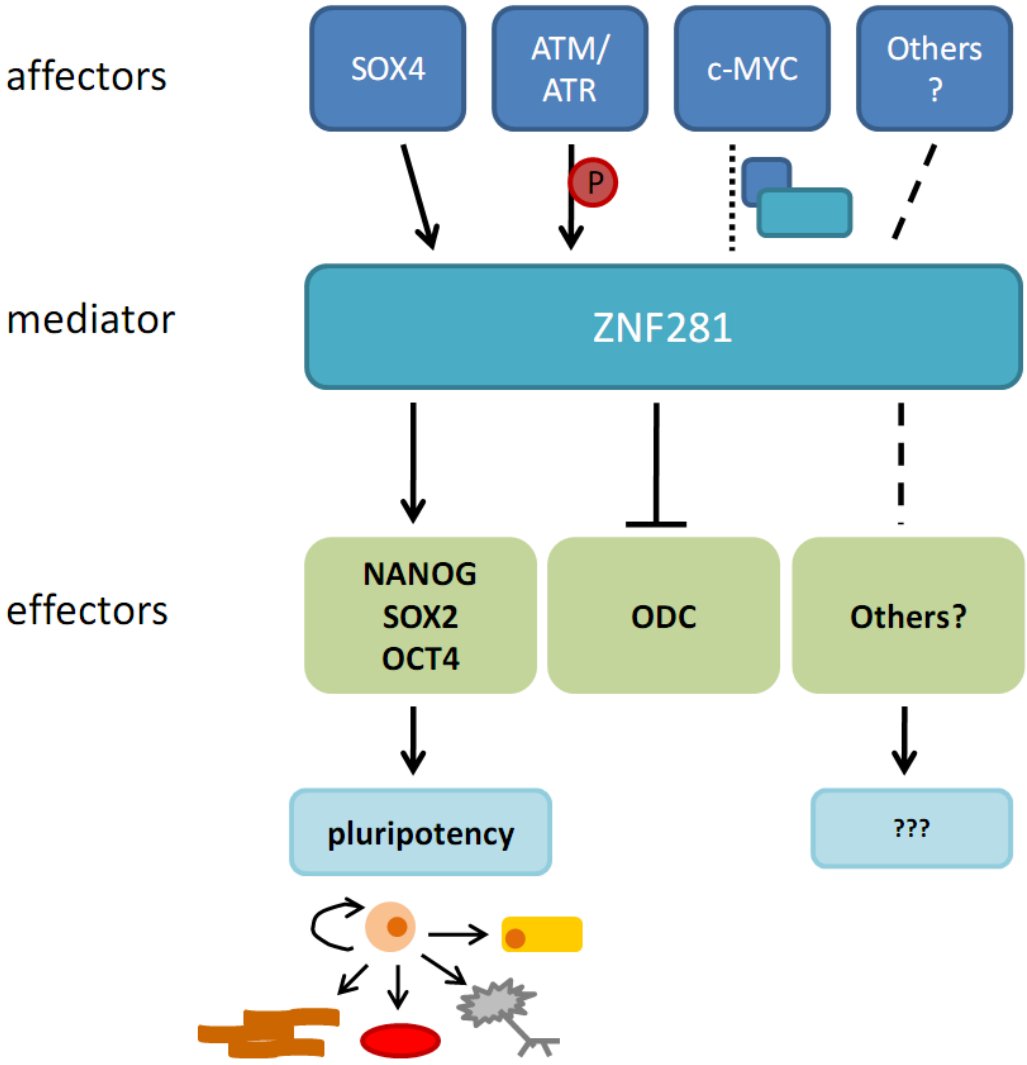

Figure 2: Cellular functions of ZNF281. The known affectors influencing ZNF281 expression or effecting ZNF281 via protein binding (dotted line) or phosphorylation are indicated in dark blue, whereas ZNF281 regulated target genes and the effected pathways are indicated by green and light blue rectangles. Dashed lines indicate connections (protein interactions, gene regulations) for which the functional consequences still have to be determined. Modified from (Hahn & Hermeking, 2014, *revised version submitted*).

1.3 Epithelial-mesenchymal transition (EMT)

The EMT is an important mechanism, which is involved in several developmental processes (see below) and represents a morphological switch in the cellular phenotype. During EMT epithelial cells lose their differentiated characteristics including cell-cell-adhesions as well as polarity and therefore their compactly layered organization and gain mesenchymal features such as decreased cell-cell contacts and loss of polarity. Thereby, EMT promotes increased motility and invasion. EMT not only plays important roles during embryonic development, but also contributes to carcinogenesis by promoting metastasis (Hugo et al, 2007; Lee et al, 2006; Polyak & Weinberg, 2009; Thiery, 2002; Thiery & Sleeman, 2006).

EMT is a morphogenic program that is involved in the formation of tissue and organs during embryonic development and wound healing. EMT has been observed in various tissue modeling events such as gastrulation (mesoderm formation), development of the prevalvular mesenchyme in the heart, formation of neural crest cells and secondary palates, the regression of the Müllerian duct as well as the process of somatogenesis (Yang & Weinberg, 2008). The key EMT programs occurring during early embryonic development are represented by the mesoderm formation and the development of the neural crest. During heart valve development and the formation of the secondary palate well-differentiated epithelial cells become mesenchymal cells (Yang & Weinberg, 2008). The latter raises the possibility that also in adult tissue EMT may appear under specific physiological or pathological conditions. Interestingly, the reverse program of mesenchymal-epithelial transition (MET) occurs during embryonic development as well as during carcinogenesis (Boyer & Thiery, 1993; Yang & Weinberg, 2008).

1.3.1 EMT and cancer

1.3.1.1 Molecular regulation of EMT

Several studies revealed that EMT can be regulated by numerous distinct signaling pathways in various organisms and different tissue culture systems. EMT is mainly regulated by extra-cellular signals such as for example by growth factors, tumor-stroma cell interactions as well as hypoxia. Furthermore, intra-cellular regulators as for example

transcription factors and non-coding RNAs control EMT (Figure 3) (Kalluri & Weinberg, 2009; Polyak & Weinberg, 2009; Yang & Weinberg, 2008).

The multiple extra-cellular mechanisms, which can initiate an EMT, are linked to a complex crosstalk between down-stream signaling pathways and transcription factors, which often includes feed-back regulations (Peinado et al, 2007; Thiery & Sleeman, 2006). Usually, the induction of EMT is accompanied by a core gene-expression signature (Peinado et al, 2007; Taube et al, 2010). So far only a few transcription factors such as SNAIL, SLUG, TWIST1/2 and ZEB1/2 are thought to constitute the central regulatory core of EMT (Peinado et al, 2007; Sanchez-Tillo et al, 2012). There exists an extensive crosstalk between EMT regulating pathways and EMT-inducers, which triggers this program commonly by down-regulating e.g. the scaffold protein and epithelial marker E-cadherin and further regulation of specific epithelial and mesenchymal genes (Thiery, 2002; Zeisberg & Neilson, 2009). The zinc-finger transcription factor SNAIL is one of the best studied inducers of EMT (de Herreros et al, 2010). SNAIL directly binds to E-Box motifs (CACCTG) in the promoter region to repress *CDH1*/E-cadherin (Batlle et al, 2000; Cano et al, 2000; de Herreros et al, 2010). SNAIL expression correlates with the hypermethylation of the *CDH-1*/E-cadherin promoter (Takeno et al, 2004). SNAIL mainly acts as transcriptional repressor, however recent data also show direct induction of target genes by SNAIL (De Craene et al, 2005; Guaita et al, 2002; Rembold et al, 2014; Vetter et al, 2010). Moreover, SNAIL is expressed in invasive carcinoma cells (Batlle et al, 2000; Cano et al, 2000) and SNAIL expression has been associated with repression of E-cadherin, poor prognosis, tumor recurrence and metastasis in breast carcinomas (Peinado et al, 2007). SNAIL can be induced by TGF-β (Peinado et al, 2003) and forms a complex with SMAD proteins to bind in concert to the *CDH1*-promoter (Vincent et al, 2009). The ZEB (zinc finger E-box-binding homeobox protein) family of transcription factors, consisting of ZEB1 and ZEB2, are also inducers of EMT and repressors of *CDH-1* (Vandewalle et al, 2005). ZEB expression further resulted in the repression of other components of tight and adherens junctions as well as desmosomes (Vandewalle et al, 2005). Inhibition of ZEB by the microRNA-200 family (miR-200) restores the expression of E-cadherin (Gregory et al, 2008; Park et al, 2008). ZEB expression is elevated in a variety of cancer types including ovarian, gastric, pancreatic and colorectal tumors (Peinado et al, 2007).

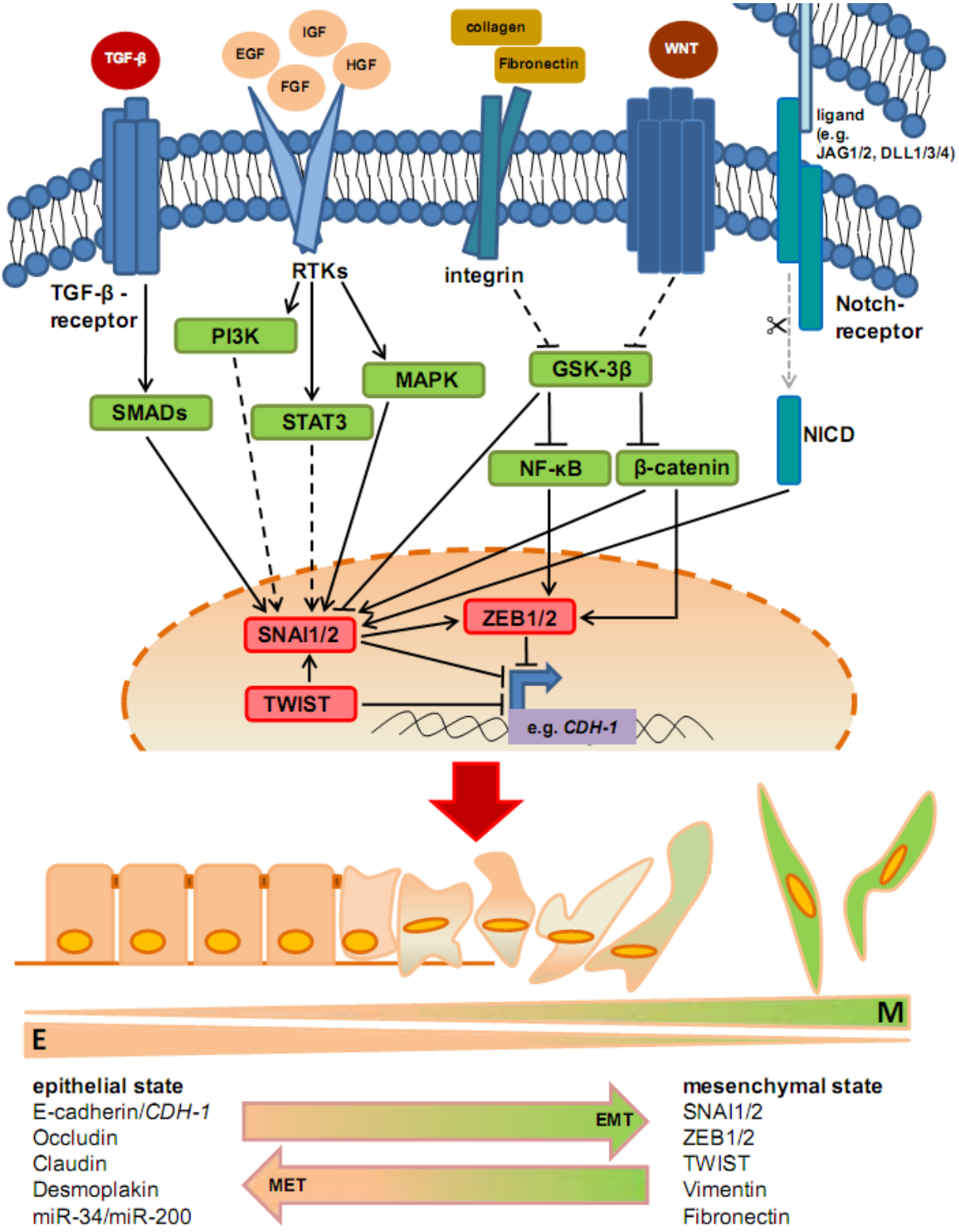

Figure 3: Schematic summary of molecular mechanisms regulating EMT. During EMT (epithelial-mesenchymal transition) epithelial cells (pale orange, E) are converted into mesenchymal-like cells (green, M). The reverse transition from mesenchymal to epithelial cells is known as MET (mesenchymal-epithelial transition) (Hahn & Hermeking, 2014, *revised version submitted*).

Members of the TGF-β family constitute some of the best characterized activators of EMT (Massague, 2008; Yang & Weinberg, 2008). In normal epithelial cells TGF-β can act growth-inhibitory, whereas in transformed cells it can promote carcinogenesis by induction of EMT (Shi & Massague, 2003; Siegel & Massague, 2003). Besides the direct TGF-β-mediated activation of the core EMT transcription factors TGF-β can induce EMT through multiple mechanisms since it influences cell polarity and tight junction formation by phosphorylating SMAD proteins and PAR6A, which leads to the loss of apical-basal polarity via dissolving tight junctions (Ozdamar et al, 2005; Polyak & Weinberg, 2009). Additionally, TGF-β signaling has been linked to the regulation of stem cell phenotypes in breast cancer and the maintenance of human embryonic stem cell pluripotency (James et al, 2005; Mani et al, 2008; Morel et al, 2008).

Another EMT-inducing signaling pathway, which is also linked to stemness, is the WNT-signaling pathway. Normally, β-catenin gets degraded upon phosphorylation by glycogen synthase kinase-3β (GSK3β). Inhibition of GSK3β or APC inactivation leads to nuclear localization and transcriptional activity of the β-catenin protein. Colorectal cancer cells undergoing EMT show an accumulation of β-catenin in the nucleus, which is reversed in metastases (reviewed in (Brabletz et al, 2005a)). Moreover, the loss of the scaffold protein E-cadherin, which is associated with the EMT process and therefore the abolishment of E-cadherin-mediated sequestration of β-catenin at the cellular membrane, allows the translocation of β-catenin to the nucleus. In the nucleus β-catenin mediates WNT-target gene activation through association with lymphoid-enhancer binding factor 1/ T-cell factor 4 (LEF-1/TCF4) (Orsulic et al, 1999; Sadot et al, 1998).

Furthermore, Notch-signaling also plays a pivotal role for EMT during embryogenesis as well as tumorigenesis (Timmerman et al, 2004). Activation of the Notch-pathway upon Jagged-1 stimulation (Noseda et al, 2004) as well as in platelet-derived growth factor-β (PDGF-β)-driven processes results in morphological and functional changes consistent with EMT. Several mechanisms lead to Notch-mediated induction of SNAIL. Notch-intracellular domain (NICD) recruitment to the *SNAIL* promoter results in direct up-regulation of SNAIL (Sahlgren et al, 2008). Additionally, Notch promoted hypoxia-inducible factor-1α (HIF-1α) gets recruited to the *lysyl oxidase* (*LOX*) promoter, leading to increased expression of LOX and to further posttranslational stabilization of SNAIL by LOX (Sahlgren et al, 2008). Moreover, recent studies revealed an extensive cross-talk

between Notch signaling and the TGF-β-pathway, which underscores the complexity of EMT-driving signaling pathways (Niimi et al, 2007; Zavadil et al, 2004).

Receptor tyrosine kinases activation may also induce EMT during embryonic and pathological processes (Baum et al, 2008; Hugo et al, 2007; Thiery & Sleeman, 2006; Yang & Weinberg, 2008). For example, exposure to hepatocyte growth factor (HGF)/scatter factor activates c-Met-signaling and is sufficient to induce the EMT-like morphological changes of epithelial Madin-Darby canine kidney (MDCK) cells via activation of several down-stream pathways including Ras, MAP kinase, PI3 kinase and Rac/CDC42 (Birchmeier et al, 1997). The scattering of the cells can also occur after exposure to FGF1, EGF or HGF (Boyer et al, 1997). The discovery of the induction of a PDGF/PDGF-receptor autocrine loop during TGF-β-mediated EMT further linked RTK-signaling to the regulation of EMT (Grunert et al, 2003; Jechlinger et al, 2003).

Hypoxia induces EMT by activation of HIF-1α, HGF, SNAIL and TWIST1 as well as by promoting Notch- and NFκB-signaling (Gort et al, 2008). Furthermore, it has been shown that low O_2 levels lead to an induction of EMT by GSK-3β inhibition. The resulting accumulation of free β-catenin and subsequent activation of the WNT-signaling, followed by SNAIL-induction and further repression of E-cadherin leads to a positive feed-back loop involving EMT-regulating transcription factors and the WNT-pathway (Cannito et al, 2008; Jiang et al, 2011).

1.3.1.2 EMT in cancer progression and the invasion-metastasis cascade

EMT has been tightly associated with the acquisition of metastatic and stem cell traits in tumor cells. Around 90% of all cancer-related deaths are caused by the metastatic spread of cancer cells to distant sites instead of by the growth of the primary tumor (Nguyen et al, 2009; Valastyan & Weinberg, 2011). During metastasis formation cells spread from the primary tumor to distant organs, where they have devastating effects (Fidler, 2003; Sleeman & Steeg, 2010). The series of distinct steps leading to the formation of metastases is often referred to as the “invasion-metastasis-cascade” (Valastyan & Weinberg, 2011). During primary tumor growth cancer cells accumulate genetic and epigenetic changes, which enable a specific subset of the cells to escape from the tumor mass and invade into surrounding tissue (Scheel & Weinberg, 2012; Zheng & Kang, 2013). Alterations in gene expression in the tumor microenvironment

may also contribute to this process (Beauchemin, 2011; Joyce & Pollard, 2009). An initial step in metastasis is the dissemination of some tumor cells from the solid tumor mass. This can occur as collective migration by a small group of cells or by the mechanism of mesenchymal or amoeboid migration by single cells (Friedl & Alexander, 2011). During mesenchymal migration intercellular junctions are dissolved, polarity is lost and migration and invasion of single cells into the tumor surrounding stroma occurs. This is often achieved by the activation of the cellular program of EMT (Thiery et al, 2009; Thompson & Williams, 2008). In patient samples it could be shown that cells in the invasive front of various tumor types display characteristics of EMT (Brabletz et al, 2001; Franci et al, 2006; Thiery, 2002). Furthermore, the invasive abilities enable the disseminated cancer cells to enter the systemic circulation (intravasation) and thereby spread to secondary organs. In order to allow the metastatic growth of tumor cells in distant organs after exiting from the vasculature into surrounding tissues (extravasation) this EMT-process is reversed (Scheel & Weinberg, 2012; Zheng & Kang, 2013): cells undergo a mesenchymal-epithelial transition (MET), revert to the epithelial state and proliferate, which is necessary for the outgrowth of the micro- to a macrometastasis at the distant site (see Figure 4) (Thiery, 2002; Thiery et al, 2009).

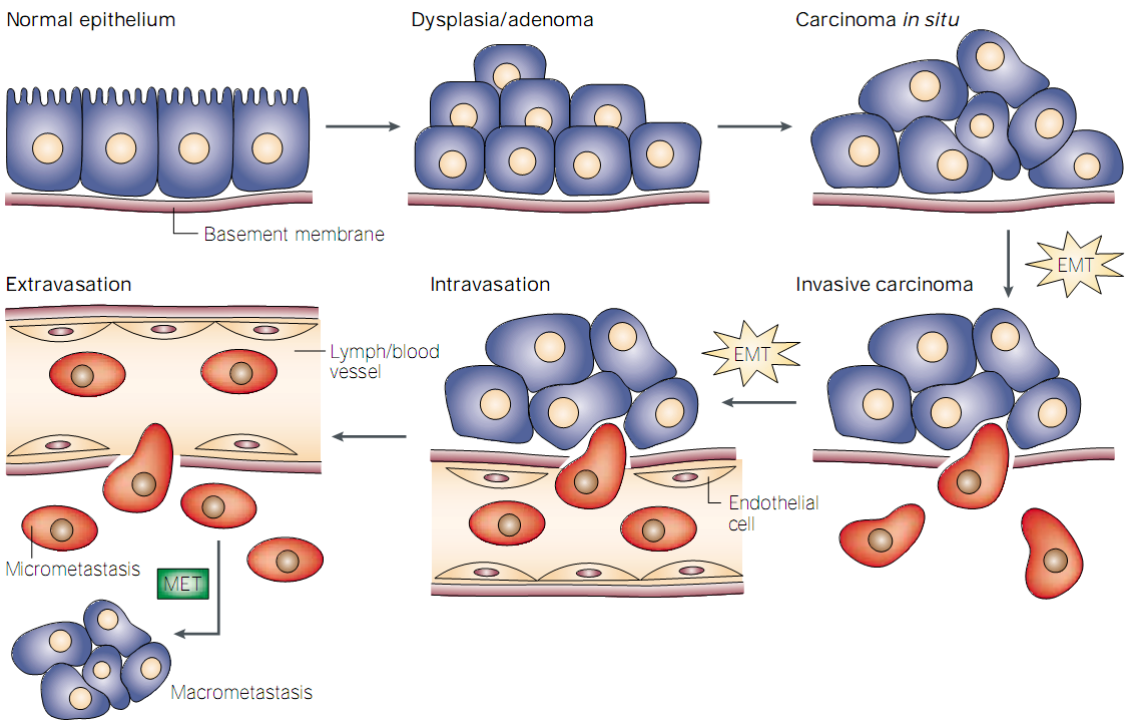

Figure 4: EMT and MET in the progression of carcinoma and metastases. Normal epithelial cells lined by the basement membrane can proliferate locally, thereby giving rise to an adenoma. Further epigenetic changes as well as genetic alterations lead to transformation of the cells, resulting in a carcinoma *in situ*. Additional alterations can yield to the local dissemination of some carcinoma cells by an epithelial-mesenchymal transition (EMT) and the concomitant fragmentation of the basement membrane. The cells then intravasate into lymph or blood vessels. At distant sites, solitary carcinoma cells extravasate and either remain solitary (micrometastasis) or grow out to a macrometastasis through an mesenchymal-epithelial transition (MET) (Thiery, 2002).

EMT occurs also at later steps of the metastasizing process, besides invasion into stroma as crucial initial step in the metastasis formation cascade. EMT also contributes to tumor stemness, evasion of the immune system, escape from senescence, chemoresistance as well as tumor relapse (Zheng & Kang, 2013). Cancer cells undergoing EMT have been shown to acquire properties of cancer stem cells (CSCs) or tumor-initiating cells (TICs), which are necessary for metastasis formation (Brabletz et al, 2005b; Mani et al, 2008). Interestingly, the ability to induce both stemness and EMT is shared by the EMT-transcription factors (EMT-TFs) SNAIL, TWIST and ZEB1 (Mani et al, 2008; Wellner et al, 2009). Therefore, EMT-TFs not only contribute to the change of epithelial towards mesenchymal cell characteristics, but also play a crucial role in seeding of cancer cells by confering them with traits of self-renewal to support the formation of metastases (Scheel & Weinberg, 2012).

1.4 microRNAs

microRNAs (miRNAs) are small non-coding, single-stranded RNA molecules consisting of ~ 22 nucleotides, which specifically repress the translation of target mRNAs. (Esquela-Kerscher & Slack, 2006). miRNAs regulate various processes such as cell growth, differentiation and apoptosis as well as tumorigenesis (Esquela-Kerscher & Slack, 2006). Transcription of miRNAs generally is driven by RNA polymerase II (RNAPol II) resulting in a precursor transcript, the so-called primary (pri-) miRNA (Bartel, 2004). This is further processed in the nucleus by Drosha, a RNase III enzyme, and Pascha (DGCR8), a protein which binds to double-stranded RNAs. The resulting cleaved precursor (pre-) miRNA is ~ 70-nucleotides in length and folds imperfectly into a stem-loop structure. The pre-miRNA is exported from the nucleus to the cytoplasm by Exportin-5, which is a RAN GTP-dependent transporter (Brownawell & Macara, 2002). In the cytoplasm another processing step occurs, by which a ~ 22 nucleotide long double-stranded RNA (miRNA:miRNA* duplex) arises due to enzymatic cleavage of the pre-miRNA hairpin by Dicer, another RNase III enzyme (Hutvagner et al, 2001). This duplex then gets incorporated into the multiprotein RNA-induced silencing complex (RISC) including the Argonaute (Ago) protein. Often, a single miRNA targets the expression of numerous mRNAs (reviewed in (Bartel, 2009)) and more than 60% of all human protein-coding genes are presumably targeted by miRNAs (Friedman et al, 2009). The targeting of selected mRNAs by RISC-incorporated miRNAs occurs via the up to seven nucleotides long seed sequence of the miRNA and the complementary site (seed-matching sequence) in the target 3´- untranslated region (3´-UTR) and results in the degradation or translational repression of the target mRNA (Figure 5) (Esquela-Kerscher & Slack, 2006; Winter et al, 2009).

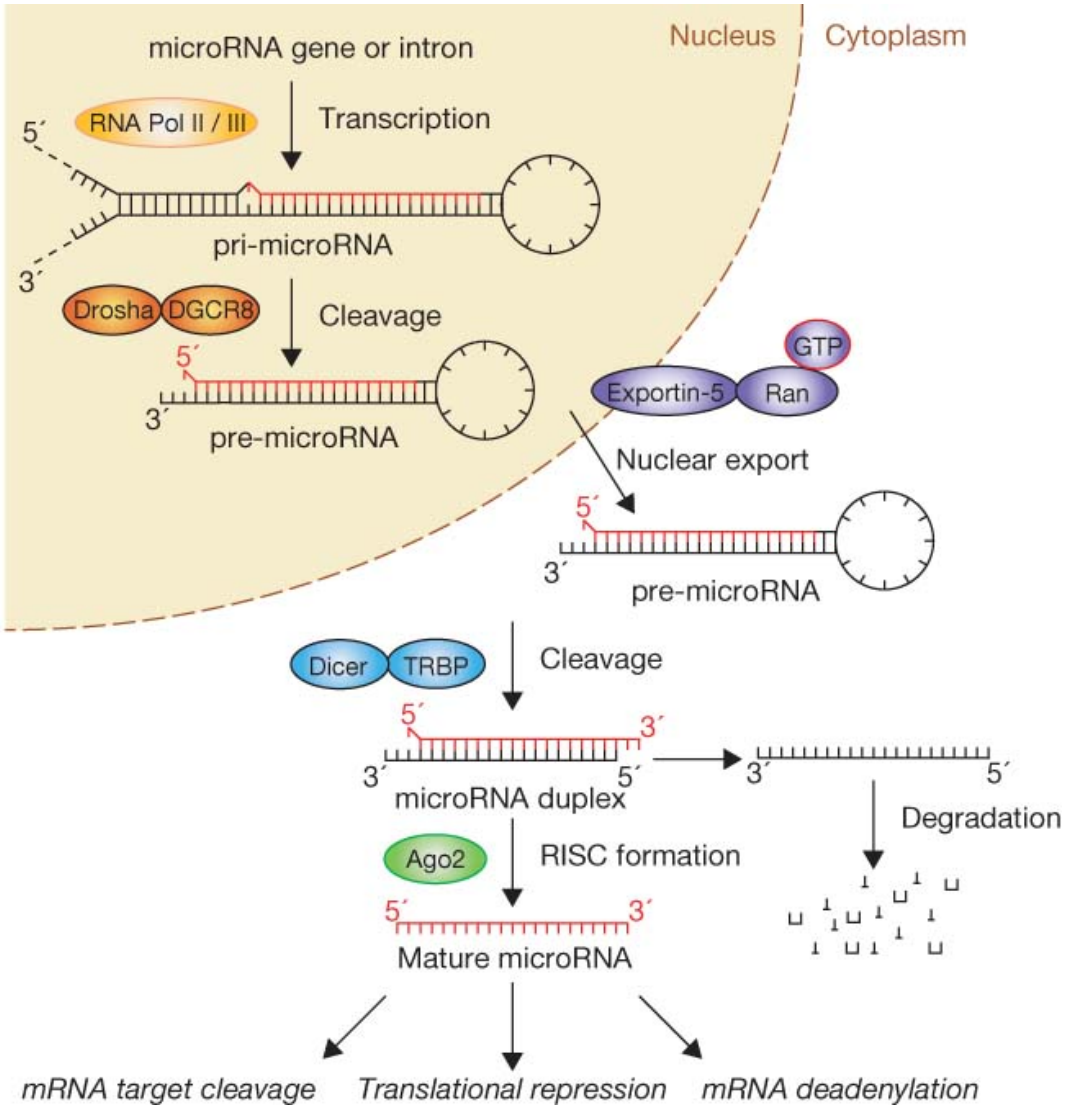

Figure 5: The biogenesis and function of microRNAs. In the nucleus microRNA (miRNA) genes are generally transcribed by RNA Polymerase II (RNA Pol II) to form pri-miRNA transcripts. These pri-miRNA transcripts are further processed by Drosha, an RNase III enzyme, and its co-factor, Pasha, in order to generate the ~70-nucleotide pre-miRNA precursor product (The mature miRNA sequence is shown in red.). The transport of the pre-miRNA into the cytoplasm occurs via RAN–GTP and Exportin-5. In the cytoplasm Dicer, another RNase III enzyme, processes the pre-miRNA to generate a transient ~22-nucleotide miRNA:miRNA* duplex. This duplex becomes integrated into the miRNA-associated multiprotein RNA-induced silencing complex (miRISC). This complex includes the Argonaute (Ago) proteins and preferentially the mature single-stranded miRNA (red). The targeting of selected mRNAs by miRNAs occurs via a stretch of seven nucleotides (the so-called seed-sequence) (Winter et al, 2009).

1.4.1 The miR-34 family: members, regulation and the role in cancer

The miR-34 family consists of the miRNAs miR-34a/b/c, which are encoded by two different genes, and the miRNAs miR-449a/b/c. The m*iR-34a* gene is located on chromosome 1p36. The transcript encoding for *miR-34b* and *miR-34c* is located on chromosome 11q23 and miR-34b/c share the same pri-miRNA (reviewed and illustrated in (Hermeking, 2010)). The miR-449 cluster is located on chromosome five in a highly conserved region within the second intron of the *CDC20B* gene (Lize et al, 2011).

The *miR-34* genes are directly induced by p53 via consensus p53-binding sites in the proximal promoter regions of the encoding genes (Bommer et al, 2007; Chang et al, 2007; He et al, 2007; Raver-Shapira et al, 2007; Tarasov et al, 2007). It has been shown that ectopic expression of miR-34 family members causes a G1 arrest, cellular senescence or apoptosis (Bommer et al, 2007; He et al, 2007; Tarasov et al, 2007). Therefore, miR-34 presumably is a mediator of tumor suppression by p53. p63, a relative of p53 lacking a transactivation domain, directly represses *miR-34a/c* to maintain cell cycle progression *(*Antonini et al, 2010; Boominathan, 2010*)*. Moreover, *miR-34b/c* is induced by activation of the WNT-signaling or by FOXO3a (Kress et al, 2011; Tamura et al, 2013). Up-regulation of miR-34a has been shown upon oncogene-induced senescence mediated by the ETS family transcription factor ELK1 (Christoffersen et al, 2010). In contrast, cytokine IL-6 activated oncogenic STAT3 transcription factor directly represses the *miR-34a* gene via a conserved STAT3 binding site (Rokavec et al, 2014). The genetic ablation of *miR-34a* allowed the invasion of colitis-associated colon cancer by activation of an IL6R/STAT3/miR-34a feedback loop (Rokavec et al, 2014). Furthermore, loss of *miR-34a/b/c* cooperates with *p53* loss in prostate cancer progression in mouse tumor models (Cheng et al, 2014). In addition, *miR-34a/b/c* deletion cooperates with deletion of one *p53* allele in a lung cancer model (Okada et al, 2014). The EMT-TFs SNAIL and ZEB1 have been shown to directly repress miR-34 by binding to E-boxes in the *miR-34* promoters (Siemens et al, 2011). Therefore, *miR-34a/b/c* genes have tumor suppressive properties, which are mediated by down-regulation of different tumor-promoting factors. Furthermore, it has been demonstrated that TGF-β signaling suppresses miR-34a expression, probably via the TGF-β-mediated induction of the EMT-TF SNAIL (Siemens et al, 2011; Yang et al, 2012).

Low miR-34a expression levels were detected in neuroblastoma showing a frequent deletion of chromosome 1p36 (Welch et al, 2007). Moreover, others observed that down-regulation of miR-34 in various tumor types is not solely based on inactivating mutations of p53, but is also caused by epigenetic changes (reviewed in (Hermeking, 2010)). The promoters of the *miR-34* genes are located within CpG islands, which are sites of hyper-methylation. Methylation occurs upon transfer of a methyl-group by DNA-methyltransferases (DNMTs) from *S*-adenosylmethionine to the C-5 position of cytosine, located 5' to a guanosine which then form a CpG dinucleotide (Iacobuzio-Donahue, 2009). This DNA methylation directly leads to the transcriptional silencing of genes via affecting the chromatin status. Thereby, the binding of promoter activating transcription factors is inhibited and recruitment of methyl-CpG-binding proteins and their associated repressive chromatin remodelling activities occurs (Robertson, 2005). Recently, it has been shown that EMT-TFs are linked to the control of the chromatin configuration resulting from different histone modifications (reviewed in (Tam & Weinberg, 2013)).

Furthermore, miRNAs have emerged as major regulators of EMT (Brabletz, 2012; Hermeking, 2012). For example, miR-34a/b/c promote MET by directly inhibiting the EMT-inducing factor SNAIL (Kim et al, 2011; Siemens et al, 2011). Members of the miR-200 family and miR-205 achieve the same effect by targeting ZEB1/2 (Gregory et al, 2008; Park et al, 2008). Moreover, SNAIL directly represses *miR-34a/b/c* transcription (Siemens et al, 2011), which results in a double-negative feedback loop. This loop represents a bistable switch, which can be locked in the mesenchymal state by inactivation of *miR-34* genes by CpG methylation, which is often found in cancer cells (Hermeking, 2012; Siemens et al, 2013). Interestingly, the genes encoding the *miR-200* and *miR-34* families are both direct p53 targets and their mediation of MET presumably contributes to tumor suppression by p53 (Figure 6) (Hermeking, 2012).

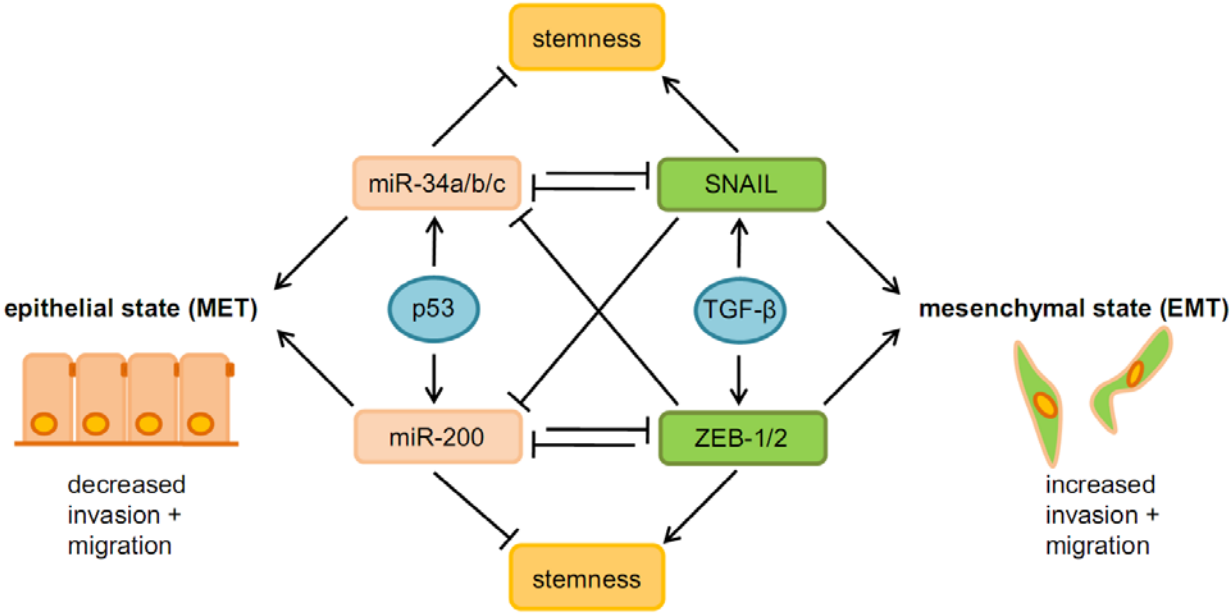

Figure 6: The functions of the p53-induced miRNAs miR-34 and miR-200 in the context of EMT and stemness. p53-induced miRNAs and TGF-β induced EMT-TFs form a double-negative feed-back loop controlling EMT and MET. Modified from (Siemens et al, 2011).

2. AIMS OF THE STUDY

The present study had the following aims:

1. Characterization of transcription factor- and microRNA-mediated regulation of ZNF281 expression.

2. Evaluation of ZNF281-mediated cellular functions in colorectal cancer cells and identification of the impact of ZNF281 knock-down

3. Determination of the role of ZNF281 for c-MYC- and SNAIL-mediated functions in colorectal cancer cells.

3. MATERIALS

3.1 Chemicals and reagents

Chemical compound	Supplier
2-(4-Amidinophenyl)-6-indolecarbamidine-dihydrochloride (DAPI)	Carl Roth GmbH, Karlsruhe, Germany
ammonium peroxodisulfate (APS)	Carl Roth GmbH, Karlsruhe, Germany
ampicillin	Sigma-Aldrich, St.Louis, MD, USA
BD Matrigel™ Basement Membrane Matrix	BD Bioscience, Heidelberg, Germany
christal violet	Carl Roth GmbH, Karlsruhe, Germany
complete mini protease inhibitor cocktail	Roche Diagnostics GmbH, Mannheim, Germany
dimethyl-sulfoxide (DMSO)	Carl Roth GmbH, Karlsruhe, Germany
dNTPs (deoxynucleotides triphosphate)	Thermo Fisher Scientific, Inc., Waltham, MA, USA
doxycycline hyclate	Sigma-Aldrich, St.Louis, MD, USA
ECL/HRP substrate	Immobilon, Merck Millipore, Billerica, MA, USA
ethidium bromide	Carl Roth GmbH, Karlsruhe, Germany
Fast SYBR® Green Master Mix	Applied Biosystems, Foster City, CA, USA
Fast SYBR Green Master Mix Universal RT	Exiqon A/S, Vedbaek, Denmark
FCS (Fetal calf serum)	Gibco®, Life Technologies GmbH, Darmstadt, Germany
FuGENE®6 Transfection Reagent	Promega, Madison, WI, USA
Hi-Di™ Formamide	Applied Biosystems, Foster City, CA, USA
HiPerFect Transfection Reagent	Qiagen GmbH, Hilden, Germany
Hygromycin B	Invitrogen GmbH, Karlsruhe, Germany
Immobilon-P Transfer Membrane	Immobilon, Merck Millipore, Billerica, MA, USA
LB-Agar (Lennox)	Carl Roth GmbH, Karlsruhe, Germany
LB-Medium (Luria/Miller)	Carl Roth GmbH, Karlsruhe, Germany
methyl cellulose	Sigma-Aldrich, St.Louis, MD, USA
Mitomycin C	Sigma-Aldrich, St.Louis, MD, USA
Nonidet®P40 substitute	Sigma-Aldrich, St.Louis, MD, USA
Opti-MEM® Reduced Serum Medium	Life Technologies GmbH, Darmstadt, Germany
paraformaldehyde	Merck KgaA, Darmstadt, Germany
polyHEMA (poly(2-hydroxyethyl methacrylate))	Sigma-Aldrich, St.Louis, MD, USA

Chemical compound	Supplier
ProLong Gold antifade	Invitrogen GmbH, Karlsruhe, Germany
propidium iodide	Sigma-Aldrich, St.Louis, MD, USA
puromycin dihydrochloride	Sigma-Aldrich, St.Louis, MD, USA
Rotiphorese gel 30 (37,5:1)	Carl Roth GmbH, Karlsruhe, Germany
sea plaque® agarose	Lonza Ltd, Basel, Switzerland
skim milk powder	Fluka, Sigma-Aldrich, St.Louis, MD, USA
sodium dodecyl sulfate (SDS)	Carl Roth GmbH, Karlsruhe, Germany
temed (tetramethylethylendiamin,1,2-bis (dimethylamino) –ethan)	Carl Roth GmbH, Karlsruhe, Germany
TritonX 100	Carl Roth GmbH, Karlsruhe, Germany
Tween20	Sigma-Aldrich, St.Louis, MD, USA
water (molecular biological grade)	Gibco®, Life Technologies GmbH, Darmstadt, Germany

3.2 Enzymes

Enzyme	Supplier
DNase I (RNase-free)	Sigma-Aldrich, St.Louis, MD, USA
FIREPol® DNA Polymerase	Solis BioDyne, Tartu, Estonia
Platinum® *Taq* DNA polymerase	Invitrogen GmbH, Karlsruhe, Germany
proteinase K	Sigma-Aldrich, St.Louis, MD, USA
restriction endonucleases	New England Biolabs GmbH, Frankfurt, Germany
RNase A	Sigma-Aldrich, St.Louis, MD, USA
T4 DNA ligase	Thermo Fisher Scientific, Inc., Waltham, MA, USA
trypsin (10x, phenol-red free)	Invitrogen GmbH, Karlsruhe, Germany

3.3 Kits

Kit	Supplier
BCA Protein Assay Kit	Pierce, Thermo Fisher Scientific, Inc., Waltham, MA, USA
BigDye® Terminator v3.1 Cycle Sequencing Kit	Life Technologies GmbH, Darmstadt, Germany
Dneasy® Blood&Tissue Kit	QIAGEN GmbH, Hilden, Germany
DyeEx® 2.0 Spin Kit	QIAGEN GmbH, Hilden, Germany
High Pure RNA Isolation Kit	Roche Diagnostics GmbH, Mannheim, Germany
miRCURY LNA™ Universal RT microRNA PCR – Universal cDNA Synthesis Kit II	Exiqon A/S, Vedbaek, Denmark
Pure Yield™ Plasmid Midiprep System	Promega GmbH, Mannheim, Germany
QIAprep Spin Miniprep Kit	QIAGEN GmbH, Hilden, Germany
QIAquick Gel Extraction Kit	QIAGEN GmbH, Hilden, Germany
QuikChange II Site-Directed Mutagenesis Kit	Stratagene, Agilent Technologies GmbH & Co.KG, Waldbronn, Germany
Verso cDNA Kit	Thermo Fisher Scientific, Inc., Waltham, MA, USA

3.4 Antibodies

3.4.1 Primary antibodies

Epitope	Clone	Ordering no.	Company	Use	Dilution	Source
α-tubulin	DM 1A	# T-9026	Sigma	WB	1:1000	mouse
β-actin		# A2066	Sigma	WB	1:1000	rabbit
β-catenin		# 610154	BD PharMingen	WB	1:1000	mouse
β-catenin		# 1247-1	Epitomics	IF	1:200	rabbit
E-cadherin	4A2C7	# 334000	Invitrogen	WB; IF	1:1000; 1:50	mouse
goat IgG		# AB-108-C	R&D Systems	ChIP		goat
rabbit IgG		# R-5506	Sigma	ChIP		rabbit
SNAIL		# 3879S	Cell Signaling	WB; IF	1:200; 1:100	rabbit
SNAIL		# AF3639	R&D Systems	ChIP		goat
Vimentin	EPA3776	# 2707-1	Epitomics	WB; IF	1:5000; 1:50	rabbit

Epitope	Clone	Ordering no.	Company	Use	Dilution	Source
VSV		# V4888	Sigma	WB; ChIP	1:7500	rabbit
ZNF281				WB; ChIP	1:1000	rabbit

WB = Western blot, IF = immunofluorescence, ChIP = chromatin immunoprecipitation

3.4.2 Secondary antibodies

Name	Source	Application	Supplier
anti-mouse HRP	goat	WB	Promega GmbH, Mannheim, Germany
anti-mouse-Alexa Fluor-555	goat	IF	Invitrogen GmbH, Karlsruhe, Germany
anti-rabbit HRP	goat	WB	Sigma-Aldrich, St.Louis, MD, USA
anti-rabbit-Cy3	donkey	IF	Jackson Immuno-Research Europe Ltd., Newmarket, Suffolk, UK
Phalloidin-Alexa-647		IF	Invitrogen GmbH, Karlsruhe, Germany

WB = Western blot, IF = immunofluorescence

3.5 Vectors and oligonucleotides

3.5.1 Vectors

Name	ORF/Rep	Reference
pRTR		(Jackstadt et al, 2013)
pRTR-p53-VSV	p53	(Siemens et al, 2011)
pRTR-*pri-miR-34a*	miR-34a	(Kaller et al, 2011)
pRTR-SNAIL-VSV	SNAIL	(Siemens et al, 2011)
pRTR-ZNF281-VSV	ZNF281	this work
pRTR-c-MYC-VSV	c-MYC	(Jackstadt et al, 2013)
pUC19SfiI		kind gift from Andreja Vasiljev
pBV		(He et al, 1999)
pBV-*ZNF281* wt	2 kb human *ZNF281* wild-type promoter	this work
pBV-*ZNF281 SBS2* mut	human *ZNF281* promoter mutated *SBS2*	this work

Name	ORF/Rep	Reference
pBV-*ZNF281 SBS3 mut*	human *ZNF281* promoter mutated *SBS3*	this work
pBV-*ZNF281 SBS2+3 mut*	human *ZNF281* promoter mutated *SBS2+3*	this work
pXP2-*E-cadherin/CDH1*	E-cadherin	(Yang et al, 2010)
pXP2-*E-cadherin/CDH1*	E-cadherin SBSs mutated	(Yang et al, 2010)
pGL3-control-MCS		(Kaller et al, 2011; Welch et al, 2007)
pGL3-*ZNF281wt_77bp*	human ZNF281 wild-type 3´UTR	this work
pGL3-*ZNF281wt_fl*	human ZNF281 wild-type 3´UTR	this work
pGL3-*ZNF281mut_77bp*	human ZNF281 mutated 3´UTR	this work
pGL3-TPD52	human TPD52 3´UTR	(Kaller et al, 2011)
pGL3-*SNAIL* promoter -1158/+92	human *SNAIL* promoter	(Barbera et al, 2004)
pGL3-*SNAIL* promoter -869/+59	human *SNAIL* promoter	(Barbera et al, 2004)
pGL3-*SNAIL* promoter -514/+59	human *SNAIL* promoter	(Barbera et al, 2004)
pGL3-*SNAIL* promoter -194/+59	human *SNAIL* promoter	(Barbera et al, 2004)
pGL3-*SNAIL* promoter -78/+59	human *SNAIL* promoter	(Barbera et al, 2004)
RL	Renilla	(Pillai et al, 2005)
pcDNA3-SNAIL-VSV	SNAIL	kind gift from Markus Kaller
pcDNA3-ZNF281-VSV	ZNF281	kind gift from Ru Zhang
pRTS		(Bornkamm et al, 2005)
pRTS-non-spec.-miRNA	non specific microRNA	kind gift from Ru Zhang
pRTS-*ZNF281*-spec.-miRNA #1	*ZNF281*-specific microRNA #1	kind gift from Ru Zhang
pRTS-*ZNF281*-spec.-miRNA #2	*ZNF281*-specific microRNA #2	kind gift from Ru Zhang
pRTS-ZNF281-VSV	ZNF281	kind gift from Ru Zhang
pRTS-*pri-miR-34a*	miR-34a	(Tarasov et al, 2007)
pBabe		(Morgenstern & Land, 1990)
pBabe-SNAIL-VSV	SNAIL	(Siemens et al, 2011)
pcDNA3-Luc2-tdTomato	Luc2-tdTomato	(Patel et al, 2010)
pLXSN-Luc2-tdTomato	Luc2-tdTomato	kind gift from Rene Jackstadt

ORF = open reading frame, wt = wild-type, mut = mutant, SBS = SNAIL binding site, MCS = multiple cloning site, fl = full-length

3.5.2 Oligonucleotides

3.5.2.1 Oligonucleotides used for qChIP

Name	Sequence (5' to 3')
ZNF281 SBS1 fwd	AGGCTGGTCTTGAACTCCTG
ZNF281 SBS1 rev	GGAAACAATCCCAGAACAAAG
ZNF281 SBS2+3 fwd	GTACCACTAATTGCGGTTTCAA
ZNF281 SBS2+3 rev	TAATGGGCGCATATCCTTTG
ZNF281 SBS4 fwd	TGTAGTGCTGCTTTCCGAAG
ZNF281 SBS4 rev	ATGCTGCACTGATCACATCC
ZNF281 SBS5 fwd	AGGACACATGGTCTCCCAAC
ZNF281 SBS5 rev	AAATCCACTCGTGGTTCTGC
SNAIL A fwd	CCCTATGGAGCCGTGTTACAG
SNAIL A rev	GAGTTTCGTTGAAAAAGATCCCTG
SNAIL B fwd	AACGGGTGCTCTTGGCTA
SNAIL B rev	GAAGCGAGGAAAGGGACAC
SNAIL C fwd	GGAGTACTTAAGGGAGTTGGCGG
SNAIL C rev	GAACCACTCGCTAGGCCGT
SNAIL D fwd	GACTCAGATTGGGTGACCTGG
SNAIL D rev	ACTCAATCAACAAACATGAGCCC
CDH-1 TSS fwd	TGAACCCTCAGCCAATCAG
CDH-1 TSS rev	AGTTCCGACGCCACTGAG
CDH-1 -10kb fwd	GCCTGGGACTGAAAGTCTTG
CDH-1 -10kb rev	CAGGGTTCTCCCAAGAACAG
OCLN TSS fwd	CGAGTTTCAGGTGAATTGGTC
OCLN TSS rev	CGGGAGTGTAGGTGTGGTGT
OCLN -5kb fwd	TCCCAAAGTGCTGGGATTAC
OCLN -5kb rev	GGCTCACTGCAGCCTCTATC
CLDN-7 TSS fwd	TTTGAGAGGGCAAAACAAAG
CLDN-7 TSS rev	CAGTTTCCTCCCAATCTTCC
CLDN-7 -3kb fwd	TGAAAGCAAAGTACTGGTAGCC
CLDN-7 -3kb rev	CCACCCACCTTCCTCTATCC
Axin2 fwd	CCAACTCACTCAGGGGAGAC
Axin2 rev	GATTCTTGGCACAGGCAGTAG
LGR5 fwd	TCTCCCAGGTCTGGTGTGTT
LGR5 rev	CACCCTGAGCAACATCCTG
CD133 fwd	AACCCAAACAAAGCAAAACC
CD133 rev	TTTGCACAGAAGCAGAAAGC
Chr. 16q22 fwd	CTACTCACTTATCCATCCAGGCTAC
Chr. 16q22 rev	ATTTCACACACTCAGACATCACAG

fwd = forward, rev = reverse, SBS = SNAIL binding site, TSS = transcription start site

3.5.2.2 Oligonucleotides used for qPCR

Designation	Sequence (5' to 3')
β-actin fwd	TGACATTAAGGAGAAGCTGTGCTAC
β-actin rev	GAGTTGAAGGTAGTTTCGTGGATG
ZNF281 fwd	TCTTCACCTCTCCACAACCAC
ZNF281 rev	TGTAGCATCCAAAGCAGACAA
pri-miR-34a fwd	CGTCACCTCTTAGGCTTGGA
pri-miR-34a rev	CATTGGTGTCGTTGTGCTCT
SNAIL fwd	GCACATCCGAAGCCACAC
SNAIL rev	GGAGAAGGTCCGAGCACA
CDH-1 fwd	CCCGGGACAACGTTTATTAC
CDH-1 rev	GCTGGCTCAAGTCAAAGTCC
VIM fwd	TACAGGAAGCTGCTGGAAGG
VIM rev	ACCAGAGGGAGTGAATCCAG
SLUG fwd	TGGTTGCTTCAAGGACACAT
SLUG rev	GTTGCAGTGAGGGCAAGAA
ZEB1 fwd	TCAAAAGGAAGTCAATGGACAA
ZEB1 rev	GTGCAGGAGGGACCTCTTTA
FN-1 fwd	CTTTGGTGCAGCACAACTTC
FN-1 rev	TCCTCCTCGAGTCTGAACCA
OCLN fwd	GGCCTCTTGAAAGTCCACCT
OCLN rev	CTGAGAGAGCATTGGTCGAA
CLDN-7 fwd	AGTTGCTGGGCTTCTCCAT
CLDN-7 rev	TTGGAAGAGTTGGACTTAGGG
CDH-3 fwd	ATGACGTGGCACCAACCAT
CDH-3 rev	GTTAGCCGCCTTCAGGTTCTC
ZO-3 fwd	CGTCGCCTCTACGCACAAG
ZO-3 rev	TGAAGAGGTGGCTGCTGTGTT
PKP-2 fwd	CGGAAATCTTCACCGAACCA
PKP-2 rev	AACGGCCTCCAACAAAATCAT
DSP fwd	CAGTGGTGTCAGCGATGATGT
DSP rev	TGACGCTGGATATGGTGGAA
CLDN-1 fwd	GCCCCAGTGGATTTACT
CLDN-1 rev	GTTTTGGATAGGGCCTTGGT
TSPAN-31 fwd	CGCTCTCAACGTGGTCTACA
TSPAN-31 rev	ACTCCCACAGCAATGACTCC
ZO-1 fwd	CAGGAAATCTATTTCAAGGTCTGC
ZO-1 rev	CATCACCAAAGGACTCAGCA
β-catenin fwd	AGCTGACCAGCTCTCTCTTCA
β-catenin rev	CCAATATCAAGTCCAAGATCAGC
LGR5 fwd	GCATTTGGAGTGTGTGAGAA
LGR5 rev	AGGGCTTTCAGGTCTTCCTC

Designation	Sequence (5' to 3')
CD133 fwd	TCCACAGAAATTACCTACATTGG
CD133 rev	CAGCAGAGAGCAGATGACCA
Axin2 fwd	CCACACCCTTCTCCAATCC
Axin2 rev	TGCCAGTTTCTTTGGCTCTT
GAPDH fwd	GCTCTCTGCTCCTCCTGTTC
GAPDH rev	ACGACCAAATCCGTTGACTC

fwd = forward, rev = reverse

3.5.2.3 Oligonucleotides used for cloning and mutagenesis

Name	Sequence (5' to 3')
human *ZNF281*_77bp_UTR fwd	GTGGCCAGGCTGGAGGTCTTCTAATGTAATTTTGTTTTATTTTGAG
human *ZNF281* wt_77bp_UTR rev	GGATCGTGTAGAAACATTCCAATGGCAGTGTTCTCAAAATAAAACA AAA
human *ZNF281* mut_77bp_UTR rev	GGATCGTGTAGAAACATTCCAATCCGACTGTTCTCAAAATAAAACA AAA
human *ZNF281* wt_fl_UTR fwd	TTTACCGGTGGTCCCAAAAGTGGCCAG
human *ZNF281* wt_fl_UTR rev	TTTCTGCAGGCGTTTAAAACATTTGGGC
human *ZNF281* promoter fwd NheI	TTTGCTAGCCCCCTTCCTTGGGCTTGA
human *ZNF281* promoter rev EcoRI	TTTGAATTCGCCTCCCGTGTACTGCG
SBS2 mut fwd	GCGTGTTTTACAGGACTGCTGACTCCTGATTACGCTCGGTTTCCT CTTC
SBS2 mut rev	GAAGAGGAAACCGAGCGTAATCAGGAGTCAGCAGTCCTGTAAAACACG
SBS3 mut fwd	GCTTCCAAATTCAAAGGGATAACATAAGACTCCTTTTTAATAAATGTTGAGC AATTTGGAG
SBS3 mut rev	CTCCAAATTGCTCAACATTTATTAAAAAGGAGTCTTATGTTATCCCTTTGAAT TTGGAAGC

fwd = forward, rev = reverse, wt = wild-type, mut = mutant, SBS = SNAIL binding site, fl = full-length

3.5.3 microRNA mimics and antagomiRs

The following pre-microRNA mimics and antagomiRs were purchased from Ambion:

- pre-miR-control
- pre-miR-34a
- anti-miR-control
- anti-miR-34a

3.6 Buffers and solutions

2x Laemmli buffer:

- 125 mM TrisHCl (pH 6.8)
- 4% SDS
- 20% glycerol
- 0.05% bromophenol blue (in H_2O)
- 10% β-mercaptoethanol (added right before use)

Propidium iodide staining solution:

- 800 µl propidium iodide (1.5 mg/ml)
- 1000 µl RNase A (10 mg/ml)
- ad 20 ml PBS 0.1% TritonX 100

10x 'Vogelstein' PCR buffer:

- 166 mM NH_4SO_4
- 670 mM Tris (pH 8.8)
- 67 mM $MgCl_2$
- 100 mM β-mercaptoethanol

RIPA buffer (for protein lysates):

- 1% NP40
- 0.5% sodium deoxycholate
- 0.1% SDS
- 250 mM NaCl
- 50 mM TrisHCl (pH 8.0)

SDS buffer:

- 50 mM Tris (pH 8.1)
- 100 mM NaCl
- 0.5% SDS
- 5 mM EDTA

10x Tris-glycine-SDS running buffer (5l, for SDS-PAGE):

- 720 g Glycin
- 150 g Tris base
- 50 g SDS
- pH 8.3-8.7
- ad 5 l ddH_2O

Triton dilution buffer:

- 100 mM Tris-HCl (pH 8.6)
- 100 mM NaCl
- 5 mM EDTA (pH 8.2)
- 0.2% NaN_3
- 5% TritonX-100

Towbin buffer (for Western blotting):

- 200 mM glycine
- 20% methanol
- 25 mM Tris base (pH 8.6)

10x TBS-T (5l):

- 500 ml 1M Tris (pH 8.0)
- 438.3 g NaCl
- 50 ml Tween20
- ad 5 l ddH_2O

3.7 Laboratory equipment

Device	Supplier
5417C table-top centrifuge	Eppendorf AG, Hamburg, Germany
ABI 3130 genetic analyzer capillary sequencer	Applied Biosystems, Foster City, USA
Axiovert 25 microscope	Carl Zeiss GmbH, Oberkochen, Germany
BD Accuri™ C6 Flow Cytometer Instrument	Accuri, Erembodegem, Belgium
Biofuge *fresco*	Heraeus; Thermo Fisher Scientific, Inc., Waltham, MA, USA
Biofuge *pico* table top centrifuge	Heraeus; Thermo Fisher Scientific, Inc., Waltham, MA, USA
Boyden chamber transwell membranes (pore size 8.0 µm)	Corning Inc., Corning, NY, USA
Cflow® software	Accuri, Erembodegem, Belgium
CF40 Imager	Kodak, Rochester, New York, USA
Falcons, dishes and cell culture materials	Schubert & Weiss OMNILAB GmbH & Co. KG
Fisherbrand FT-20E/365 transilluminator	Fisher Scientific GmbH, Schwerte, Germany
Forma scientific CO_2 water jacketed incubator	Thermo Fisher Scientific, Inc., Waltham, MA, USA
GeneAmp® PCR System 9700	Applied Biosystems, Foster City, USA
Herasafe KS class II safety cabinet	Thermo Fisher Scientific, Inc., Waltham, MA, USA
HTU SONI130	G. Heinemann Ultraschall- und Labortechnik, Schwäbisch Gmünd, Germany
KAPPA ImageBase software	KAPPA opto-electronics GmbH, Gleichen, Germany
Megafuge 1.0R	Heraeus; Thermo Fisher Scientific, Inc., Waltham, MA, USA
Mini-PROTEAN®-electrophoresis system	Bio-Rad, München, Germany
MultiImage Light Cabinet	Alpha Innotech, Johannesburg, South Africa
ND 1000 NanoDrop Spectrophotometer	NanoDrop products, Wilmington, DE, USA
Neubauer counting chamber	Carl Roth GmbH & Co, Karlsruhe, Germany
Orion II luminometer	Berthold Technologies GmbH & Co. KG, Bad Wildbad, Germany
PerfectBlue™ SEDEC 'Semi-Dry' blotting system	*PEQLAB* Biotechnologie GmbH, Erlangen, Germany
real-time cell analyzer (RTCA)	xCELLigence RTCA SP; Roche Diagnostics GmbH, Penzberg, Germany

Device	Supplier
Varioskan Flash Multimode Reader	Thermo Scientific, Inc., Waltham, MA, USA
waterbath	Memmert GmbH, Schwabach, Germany

4. METHODS

4.1 Bacterial cell culture

4.1.1 Propagation and seeding

For replication of plasmids carrying an ampicillin resistance the *E.coli* XL1-blue strain was used. The bacterial cells were cultured in lysogeny both (LB) -medium by agitation (225 rpm) or on LB agar plates to obtain single cell clones. Each LB was supplemented with 100 µg/ml ampicillin for selection at 37°C overnight.

4.1.2 Transformation

For transformation competent *E.coli* XL1-blue were used. The plasmid DNA was added to the bacterial cells and incubated on ice for 30 minutes. The cells were subjected to a heat-shock at 42°C for 45 seconds and replaced on ice for additional two minutes. To increase the transformation efficiency the transformed cells where pre-incubated at 37°C for one hour. Next, the cells were plated on LB-agar plates containing ampicillin and cultivated at 37°C overnight. For further propagation of the plasmid a transformed single cell clone was used to inoculate the respective amount of LB-medium containing the antibiotics, incubated at 37°C overnight and subjected to the procedure of choice to purify the plasmid DNA.

4.1.3 Purification of plasmid DNA from *E.coli*

For the preparation of smaller amounts of plasmid DNA 5 ml of LB-medium supplemented with ampicillin were inoculated with the respective single clone of the transformed bacterial cells. The plasmid DNA was isolated according to the manufacturer's instructions of the QIAprep Spin Miniprep Kit (Qiagen). This method was preferentially used due to the better yields and quality of the DNA leading to better transfection efficiencies.

In order to generate larger amounts of plasmid DNA 150 ml of LB-medium containing ampicillin were used for bacterial cell inoculation. For DNA purification the Pure Yield™ Plasmid Midiprep System (Promega) was used according to the protocol of the manufacturer.

4.2 Chromatin immunoprecipitation (ChIP) assay

DLD-1 colorectal cancer cells and their derivatives were cultured as described above. Before cross-linking, the cells were treated with DOX [100 ng/ml] for 24 hours to induce ectopic expression of VSV-tagged proteins. Cross-linking was performed with formaldehyde (Merck) at a final concentration of 1% and terminated after five minutes by addition of glycine at a final concentration of 0.125 M. Cells were harvested with SDS buffer (50 mM Tris pH 8.1, 0.5% SDS, 100 mM NaCl, 5 mM EDTA), pelleted and resuspended in IP buffer (2 parts of SDS buffer and 1 part Triton dilution buffer (100 mM Tris-HCl pH 8.6, 100 mM NaCl, 5 mM EDTA, pH 8.0, 0.2% NaN_3, 5.0% TritonX 100). Chromatin was sheered by sonication (HTU SONI 130, G. Heinemann) to generate DNA fragments with an average size of 500 bp. Preclearing and incubation with polyclonal VSV (V4888, Sigma) antibody, polyclonal ZNF281 antibody or the rabbit IgG antibody control (R-5506, Sigma) for 16 hours was performed as previously described (Menssen et al, 2007). Washing and reversal of cross-linking was performed as described (Amati et al, 2001). The ChIP assay against endogenous SNAIL was performed according to the manufacturer's instructions using the QuickChIP Kit (Imgenex Corporations) and a polyclonal antibody against SNAIL (AF3639, R&D Systems) or the goat IgG control (AB-108-C, R&D Systems). Immunoprecipitated DNA was analyzed by qPCR and the enrichment was expressed as percentage of the input for each condition (Amati et al, 2001). To calculate the binding to the DNA region analyzed, the enrichment using the specific antibody (AB) compared to the isotype control (IgG) IP is expressed as % input. The calculation was done as indicated below:

$$\frac{2^{((CP\,input)-(CP\,IP))_{AB}}}{2^{((CP\,input)-(CP\,IP))_{IgG}}} = \%\,input\,/\,IgG$$

Binding to a region on chromosome *16q22* served as negative control in all ChIP assays performed. The sequences of oligonucleotides used as qChIP primers are listed in chapter 3.5.2.1.

4.3 Cell culture of human cells

4.3.1 Propagation of human cell lines

The cell lines HCT-15, HEK293T, HT29, MiaPaCa2, SKBR3, SW480 and SW620, as well as human diploid fibroblasts (HDFs) were kept in high glucose Dulbecco`s modified Eagles medium (DMEM, Invitrogen). DLD-1, HCT116 *p53* -/- and HCT116 *p53* +/+ cells were cultured in McCoys medium (Invitrogen) and Colo320 in RPMI medium (Invitrogen). Media were supplemented with 10% fetal calf serum (FCS, Invitrogen) and 1% Penicillin/Streptavidin (Invitrogen). For HEK293T cells 5% FCS was used. All cells were kept at 5% CO_2 and 37°C in a humidified incubator. The same culturing conditions were used for the respective derivatives of the cell lines. In order to avoid any confluency of the cells, they were passaged every two to four days and seeded into fresh culturing flasks.

4.3.2 Transfection of oligonucleotides and vector constructs

Transfections of oligonucleotides and vector constructs were carried out using freshly trypsinized and re-seeded (not yet settled) cells in the medium and cell culturing format of choice, preferentially into a six- or twelve-well format. In general the transfection reagent mix contained 100 µl Opti-MEM (Invitrogen), 10 µl HiPerFect (Qiagen) and 10 µl of the respective oligonucleotide [10 µM] (Ambion – Applied Biosystems, final concentration [100 nM]). In order to transfect plasmid DNA the transfection mix consisted of 150 µl Opti-MEM, X µg DNA (as indicated in the figure legend) and 5 µl FuGENE6 (Promega). The mix was incubated at RT for 15-20 minutes and afterwards added drop-wise to the cells. After the indicated incubation time the respective assays were carried out. Selection of plasmid containing cells was started 48 hours after the transfection procedure using the appropriate antibiotics.

4.3.3 Conditional expression in cell pools

Polyclonal cell pools for conditional expression were generated by transfection of the episomal expression vector pRTR (Jackstadt et al, 2013) using Fugene6 (Roche) and selection in 2 µg/ml Puromycin (Sigma; stock solution: 2 mg/ml in water) for 10 days. The percentage of eGFP-positive cells was determined 48 hours after addition of Doxycycline (DOX) at a final concentration of 100 ng/ml (Sigma; stock solution 100 µg/ml in water). Polyclonal cell pools transfected with the pRTS vector (Bornkamm et al, 2005) were similarly generated and selection occurred in 150 µg/ml Hygromycin B (Sigma; stock solution: 50 mg/ml) for up to 14 days. The percentage of mRFP-positive cells was determined 48 hours after addition of DOX at a final concentration of 1 µg/ml.

4.3.4 Cryo-preservation of mammalian cells

Sub-confluent cells in the exponential growth phase were used for cryo-preservation by trypsination, resuspended with medium and pelleted by centrifugation at 1200 rpm for five minutes. Resuspension of the cells was done in 50% FCS, 40% growth medium and 10% (v/v) DMSO (Roth). Aliquots in cryo-vials were cooled down in a freezing device at -80°C overnight and transferred into liquid nitrogen for long term storage.
In order to recover cells they were rapidly thawed in a water bath at 37°C, resuspended in medium and pelleted by centrifugation as described above. Thereafter, the cells were resuspended in the respective growth medium and plated in the desired format of a cell culture flask for further cultivation.

4.3.5 Isolation of genomic DNA from human diploid fibroblasts (HDFS)

Genomic DNA from HDFs was generated by seeding the cells on a 10 cm^2 dish at a confluency of 90% at the maximum. The DNA was isolated according to manufacturer's instructions using the Blood & Tissue Kit (Qiagen), eluted into a final volume of 50 µl and the resulting DNA content was analyzed using the Nanodrop spectrophotometer.

4.4 Determination of proliferation

4.4.1 Determination of proliferation by cell counting

The proliferation of DLD-1/pRTR-ZNF281-VSV and SW480/pRTS-miR cells was determined by seeding 1 x 10^5 cells/6-well in triplicates for the indicated time-points. Furthermore, the cells were treated with DOX (DLD-1: 100 ng/ml; SW480: 1 µg/ml) for 24 to 72 hours or left untreated as control. One day after seeding the 0 hours time-point was harvested by trypsinizing the cells and resuspending them in a defined volume of DMEM supplemented with 10% FCS to stop the reaction. Cell counting was done using the Neubauer chamber and calculation of the total cell number per well was carried out. The cells corresponding to the indicated time-points were harvested as described above. Total cell numbers are graphically shown.

4.4.2 Determination of proliferation by impedance measurement

The optimal cell concentration was determined by serial dilution for each cell line. 1 x 10^4 SW620 cells were seeded per well (96-well). Subsequently, 100 µl of cell culture media at room temperature was added into each well of an E-plate 16 (Roche). Proper electrical-contact was checked and background impedance was measured. 100 µl cell suspension was added to the medium-containing wells on the E-plate 16. After 30 minutes incubation at room temperature, the E-plate 16 was placed in the xCELLigence device (Roche) in a cell culture incubator. Impedance was monitored every 60 minutes for a period of up to 110 hours. The electrical impedance is represented as a dimension-less parameter termed cell-index (CI). All calculations were performed using the RTCA software provided with the xCELLigence system. The unit-less parameter CI represents the relative change in electrical impedance that occurs in the presence and absence of cells in the wells, which is calculated based on the following formula: $CI = (Zi - Z0)/15$, where Zi is the impedance at an individual point of time during the experiment and $Z0$ is the impedance at the start of the experiment. Impedance is measured at three different frequencies (10, 25 or 50 kHz) and a specific time (ref: Roche Diagnostics GmbH. Introduction of the RTCA DP Instrument. RTCA DP Instrument Operator‘s Manual, A. Acea Biosciences, Inc.; 2008.).

4.5 Episomal vectors for ectopic expression of proteins and miRNAs

The generation of the pRTR vector, which is an improved version of the pRTS vector is described in (Jackstadt et al, 2013). The VSV-tagged ZNF281 expression construct was generated using standard PCR and cloning techniques with pCMV-sport1-ZNF281 (kindly provided by Juanita Merchant (Law et al, 1999)) as a template and insertion into the pRTS vector by using the pUC19SfiI shuttle vector and SfiI restriction sites. The VSV-tagged sequence of ZNF281 was excised from pRTS-ZNF281-VSV and ligated into the pRTR vector via the SfiI-sites. The insert orientation was verified by sequencing. More detailed information on the generation of the pRTR-SNAIL-VSV, the pRTR-p53-VSV or the pRTR-*pri-miR-34a* vectors are provided in (Kaller et al, 2011; Siemens et al, 2011). Expression plasmids used are listed in chapter 3.5.1.

4.6 Flow cytometry

4.6.1 Analysis of the transfection efficiency (eGFP/mRFP)

In order to control the transfection efficiency of the pRTR and pRTS vectors into mammalian cells, both vectors harbor an *eGFP* or *mRFP* gene, respectively. The percentage of eGFP/mRFP-positive cells was determined 48 hours without or following addition of DOX [100 ng/ml]. A BD Accuri™ C6 Flow Cytometer instrument (Accuri) and the corresponding Cflow® software served to read out the proportion of fluorescent cells.

4.6.2 Cell cycle analysis by propidium iodide staining

The respective cells were cultured under the indicated conditions and treated with DOX or left untreated as described in the respective figure legends and depicted in the figure. Cells were harvested by trypsination, resuspended in DMEM or McCoys medium supplemented with 10% FCS respectively. Following centrifugation and removal of the supernatant the cells were resuspended and ice-cold ethanol (70%) was added drop-wise. After overnight incubation at -20°C, cells were centrifuged and resuspended in

propidium iodide (PI) staining buffer (PBS supplemented with 0.1% TritonX 100, 1.2 mg propidium iodide and 10mg RNaseA) and incubated at 37°C for 30 minutes. The distribution of the cells according to the different cell cycle stages was determined by analyzing 1 x 10^4 cells per measurement with the BD Accuri™ C6 Flow Cytometer Instrument (Accuri) and the corresponding Cflow® software. Experiments were carried out in triplicates.

4.7 Generation of Luc2 expressing SW620 cells

To generate the luciferase expressing vector pLXSN-Luc2-tdTomato, the *Luc2* and *tdTomato* ORFs were excised from the pcDNA3-Luc2-tdTomato vector (Addgene Plasmid # 32904, kindly provided by Christopher Contag (Patel et al, 2010)) by using EcoRI sites and cloned into the pLXSN retroviral vector. For retroviral infection of SW620 cells, Phoenix-A packaging cells were transfected with the pLXSN-Luc2-dtTomato vector using calcium phosphate precipitation. Retrovirus-containing supernatants were harvested 24 hours after transfection, passed through 0.45 µm filters (Millipore) and used to infect SW620 in the presence of polybrene (8 µg/ml) four times in four hours intervals. Selection was started 48 hours later by addition of 500 µg/ml geneticin (Gibco) for 14 days and subsequently a single cell clone was picked.

4.8 Immunofluorescence and confocal-laser scanning microscopy

For immunofluorescence analysis, cells cultivated on glass cover-slides were fixed in 4% paraformaldehyde/PBS for 10 minutes, permeabilized with 0.2% TritonX 100 for 20 minutes and blocked in 100% FBS for 30 minutes. Primary and secondary antibodies are listed in chapter 3.4. F-Actin was detected with Phalloidin conjugated with Alexa Flour 647 (Invitrogen). Chromatin was stained by DAPI (Roth). Finally, slides were covered with ProLong® Gold antifade (Invitrogen).

Laser scanning microscopy (LSM) images were captured with a confocal microscope (LSM 700, Zeiss) using a Plan Apochromat 20x/0.8 M27 objective, ZEN 2009 software (Zeiss) and the following settings were used: image size 2048x2048 and 16 bit,

pixel/dwell of 25.2 µs, pixel size 0.31 µm, laser power 2% and master gain 600-1000. After image capturing the original LSM files were converted into TIFF files.

4.9 *In vivo* lung metastasis assay

72 hours after siRNA transfection 4 x 10^6 SW620-Luc2 cells were resuspended in PBS in a total volume of 0.2 ml and injected into the lateral tail vein of a six- to eight-week-old male nonobese diabetic/severe combined immunodeficient (NOD/SCID) mouse using a 25-gauge needle. For monitoring of the injected cells mice were injected intraperitoneal with d-luciferin (150 mg/kg) and were imaged under anaesthesia with the IVIS Illumina System (Caliper Life Sciences) 30 minutes after tail vein injection in order to have a reference point. The acquisition time was set to two minutes and imaging was repeated once a week to monitor the seeding and outgrowth of the cells. After nine weeks complete lungs were resected and photographed. For hematoxylin and eosin (H&E) staining, lungs were fixed with 4% paraformaldehyde and 5 µm paraffin sections were stained with H&E. The number of metastases was determined microscopically. Mice were kept under IVC conditions and experiments were performed with permission of the Bavarian state.

4.10 Isolation of RNA and reverse transcription

The High Pure RNA Isolation Kit (Roche) was used to isolate total RNA from human cancer cells according to the manufacturer's instructions. Elution occurred by using 50 µl elution buffer. Amount and quality of the RNA were determined using a Nanodrop spectrophotometer. cDNA was generated from 1 µg of total RNA per sample using anchored oligo(dT) primers (Verso cDNA synthesis Kit) following the manufacturer's instructions. For the detection of mature miRNAs cDNA was generated from 300 ng total RNA per sample using the Universal cDNA Synthesis Kit from the miRCURY LNA Universal RT microRNA PCR Kit (Exiqon, 203300) according to the manufacturer´s instructions. As primers miRNA LNA PCR primers specifically for *miR-34a/b/c* (Exiqon: 204486, 204005, 204407) and the respective control primer SNORD48 (Exiqon: 203903) were used.

4.11 Luciferase assay

DLD-1 cells were seeded in 12-well format dishes at 1.5 x 10^5 cells/well and transfected with FuGene Reagent (Roche) for 48 hours with 100 ng of the indicated firefly luciferase reporter plasmid (pBV), 100 ng of the respective pcDNA3 vector and 20 ng of *Renilla* reporter plasmid (pRL) as a normalization control. SW480 cells were seeded in 12-well format dishes at 3 x 10^5 cells/well and transfected for 72 hours with 100 ng of the indicated firefly luciferase reporter plasmid, 20 ng of *Renilla* reporter plasmid as a normalization control and 25 nM of *miR-34a* pre-miRNA oligonucleotides (Ambion, PM11030), or a negative control oligonucleotides (Ambion, neg. control #1). HEK293T cells were seeded in 12-well format dishes at 1.5 x 10^5 cells/well and transfected with FuGene Reagent (Roche) for 48 hours. 100 ng of the indicated firefly luciferase reporter plasmid (pGL3), 500 ng of the pcDNA3 vector as indicated and 20 ng of *Renilla* reporter plasmid as a normalization control were used. The pGL3-*SNAIL* promoter constructs were kindly provided by Antonio Garcia de Herreros and Lionel Larue (Barbera et al, 2004). The analyses were performed with the Dual Luciferase Reporter assay kit (Promega) according to the manufacturer's instructions. Luminescence intensities were measured with an Orion II luminometer (Berthold) in 96-well format and analyzed with the SIMPLICITY software package (DLR). DLD-1 colorectal cancer cells harboring a conditional *ZNF281* allele and SW480 cells in 12-well plates were transfected using FuGene Reagent (Roche) supplemented with 10 ng of Renilla luciferase control reporter plasmid, 100 ng Topflash or Fopflash luciferase reporter constructs containing either wild-type or mutant TCF binding sites (Veeman et al, 2003). The conditional *ZNF281* allele was activated by addition of Doxycycline (DOX; 100 ng/ml) for 72 hours. Firefly and Renilla luciferase activities were measured 72 hours after transfection using the Dual Luciferase Reporter assay kit (Promega) as mentioned above.

4.12 Migration and invasion analysis in Boyden-chambers

DLD-1 and SW480 cells expressing DOX-inducible pRTR or pRTS vectors were cultured for the indicated periods in presence or absence of DOX [pRTR: 100 ng/ml; pRTS: 1 µg/ml]. Cells were deprived of serum (0.1%) for 48 hours before the analysis. To analyze migration 5 x 10^4 cells were seeded in the upper chamber (8.0 µm pore

size; Corning) in serum-free medium. To analyze invasion membranes were coated with Matrigel (BD Bioscience) at a dilution of 3.3 mg/ml in medium without serum. After coating 7 x 10^4 cells were seeded on Matrigel in the upper chamber. As chemo-attractant 10% FCS was used in the lower chamber. Cultures were maintained for 48 hours, then non-motile cells at the top of the filter were removed and the cells in the lower chamber were fixed with methanol and stained with DAPI. Either the number of cells per well or five different fields per condition were counted by microscopy. The relative invasion/migration was expressed relative to the control.

4.13 NCI-60 database analysis

The NCI-60 dataset contains microarray expression analysis results of various human cancer cell lines derived from multiple tumor types (Shoemaker, 2006). Results derived from seven colon cancer cell lines were chosen for further analysis.

4.14 Oncomine analysis

The Oncomine tool (Rhodes et al, 2004) was used in order to assess the differential expression of *ZNF281* mRNA in human cancer datasets. The following settings were used: p-value of 0.05 and gene rank in the top 10% among all differentially expressed genes. For the listed analyses, the statistical results were provided by Oncomine and linked to a graphical representation of the original microarray dataset samples.

4.15 Polymerase chain reaction (PCR) methods

4.15.1 Colony PCR

The identity and orientation of the insert of bacterial cell clones was verified by colony PCR. For this 20µl PCR master mix containing vector and/or insert specific primers, dNTPs, 10x Vogelstein PCR buffer and FIREPol® DNA polymerase were prepared. Single colonies were picked from the LB-agar plate and transferred each into a single PCR tube. PCR cycling conditions were as exemplarily given: five minutes at 95°C,

followed by 25 cycles of 95°C for 20 seconds, 58°C for 30 seconds and 72°C for X minute/s (1 minute per 1 kb length of the expected PCR product). PCR fragment length was analyzed by supplementing the sample with loading dye and loading it to an agarose gel (percentage of the gel adjusted to the fragment length).

4.15.2 PCR amplification from HDF DNA

4.15.2.1 Cloning of 3´-UTR sequences

The full-length and shortened version of the 3´-UTR of the human *ZNF281* mRNA containing the putative *miR-34a* binding site were PCR-amplified from genomic DNA from HDFs using specific primers to clone the full-length (fl) 3´-UTR and the 77 bp long version of the 3´-UTR (3´-UTR fragment). The resulting 3´-UTR or the 3´-UTR fragment were cloned into the shuttle vector pGEM-T-Easy (Promega) respectively. After excision with EcoRI and SpeI the respective 3´-UTRs were cloned into the pGL3-control-MCS (Welch et al, 2007) and were verified by sequencing. Oligonucleotides used for cloning and mutagenesis are given in chapter 3.5.2.3.

4.15.2.2 Cloning of the *ZNF281* promoter constructs

The human *ZNF281* promoter (-1967/+34) containing the SNAIL binding sites (SBS) 2+3 (SBS2+3) was PCR-amplified from genomic DNA from HDFs using specific primers adding NheI and EcoRI restriction sites to the ends of the PCR product. After restriction with NheI and EcoRI the respective promoter construct was cloned into the pBV-MCS and were verified by sequencing. Oligonucleotides used for cloning and mutagenesis are given in chapter 3.5.2.3.

4.16 Protein isolation, SDS-PAGE and Western blot

Protein lysate generation, SDS-PAGE and Western blot analyses were performed according to standard protocols. Briefly, cells were lysed in RIPA lysis buffer (50 mM Tris/HCl, pH 8.0, 250 mM NaCl, 1% NP40, 0.5% (w/v) sodium deoxycholate,

0.1% sodium dodecylsulfate, complete mini protease inhibitor tablets (Roche)). Lysates were sonicated using a HTU SONI130 (G. Heinemann Ultraschall- und Labortechnik) for three consecutive five-second pulses with an intensity of 85% and centrifuged at 16.060 g for 15 minutes at 4°C in order to separate the protein containing supernatant from any cell debris. The BCA Protein Assay Kit (Pierce, Thermo Scientific) was used to determine the protein concentrations according to the manufacturer's instructions. The protein concentration was measured with a Varioskan Flash Multimode Reader using the SkanIt RE for Varioskan 2.4.3 software (Thermo Scientific). Afterwards, 30 to 80 µg of the respective protein lysates supplemented with Laemmlie buffer were denatured at 95°C for five minutes and loaded on 10% or 12% SDS-acrylamide gels according to the protein size. A pre-stained protein ladder (Fermentas) served as size control and the separation of the proteins by electrophoresis was performed at 60-130 V in a Mini-PROTEAN®-electrophoresis system (Bio-Rad) with Tris-glycine-SDS running buffer. Afterwards the proteins were transferred onto Immobilon PVDF membranes (Millipore) using Towbin buffer and the PerfectBlue™ SEDEC blotting system (Peqlab) and a EPS 600 power supply (Pharmacia Biotech) constantly at 125 mA per gel and a maximum voltage of 10 V. Thereafter, the membranes were incubated for one hour in 5% skim milk/TBS-Tween20 (TBS-T) to block unspecific protein binding. Incubation with the primary antibodies (diluted in TBS-T) occurred at 4°C overnight. Horseradish-peroxidase (HRP)-conjugated secondary antibodies were incubated for one hour at RT. In between, membranes were washed twice in TBS-T for 15 minutes each. ECL/HRP substrate (Immobilon) was added to the membrane. ECL signals were recorded using a CF440 Imager (Kodak). The polyclonal anti-ZNF281 antibody was generated by immunizing rabbits with a purified recombinant GST-ZNF281 fusion protein (amino acids 1-330) and purified by affinity chromatography with a Sulfo-Link (Pierce) coupled immunogen. Antibodies used here are listed in chapter 3.4.

4.17 Quantification of Western blot signals

Intensities of protein expression signals generated by Western blot were quantified using the ImageJ software (Schneider et al, 2012). ImageJ is inspired by NIH Image and offers a processing and analysis program. Upon up-loading of the respective images it allows the user to carry out a calculation of area and pixel value statistics. The

resulting values were used for calculation of a ratio of the respective protein of interest and the loading control, whereas the quotient of the respective experimental control was set equal to one.

4.18 Quantitative real-time PCR (qPCR) and Exiqon qPCR

Quantitative real-time PCR (qPCR) was performed by using the LightCycler 480 (Roche) and the Fast SYBR Green Master Mix (Applied Biosystems) and *β-actin* or *GAPDH* as control as previously described in (Menssen & Hermeking, 2002). Only primer pairs resulting in a single peak in the melting curve analysis were used. A list of all qPCR-primers is provided in chapter 3.5.2.2. The qPCR results were analyzed using the ΔΔcp method (Livak & Schmittgen, 2001).

qPCR for mature miRNAs was performed using the LightCycler 480 (Roche) and the Fast SYBR Green Master Mix Universal RT (Exiqon, 203450) according to the manufacturer's instructions.

4.19 Retroviral infections

For pBabe-SNAIL-VSV generation, SNAIL-VSV (Siemens et al, 2011), was cloned into the pBabe-empty vector. For retrovirus production, Phoenix-A packaging cells were transfected with pBabe-SNAIL-VSV (puromycin) or pBabe-empty vector (puromycin) using calcium phosphate transfection. 24 hours after transfection, retrovirus-containing supernatants were harvested, passed through 0.45 µm clarification filters (Millipore), and used to infect the respective cell lines four times in the presence of polybrene (8 µg/ml) in four hours intervals. After 48 hours, cells were selected by addition of 2 µg/ml puromycin (Sigma) for five days.

4.20 RNA interference

For RNA interference an episomal all-in-one vector system was employed (Epanchintsev et al, 2006). This vector allows the expression of miR-30-embedded microRNAs after addition of DOX. The target sequence for the respective *ZNF281*-specific-microRNAs used was from the RNAi codex

(http://codex.cshl.edu: sequence 1: TCATCAAACCATACCAATA; sequence 2: TCTAAATGCTGAAATTAA). The non-silencing microRNA fragment was isolated from a commercial pSM2c vector (Expression Arrest™, Cat. No. RHS1703, Open Biosystems). siRNAs (Ambion silencer siRNA negative control: #1 ID#4611; *ZNF281*-specific siRNAs: #1- ID#115950, #2- ID#3898; *SNAIL*-specific siRNA: ID#17124) were transfected at a final concentration of 10 nM for the indicated time-points using HiPerfect transfection reagent (Qiagen).

4.21 Sequencing

Sanger sequencing was performed to verify DNA sequences. For this reaction the BigDye® Terminator v3.1 Cycle Sequencing Kit (Life Technologies) was used according to the manufacturer's protocol. One µg of DNA, 5 pmol of the respective primer, the BigDye Terminator and the buffer were mixed in a total reaction volume of 10 µl. PCR-amplification was performed by 15 cycles of each ten seconds at 96°C, followed by 90 seconds at 60°C. Afterwards the samples were cooled down to RT. In order to clean up the PCR reaction, the DyeEx 2.0 Spin Kit (Qiagen) was used according to the manufacturer's instructions in a 5417C centrifuge (Eppendorf). Purified DNA was supplemented with Hi-Di formamide (Applied Biosystems) and loaded into an ABI3130 genetic analyzer capillary sequencer (Applied Biosystems). Analysis of the data was done by using the 3130 Data Collection Software v3.0 and the sequencing analysis software 5.2 (Applied Biosystems).

4.22 Site directed mutagenesis

The wild-type *ZNF281* promoter construct was further used for mutagenesis of the SNAIL binding sites 2, 3 or 2+3. The sequence of the SNAIL binding sites was mutated from CACCTG to ACTCCT. This was achieved with the QuickChangeII Site-directed Mutagenesis Kit (Agilent Technologies) using the respective mutagenic primers and performing the mutagenic reaction according to the manufacturer's instructions. Correctness of the plasmid sequences was verified by sequencing. Oligonucleotides used for cloning and mutagenesis are given in chapter 3.5.2.3.

4.23 Soft agar colony formation assay

To measure anchorage-independent cell growth, the bottom of a 12-well plate was coated with 700 µl base agar containing 0.8% low melt agarose (Lonza), which was then covered with 700 µl 0.4% agarose containing the respective cells and incubated for 24 hours at 37°C and 5% CO_2. 24 hours later 250 µl medium were added, supplemented with 10% FBS and either DOX [100 ng/ml] or water. Cells were incubated for 14 days changing the medium every three days. For determination of colony numbers cells were stained with 50 µl of 0.005% crystal violet per well for two hours and de-stained in PBS at 4°C overnight. Pictures were taken using an EOS 400D camera (Canon) and colonies were counted using image J software (Schneider et al, 2012).

4.24 Sphere formation assay

Cells were separated by treatment with trypsin after addition of DOX for 48 hours. For each triplicate 1 x 10^5 cells were seeded into a well of a 6-well-plate coated with attachment preventing poly(2-hydroxyethyl-metacrylate) (PolyHEMA, Sigma) in 5 ml sphere-medium (Yu et al, 2007). After seven days the resulting spheres were documented by phase-contrast microscopy at 100 x magnification and spheres were dissociated to single cells using a 0.05% Trypsin-EDTA solution. For quantification, 1 x 10^4 cells/well were seeded in six wells of a PolyHEMA coated 96-well plate in Yu-medium containing 1% methyl cellulose (Sigma) in the absence or presence of DOX. The number of colonies larger than 50 µm in diameter was counted after seven days.

4.25 Statistical analysis

Unless noted otherwise each experiment was carried out in triplicates. A Student's t-test (unpaired, two-tailed) was used for calculation of significant differences between two groups of samples, with $p<0.05$ considered significant. Asterisks generally indicate: *: $p<0.05$, **: $p<0.01$ and ***: $p<0.001$. For correlation analyses the SPSS software package 19 (SPSS Inc.) was used. Spearman rank correlation test was applied to the

NCI-60 data in order to correlate the *ZNF281* mRNA expression with the expression of other mRNAs.

4.26 Wound-healing assay

DLD-1 and SW480 cells harbouring a DOX-inducible *ZNF281* allele or respective microRNAs were cultured for the indicated periods in the presence of DOX [100 ng/ml for pRTR vectors and 1 µg/ml for pRTS vector systems] or left untreated before applying the wound. Mitomycin C [10 ng/ml] was applied two hours before scratching using a Culture-Insert (IBIDI). To remove Mitomycin C and detached cells, cells were washed twice in Hank's balanced salt solution (HBSS) and medium containing DOX [100 ng/ml or 1 µg/ml] was added. Cells were allowed to close the wound for the indicated periods and images were captured on an Axiovert Observer Z.1 microscope connected to an AxioCam MRm camera using the Axiovision software (Zeiss) at the respective time-points.

5. RESULTS

5.1 SNAIL and miR-34a feed-forward regulation of ZNF281/ZBP99 promotes epithelial-mesenchymal-transition

Previously, an interaction between c-MYC and ZNF281 proteins has been identified in a systematic analysis of c-MYC-associated protein complexes (Koch et al, 2007). ZNF281 was among the proteins, which were represented by the highest number of mass-spectrometric sequence reads, indicating that it is associated with a large fraction of c-MYC and presumably represents a significant regulator or effector of c-MYC. However, so far it is mainly unknown how ZNF281 expression itself is regulated and whether it participates in regulatory pathways, which might by relevant for c-MYC function and/or tumor biology.

5.1.1 SNAIL regulates ZNF281 expression

In order to identify upstream regulators of ZNF281 the *ZNF281* promoter sequence was inspected for binding sites of transcription factors, which might hint towards cancer-relevant functions of ZNF281. Thereby, several E-Box motifs (CACCTG) in the *ZNF281* promoter were identified, which represent putative SNAIL binding sites (SBS, Figure 7A). SNAIL is a known regulator of EMT (Batlle et al, 2000; Mauhin et al, 1993) and, similar to ZNF281, a zinc-finger-containing transcription factor (Nieto, 2002; Sanchez-Tillo et al, 2012). Two of the SBSs were located ~500 and ~700 base pairs (bp) upstream of the transcription start site (TSS; Figure 7A and B). SBS2 and SBS4 are conserved between the human and mouse *ZNF281* promoters, indicating functional relevance (Figure 7B). When SNAIL was ectopically expressed in DLD-1 colorectal cancer (CRC) cells using a Doxycycline (DOX) inducible episomal vector system an increase in the SNAIL occupancy of the *ZNF281* promoter was detected by chromatin immunoprecipitation (ChIP) analysis at SBS2 and SBS3, whereas SBS1, 4 and 5 did not display increased binding of SNAIL (Figure 8A). Also endogenous SNAIL protein selectively occupied SBS2 and SBS3 in SW620 CRC cells (Figure 8B).

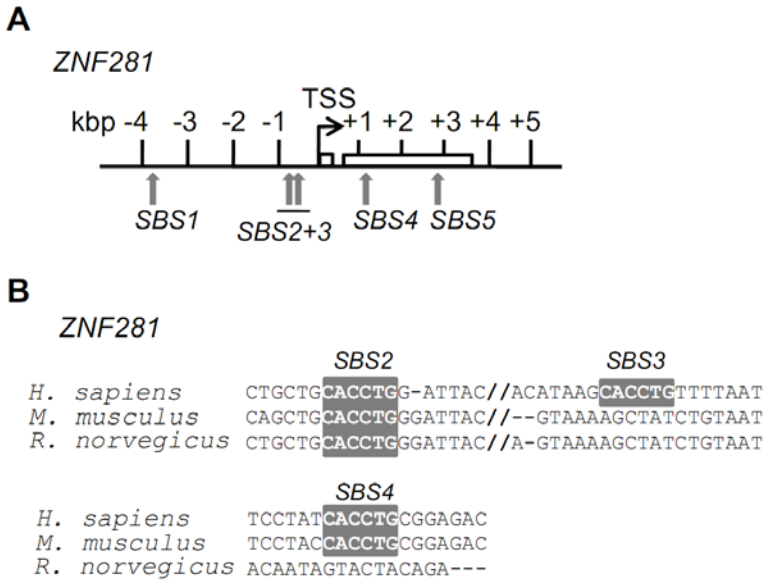

Figure 7: The *ZNF281* promoter contains putative SNAIL binding sites. (A) Scheme of the *ZNF281* promoter and SNAIL binding sites (SBS). Grey arrows indicate SNAIL binding sites; black rectangles exons and the bar a qChIP amplicon for two SBSs at the same time. TSS: transcription start site. (B) Sequence alignment of the indicated SBS in the indicated species.

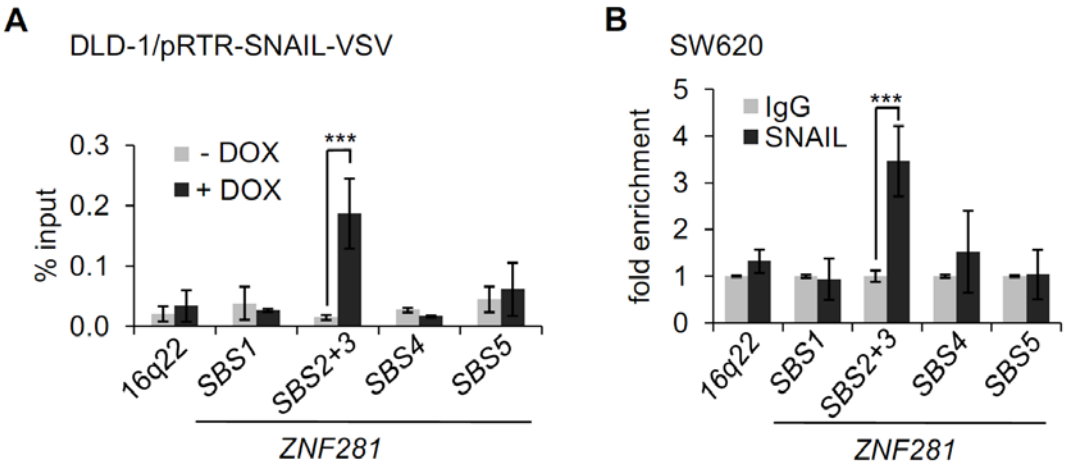

Figure 8: SNAIL occupation at the *ZNF281* promoter. Analysis of SNAIL binding to the *ZNF281* promoter at the predicted SNAIL binding motifs. (A) ChIP analysis of DLD-1/pRTR-SNAIL-VSV cells 24 hours after addition of DOX or left untreated using anti-VSV and anti-rabbit-IgG antibodies for ChIP. Results are given as the mean +/- SD (n=3). (B) ChIP assay in SW620 cells using an antibody against endogenous SNAIL. Results represent the mean +/- SD (n=3) of biological triplicates. Fold enrichment was calculated using the $2^{-\Delta\Delta cp}$ formula with the isotype control IgG set to one. Detection of SNAIL binding to *16q22* served as negative control. A Student's t-test was used with: ***: p<0.001.
DLD-1/pRTR-SNAIL-VSV cells were generated by Helge Siemens. The ChIP assays were performed by Rene Jackstadt and the resulting material was used for the qChIP measurement in (A) and (B).

Furthermore, ectopic SNAIL enhanced the expression of ZNF281 at the protein and at the mRNA level in DLD-1 cells (Figure 9A and B). SNAIL also induced ZNF281 expression in SKBR3 breast cancer and MiaPaCa2 pancreatic cancer cells (Figure 9C). Therefore, the induction of ZNF281 by SNAIL is not restricted to a specific cell type. In order to determine whether *ZNF281* is induced by SNAIL via the SBS motifs, a region encompassing 2 kbp upstream of the *ZNF281* transcriptional start site was subjected to a dual reporter assay (Figure 10). Indeed, the wild-type reporter was induced by SNAIL, whereas binding site mutation of SBS2 abolished and SBS3 mutation decreased the responsiveness to SNAIL. Also a reporter with combined mutation of SBS2 and SBS3 resulted in complete loss of responsiveness to SNAIL. A *CDH-1* reporter was repressed by SNAIL in an SBS-dependent manner in this assay.

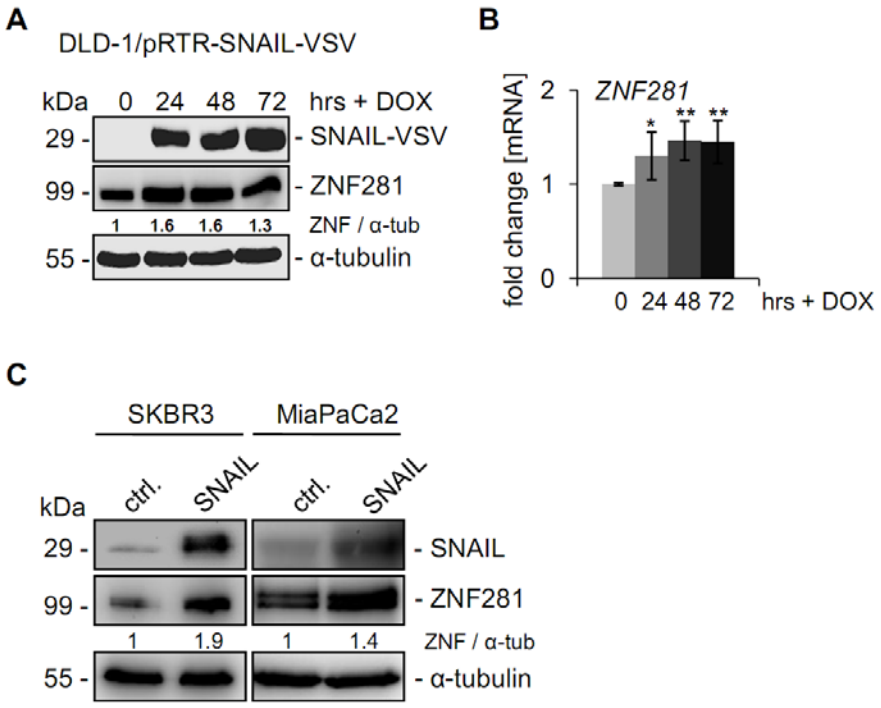

Figure 9: Ectopic SNAIL regulates ZNF281 expression. (A) DLD-1/pRTR-SNAIL-VSV cells treated with DOX for the indicated periods or left untreated were subjected to Western blot analysis of the indicated proteins at the indicated time-points. (B) qPCR analysis of *ZNF281* mRNA levels using the cells described in (A) with values representing the mean +/- SD (n=3). A Student's t-test was used. *: $p<0.05$ and **: $p<0.01$. (C) The breast cancer cell line SKBR3 and the pancreatic cancer cell line MiaPaCa2 were transduced with pBabe-SNAIL-VSV (SNAIL) or the respective control vector (ctrl.). SNAIL and ZNF281 proteins were detected by Western blot analysis. In (C) the transduction with pBabe vectors and the Western blot analysis were performed by Rene Jackstadt.
In the Western Blot analyses α-tubulin served as loading control. Relative densitometric quantifications are indicated; ZNF = ZNF281, α-tub = α-tubulin.

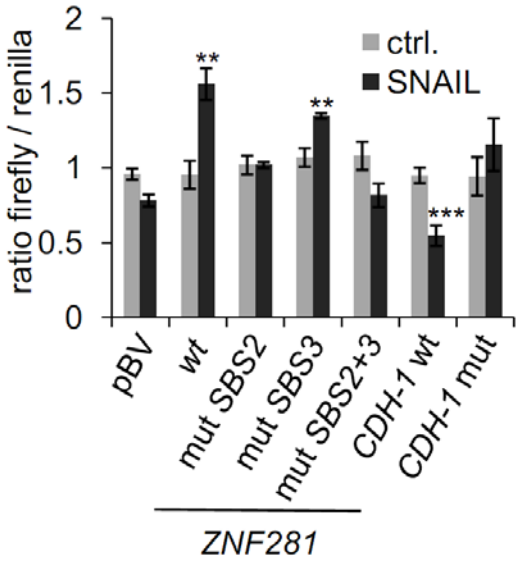

Figure 10: SNAIL regulates *ZNF281* expression directly via SBS2 and SBS3. Luciferase assay in DLD-1 cells 48 hours after transfection of pCDN3-VSV (ctrl.) or pCDNA3-SNAIL-VSV (SNAIL) vectors and the indicated pBV-*ZNF281* promoter constructs (ZNF281) or the respective pXP2-*E-cadherin/CDH-1* vectors as system controls (wt: wild-type, mut: mutated). A Student's t-test was used with: **: $p<0.01$ and ***: $p<0.001$.

ZNF281 displayed higher expression levels in CRC cell lines with mesenchymal features such as Colo320, SW480 and SW620, than in CRC cells with an epithelial phenotype such as HT29, DLD-1 and HCT-15 (Figure 11). ZNF281 expression correlated positively with SNAIL and Vimentin and inversely with E-cadherin expression (Figure 11). Moreover, analysis of publicly available mRNA expression profiles obtained from seven colorectal cancer cell lines (COLO205, HCC2998, HCT116, HCT15, HT29, KM12, SW620) within the NCI-60 panel (Shoemaker, 2006) confirmed a significant correlation between *ZNF281* and the EMT markers *SNAIL, Vimentin* and *Fibronectin-1* (Table 2). Taken together, these results suggested that the induction of ZNF281 by SNAIL might be an important component of the EMT program induced by SNAIL. Indeed, when ZNF281 was down-regulated using two different siRNAs the induction of EMT by SNAIL was prevented in DLD-1 cells (Figure 12A and B). Also the loss of the scaffold protein E-cadherin from the outer membrane, which is typical for EMT, was prevented by simultaneous siRNA-mediated down-regulation of ZNF281. Therefore, ZNF281 is required for SNAIL-induced EMT.

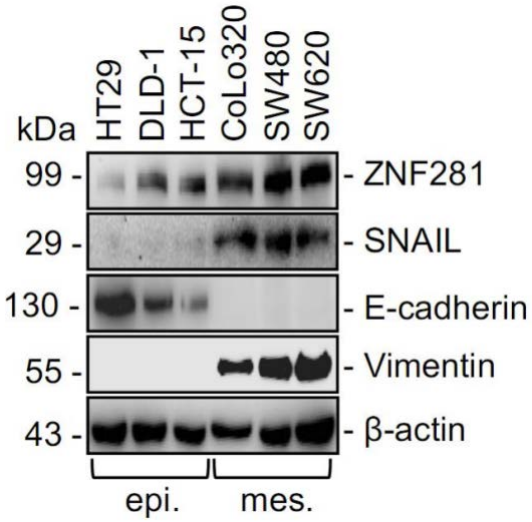

Figure 11: Expression comparison of various proteins in six different CRC cell lines. Western blot analysis of the indicated proteins in CRC cell lines. "epi." = cells with epithelial, "mes." = cells with mesenchymal phenotype. Detection of β-actin served as a loading control.

			SNAIL	*VIM*	*FN-1*	*ZNF281*
Spearman's-rho	*SNAIL*	correlation coefficient	1.000	.793*	.882**	.793*
		Sig. (2-tailed)		.033	.009	.033
		N	7	7	7	7
	VIM	correlation coefficient	.793*	1.000	.883**	.857*
		Sig. (2-tailed)	.033		.008	.014
		N	7	7	7	7
	FN-1	correlation coefficient	.882**	.883**	1.000	.775*
		Sig. (2-tailed)	.009	.008		.041
		N	7	7	7	7
	ZNF281	correlation coefficient	.793*	.857*	.775*	1.000
		Sig. (2-tailed)	.033	.014	.041	
		N	7	7	7	7

Table 2: Correlation analyses of the mRNA expression of *ZNF281* and selected target genes in seven CRC cell lines of the NCI-60 panel. Expression data obtained from the NCI-60 database representing seven different colorectal cancer cell lines were subjected to correlation analyses. The table displays the correlation between *ZNF281, SNAIL*, *Vimentin* (*VIM*) and *Fibronectin-1* (*FN-1*) mRNA expression. The significance of the calculated correlations was determined by a 2-tailed t-test and is indicated as: * = significant at 0.05 level; ** = significant at 0.01 level.

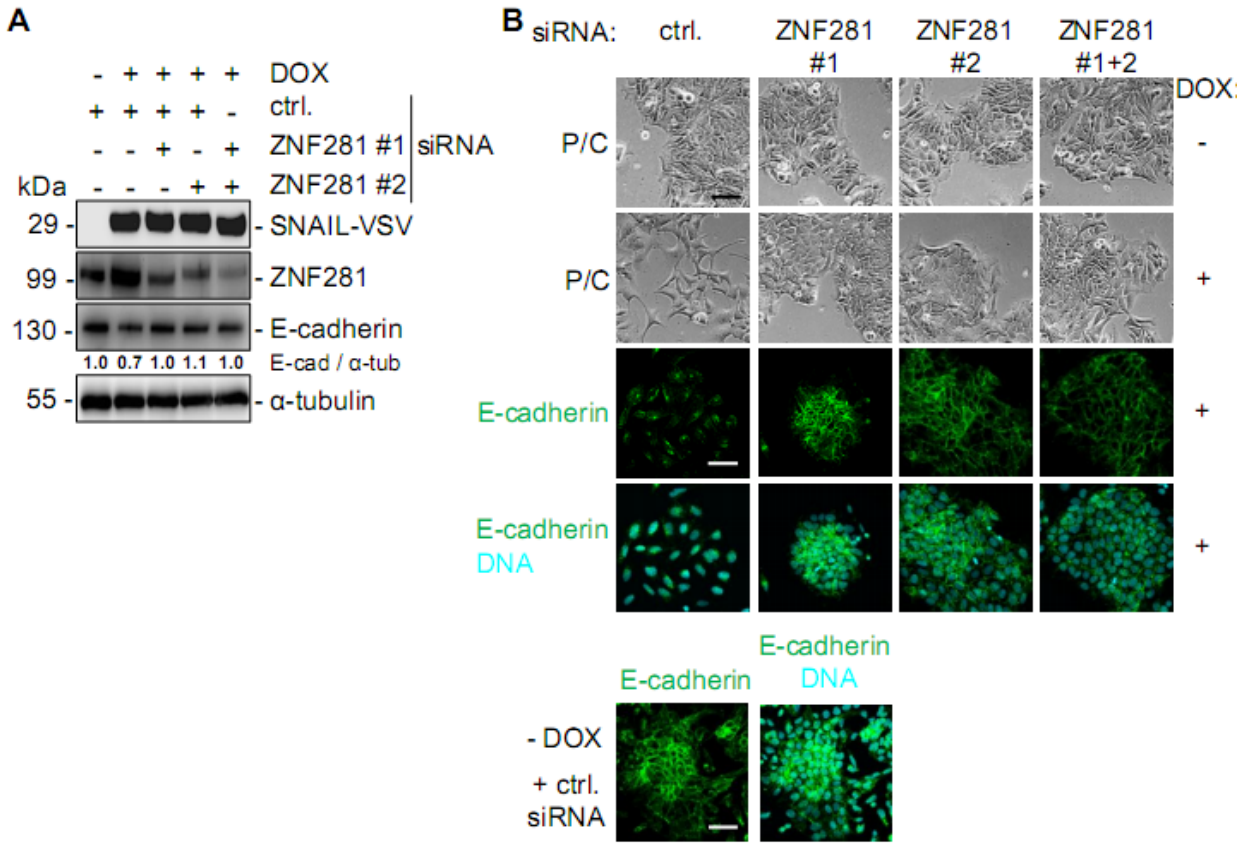

Figure 12: Requirement of ZNF281 for SNAIL-induced EMT. DLD-1/pRTR-SNAIL-VSV cells were treated with DOX (+) or left untreated (-) for 96 hours and simultaneously transfected with the indicated siRNAs. (A) The indicated proteins were detected by Western blot analysis. Detection of α-tubulin served as a loading control. Relative densitometric quantifications are indicated. E-cad = E-cadherin; α-tub = α-tubulin. (B) Two upper panels: Representative phase-contrast pictures (P/C) of the cells described in (A). 200 x magnification. Two lower panels: Detection of E-cadherin by indirect immunofluorescence and confocal microscopy. Nuclear DNA was visualized by DAPI staining. 200 x magnification. Scale bars represent 25 µm.

5.1.2 miR-34a directly regulates ZNF281 expression

The differences between the increase in ZNF281 protein levels and the minor regulation of mRNA levels after ectopic SNAIL expression suggested the possibility of an additional translational regulation mediated by miRNAs. Inspection of the *ZNF281* 3´-UTR using TargetSCAN and Miranda algorithms (Grimson et al, 2007; John et al, 2004) has revealed a conserved miR-34 seed-matching sequence (Figure 13).

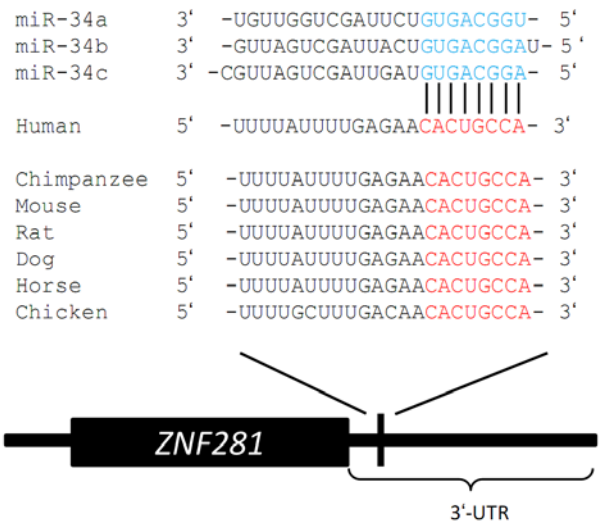

Figure 13: Putative miR-34 binding sites in the *ZNF281* 3'UTR. Schematic depiction of the miR-34 seeds (blue) and seed-matching sequences (red) in the 3´-UTR of the *ZNF281* mRNA and phylogenetic conservation among species (modified from www.targetscan.org). The position of the miR-34 seed-matching sequence in the *ZNF281* 3'-UTR is depicted as a black vertical bar.

Since it has previously been shown that the *miR-34a* and *miR-34b/c* genes are directly repressed by SNAIL (Siemens et al, 2011), it was hypothesized that at least part of the increase in ZNF281 expression observed after SNAIL induction might be due to a repression of *miR-34* genes. Indeed, ectopic *miR-34a* expression resulted in the down-regulation of endogenous ZNF281 expression on the protein and mRNA level in SW480 CRC cells (Figure 14A and B). This was also observed in MiaPaCa2 pancreatic cancer cells (Figure 14C and D). Therefore, the regulation of ZNF281 by miR-34a is not restricted to CRC cells. Furthermore, reporter constructs containing the entire 3´-UTR of *ZNF281* (720 bp) or a 77 bp fragment including the seed-matching sequence were repressed by co-transfection of pre-miR-34a, but not when the seed-matching sequence was mutated, demonstrating that it mediates repression by miR-34a (Figure 15A and B). The induction of ZNF281 by SNAIL was prevented by concomitant transfection of pre-miR-34a (Figure 16). Therefore, the previously documented repression of the *miR-34a* gene by SNAIL (Siemens et al, 2011) is presumably necessary for the SNAIL-mediated increase in ZNF281 expression. In summary, these results demonstrate that *ZNF281* is directly regulated by *miR-34a* and that SNAIL induces ZNF281, at least in part, by repressing *miR-34a*.

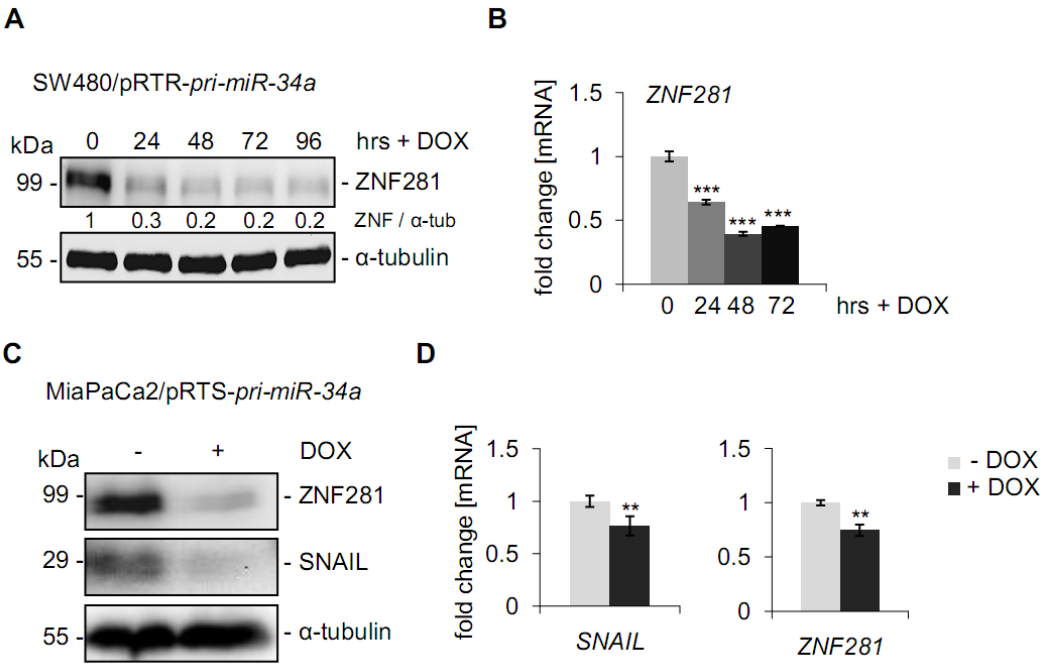

Figure 14: miR-34a represses ZNF281 expression. (A) Western blot analysis of endogenous ZNF281 protein levels in SW480 cells harboring a pRTR-*pri-miR-34a* vector after treatment with DOX for the indicated periods. Relative densitometric quantifications are indicated. ZNF = ZNF281; α-tub = α-tubulin. (B) Analysis of *ZNF281* mRNA levels in the cells corresponding to (A). Data represent the mean +/- SD (n=3). (C) MiaPaCa2 cells harboring a bicistronic pRTS-*pri-miR-34a* vector were treated with DOX for 72 hours or left untreated. The indicated proteins were detected by Western blot analysis. (D) qPCR analysis to determine the expression levels of the indicated mRNAs using the cells described in (C). Expression was normalized to GAPDH expression.
For the Western blot analyses α-tubulin served as a loading control. In (B) and (D) a Student's t-test was applied. **: p<0.01 and ***: p<0.001.
The cell lysates described in (A) and the respective cDNAs in (B) were provided by Helge Siemens. The cells used in (C) and (D) are described in (Lodygin et al, 2008).

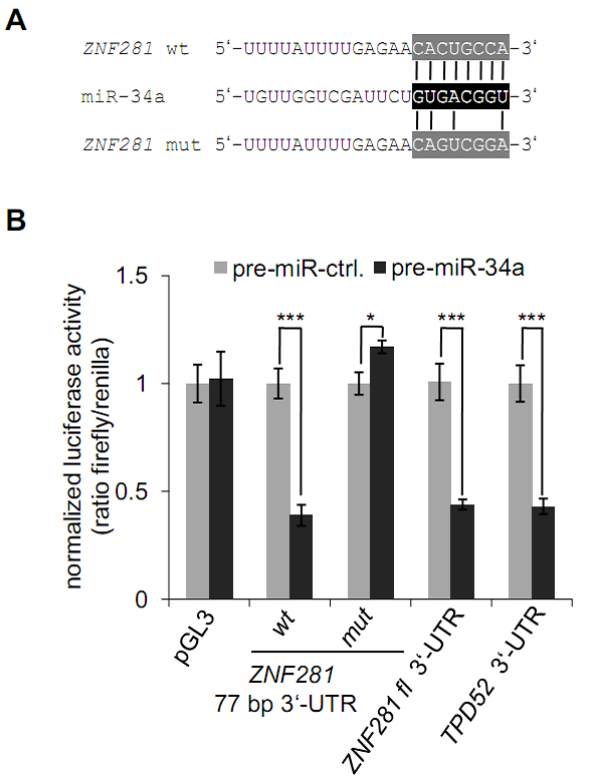

Figure 15: miR-34a represses the *ZNF281* reporter activity. (A) Mutagenesis of the *ZNF281* 3´-UTR. Black vertical bars indicate the remaining matches of the *miR-34a* seed (shaded black) with the *miR-34* seed-matching sequence (shaded gray) in the *ZNF281* 3´-UTR sequences (wt: wild-type, mut: mutated). (B) Dual luciferase reporter assay in SW480 cells 72 hours after transfection with pre-miR-34a or control oligonucleotides and the empty pGL3 vector or pGL3 harboring the indicated 3´-UTR-reporter constructs (fl: full-length). A 3´-UTR-reporter of the known *miR-34a* target *TPD52* served as a positive control. Data represent the mean +/- SD (n=3). A Student's t-test was used. *: p<0.05 and ***: p<0.001.

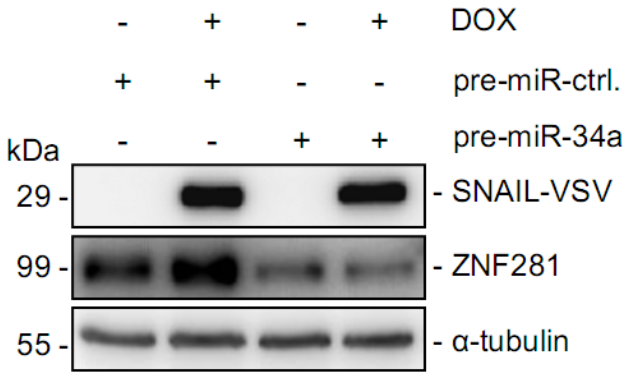

Figure 16: Transfection of pre-miR-34a oligonucleotides prevented the SNAIL-mediated induction of ZNF281. Western blot analysis of the indicated proteins in DLD-1 cells harboring a pRTR-SNAIL-VSV vector transfected with the indicated oligonucleotides for 60 hours and treated with DOX or left untreated for 36 hours prior to cell lysis. Detection of α-tubulin served as a loading control.

5.1.3 p53 represses ZNF281 via miR-34a

Since the *miR-34* genes represent direct p53 targets, it was of further interest whether p53 represses ZNF281 expression via inducing miR-34a. Indeed, ectopic expression of p53 resulted in a decrease of ZNF281 at the protein and mRNA level (Figure 17A and B). As expected, miR-34a/b/c levels were increased upon p53 activation (Figure 18A and B), which is likely to mediate the decrease in ZNF281 protein expression. Since miR-34b/c is expressed at least at 10 fold lower levels in CRC and CRC cell lines compared to miR-34a (Siemens et al, 2013; Toyota et al, 2008) further analyses were focused on miR-34a. The recovery of *ZNF281* mRNA expression by 72 hours of ectopic p53 expression (Figure 17B) is presumably due to the declining expression of ectopic p53 and therefore reduced pri-*miR-34* induction at this time-point (Figure 17A and Figure 18B). Nonetheless, ZNF281 protein was still down-regulated 72 hours after activation of p53 (Figure 17A). In order to determine whether down-regulation of ZNF281 is a result of reduced SNAIL expression caused by direct interaction of SNAIL with p53 (Lim et al, 2010) or due to p53-induced *miR-34*, direct interference with miR-34a function using antagomirs was performed. Indeed, *miR-34a*–specific antagomirs largely abolished the down-regulation of ZNF281 after p53 induction, whereas a control antagomir did not affect the repression of ZNF281 by p53 (Figure 19). The remaining minor repression of ZNF281 may be due to p53-induced *miR-34b* and *-c,* which are presumably not affected by the *miR-34a*-specific antagomir used here.

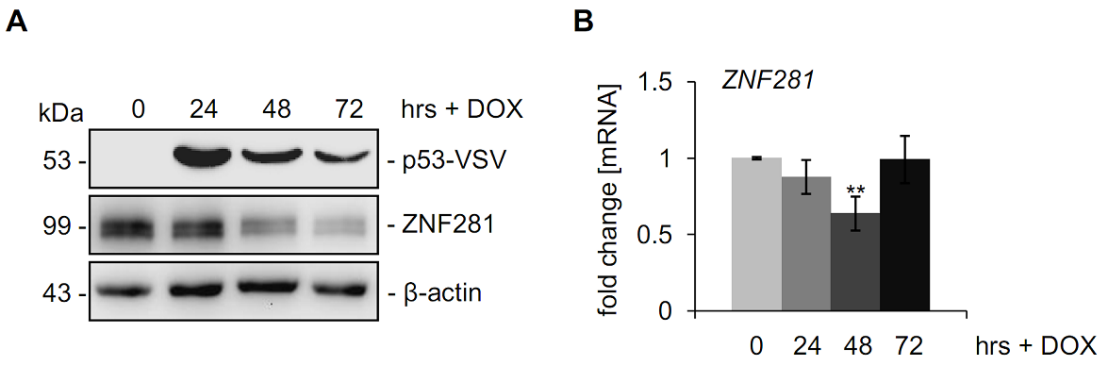

Figure 17: p53 represses ZNF281 mRNA and protein levels. SW480 cells harboring a pRTR-p53-VSV vector treated with DOX for the indicated periods or left untreated were used. (A) Western blot analysis of endogenous ZNF281 expression at the indicated time-points. (B) Ectopic p53 was expressed for the indicated periods before RNA was isolated and subjected to qPCR analysis. The values represent the mean +/- SD (n=3). Student's t-test was used. **: $p<0.01$. The SW480/pRTR-p53-VSV cells were generated by Sabine Hünten.

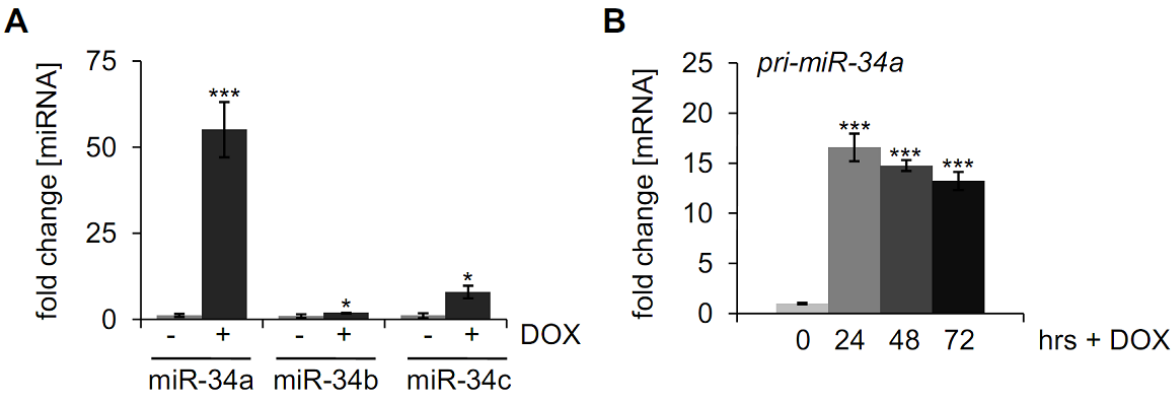

Figure 18: p53 induces miR-34. SW480/pRTR-p53-VSV vector treated with DOX for the indicated periods or left untreated were used. (A) Analysis of mature miR-34a/b/c expression levels 48 hours after addition of DOX to induce p53 or left untreated by qPCR. (B) qPCR analysis of *pri-miR-34a* mRNA levels at the indicated time-points. In (A) and (B) values represent the mean +/- SD (n=3) and a Student's t-test was used with: *: $p<0.05$ and ***: $p<0.001$.

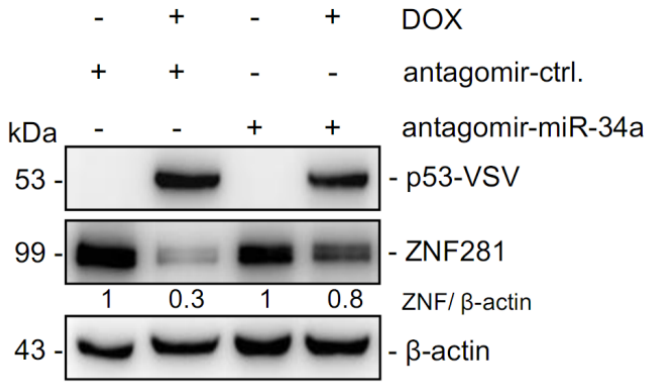

Figure 19: Transfection of a *miR-34a*-specific antagomir abolishes the p53-mediated repression of ZNF281. SW480 cells harboring a pRTR-p53-VSV vector were transfected with the respective oligonucleotides for 72 hours and treated with DOX for the last 48 hours before cell lysis or left untreated as indicated. The indicated proteins were detected by Western blot analysis. Detection of β-actin served as a loading control and was used for relative densitometric quantifications. ZNF = ZNF281.

Additionally, the expression of ZNF281 was analyzed in HCT116 *p53* +/+ cells and in the isogenic clone with homozygous deletion of p53 resembling p53 inactivation in tumors. HCT116 *p53* +/+ cells expressed lower endogenous levels of ZNF281 protein and mRNA than p53-deficient cells (Figure 20A and B). As previously described (Siemens et al, 2011), the expression of the SNAIL protein was elevated in the HCT116 *p53* -/- cells (Figure 20A). When *SNAIL* was down-regulated using a *SNAIL*-specific siRNA the expression of ZNF281 protein was only decreased to a minor extent in p53-deficient HCT116 cells (Figure 20C). Therefore, the increase in ZNF281 expression is

presumably mainly due to the decrease in miR-34a expression in p53-deficient cells (Figure 20B). Taken together, these results show that miR-34a represents an important mediator in the repression of ZNF281 by p53.

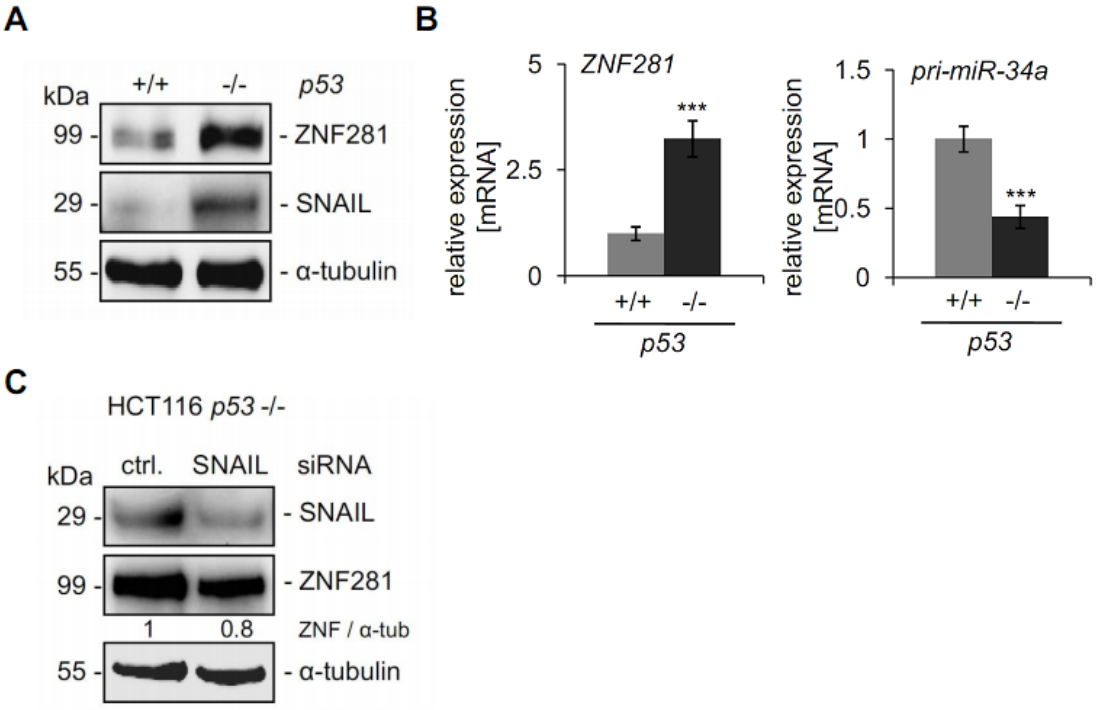

Figure 20: Regulation of ZNF281 and SNAIL in HCT116 *p53* +/+ and -/- cells. (A) Detection of the indicated proteins by Western blot analysis in HCT116 *p53* +/+ and *p53* -/- cells. (B) qPCR analysis of the *ZNF281* and *pri-miR-34a* mRNA expression in HCT116 *p53* +/+ and *p53* -/- cells. (C) Western blot analysis of the indicated proteins in HCT116 *p53* -/- cells 96 hours after transfection of a *SNAIL*-specific siRNA.
In (A) and (C) detection of α-tubulin served as a loading control and was used for relative densitometric quantifications in (C). ZNF = ZNF281; α-tub = α-tubulin. In (B) values represent the mean +/- SD (n=3). A Student's t-test was used. ***: $p<0.001$.
The cDNAs used in (B) were provided by Sabine Hünten.

5.1.4 ZNF281 induces EMT, migration and invasion

Since ZNF281 expression was induced by SNAIL and required for SNAIL-induced EMT, it was determined whether ectopic expression of ZNF281 is sufficient to promote EMT. For this purpose a pool of DLD-1 cells harboring an episomal pRTR construct that allows the DOX-inducible expression of ZNF281 was generated. After addition of DOX more than 90% of the cells were positive for eGFP (Figure 21A), which is expressed from a bidirectional promoter also driving the expression of ZNF281 (Figure 21B-C). After induction of ectopic ZNF281 expression DLD-1 cells changed from an epithelial

morphology (dense islands of cobblestone-shaped cells) to a mesenchymal morphology with spindle-shaped cells forming protrusions and displaying a scattered growth pattern (Figure 21D). This was reminiscent of the effect of ectopic SNAIL expression observed in DLD-1 cells before (Siemens et al, 2011). Also molecular markers of EMT were regulated by the expression of ZNF281 (Figure 22). The distinct membrane-bound expression of E-cadherin in DLD-1 cells was lost upon ZNF281 activation (Figure 22 upper panel). Furthermore, ZNF281-expressing cells displayed an increased cytoplasmic expression of the mesenchymal marker Vimentin (Figure 22 middle panel). In addition, F-actin, which forms stress fibers (Moreno-Bueno et al, 2009), was relocated from the membrane to the cytoplasm (Figure 22 lower panel).

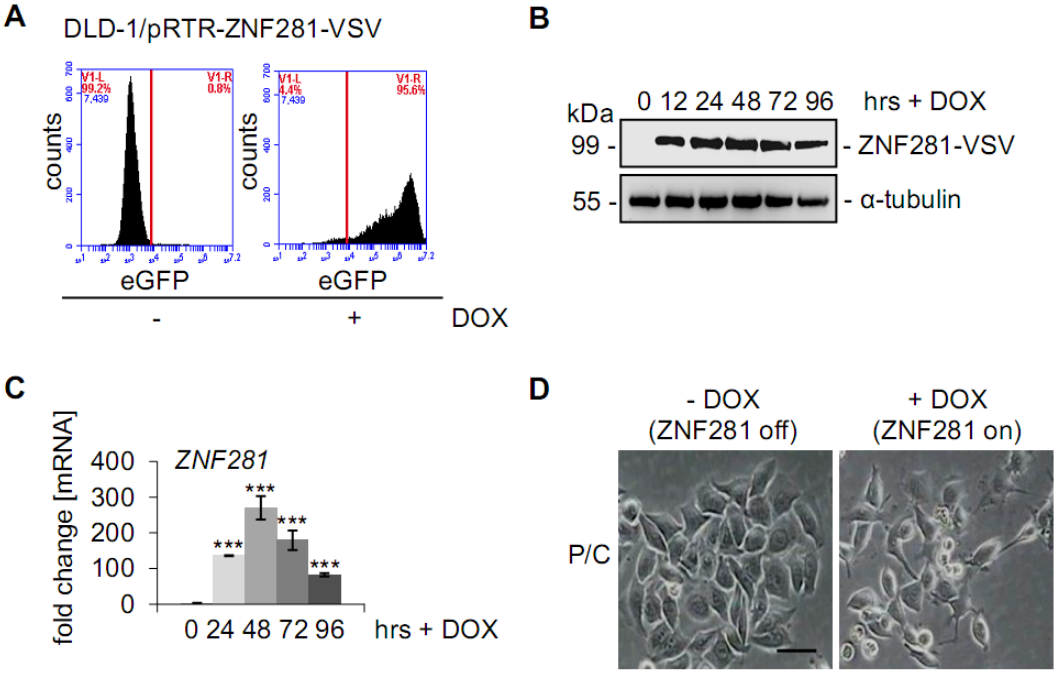

Figure 21: Ectopic expression of ZNF281 in DLD-1 cells results in morphological changes. DLD-1 cells, which harbor a bicistronic pRTR-vector expressing eGFP and ZNF281-VSV were treated with DOX for the indicated periods or left untreated. (A) Flow cytometric determination of the frequency of cells with inducible expression of eGFP in DLD-1 cell pools 48 hours after addition of DOX. (B) Detection of the indicated proteins by Western blot analysis at the respective time-points using the cells described in (A). Detection of α-tubulin served as a loading control. (C) *ZNF281* mRNA levels were determined by qPCR analysis using the indicated cells and time-points. Error bars represent +/- SD (n=3). A Student's t-test was applied with ***: $p<0.001$. (D) Representative phase-contrast (P/C) pictures of the cells treated with DOX or left untreated for 96 hours. 200 x magnification. The scale bar represents 25 µm.

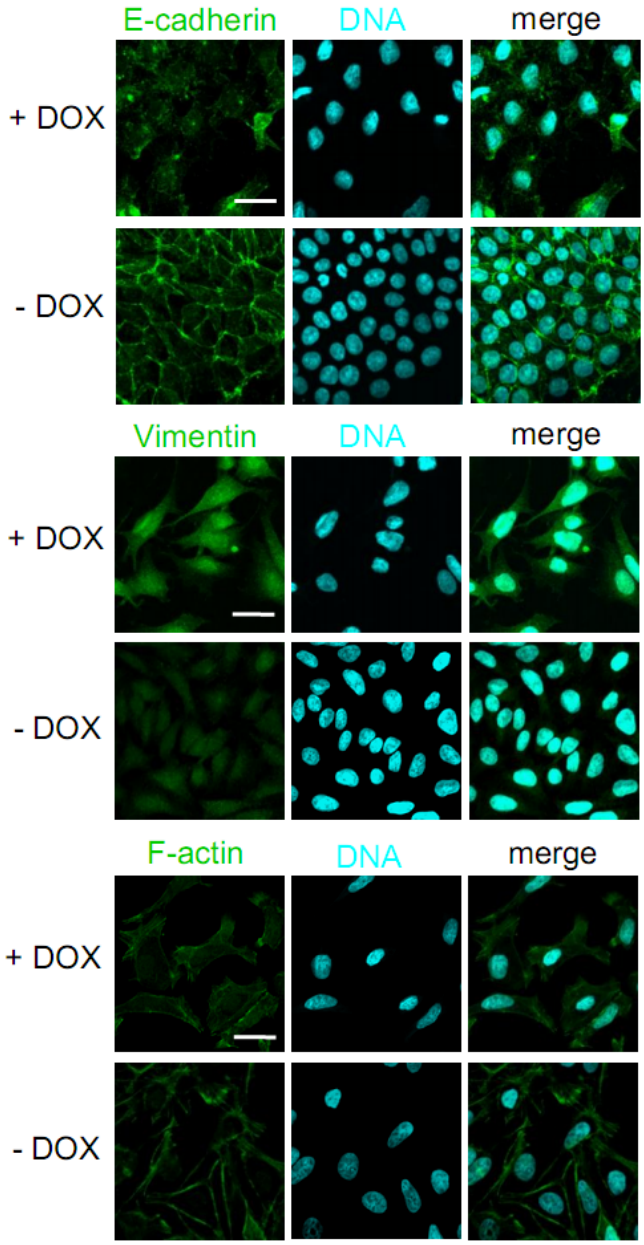

Figure 22: Regulation of epithelial and mesenchymal markers by ZNF281. DLD-1 cells harboring a pRTR-ZNF281-VSV vector treated with DOX for 96 hours or left untreated were analyzed. Confocal laser-scanning microscopy of E-cadherin, Vimentin and F-actin proteins detected by indirect immunofluorescence. Nuclear DNA was visualized by DAPI staining. 200 x magnification. The scale bars represent 25 µm.

Subsequently, it was determined whether ectopic ZNF281 expression influences cellular migration and invasion, since EMT previously has been linked to increased migration and invasion (reviewed in (Christiansen & Rajasekaran, 2006)). In a wound-healing assay ectopic ZNF281 expression resulted in a minor, but reproducible increase in the closure of a scratch in a confluent layer of DLD-1 cells (Figure 23A) compared to the controls (Figure 23A and Figure 24D). When migration and invasion were examined

in Boyden-chamber assays the effect of ectopic ZNF281 expression was more pronounced (Figure 23B and C). Furthermore, ectopic expression of ZNF281 significantly enhanced the ability of DLD-1 cells to form colonies in soft agar (Figure 23D).

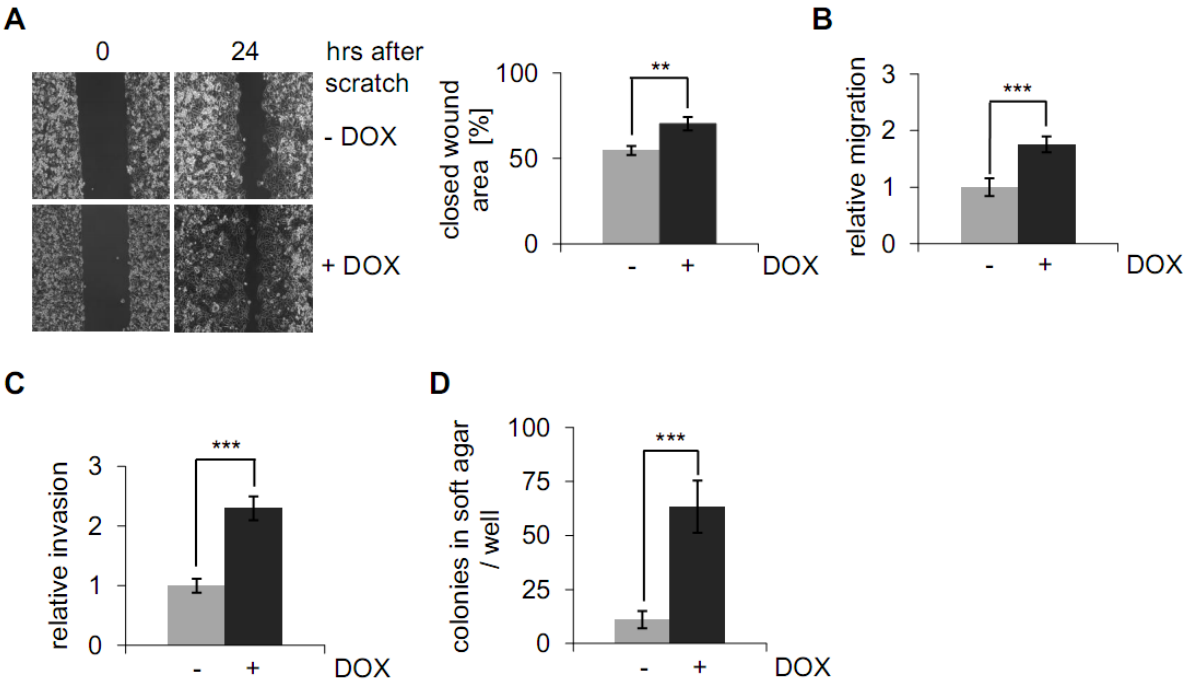

Figure 23: Ectopic expression of ZNF281 influences cellular migration and invasion of DLD-1 cells. DLD-1 cells harboring a pRTR-ZNF281-VSV vector were used for the experiments. (A) Cells were treated with DOX or left untreated for 48 hours before the scratch was applied. Left panel: representative pictures of the wound areas at the indicated time-points after scratching. 100 x magnification. Right panel: results represent the average (%) of wound closure determined by the final width of the scratch in three independent wells. Error bars represent +/- SD (n=3). Boyden-chamber assays of cellular migration (B) or invasion (C). The cells were cultivated in the presence or absence of DOX for 72 hours with serum starvation for the last 48 hours. To analyze invasion, membranes were coated with Matrigel. After 48 hours cells were fixed and stained with DAPI. The average number of cells per well was counted in three different inserts. Relative invasion or migration is expressed as the value of treated cells to control cells with controls set as one. (D) The respective cells were subjected to a soft-agar assay and treated with DOX or left untreated. Two weeks after seeding the resulting colonies were stained with crystal violet. Results represent the mean number of colonies in soft agar per well +/- SD (n=3).
(A-D) A Student's t-test was used. **: $p<0.01$ and ***: $p<0.001$.

The addition of DOX to DLD-1 cells harboring an empty vector control did not result in EMT-related morphological changes or significant effects in the above mentioned assays (Figure 24A-D). The effects of ectopic ZNF281 were not due to increased proliferation, since *ZNF281* activation had a slight anti-proliferative effect (Figure 25), which has also been described before for other EMT-TFs such as SNAIL (Peinado et al, 2007). Taken together, these results show that ectopic expression of ZNF281 is sufficient to mediate EMT and to enhance migration, invasion and anchorage independent growth.

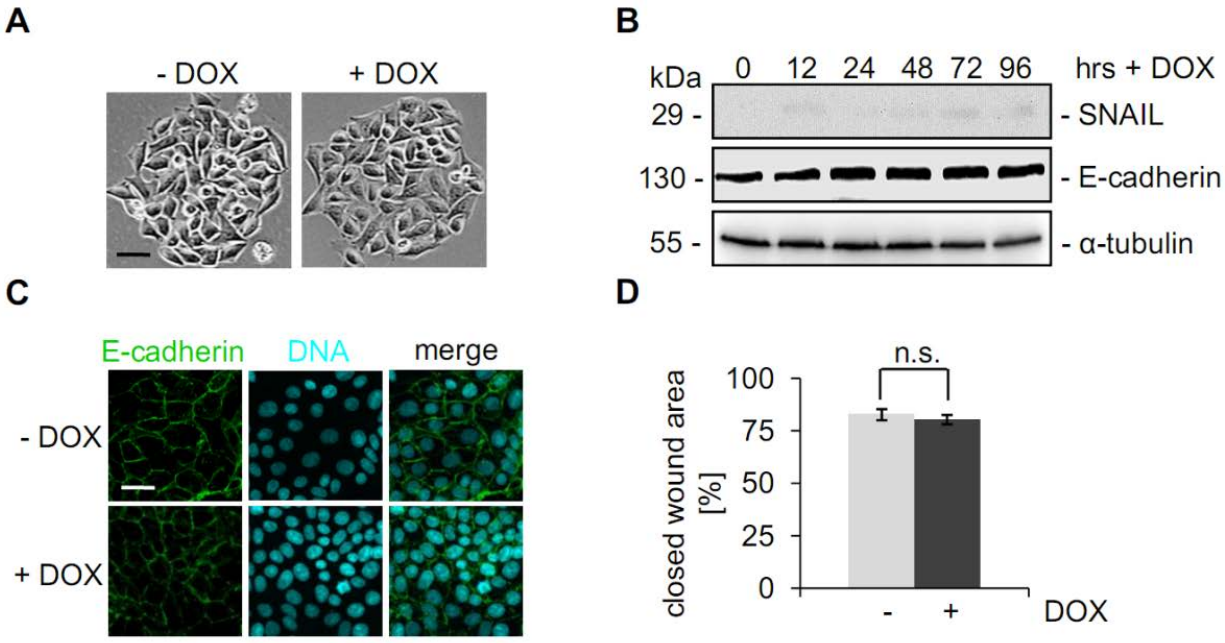

Figure 24: Expression of the vector control in DLD-1 cells does not result in morphological or migratory changes. DLD-1 cells harboring the empty vector control were used for the experiments. (A) Representative phase-contrast pictures of the cells 96 hours after treatment with DOX or left untreated. 200 x magnification. (B) Western blot analysis of the indicated proteins after addition of DOX for the indicated periods. Detection of α-tubulin served as a loading control. (C) Confocal microscopy of E-cadherin protein visualized by indirect immunofluorescence. Nuclear DNA was visualized by DAPI staining. 200 x magnification. (D) Analysis of cell migration using a wound healing assay. The cells were treated with DOX or left untreated 48 hours before a scratch was applied. Results represent the average percentage of closed wound area in three independent wells. The error bars represent +/- SD (n=3). A Student's t-test was applied with $p>0.05$ being considered non-significant (n.s.).
In (A) and (B) the scale bars represent 25 µm.

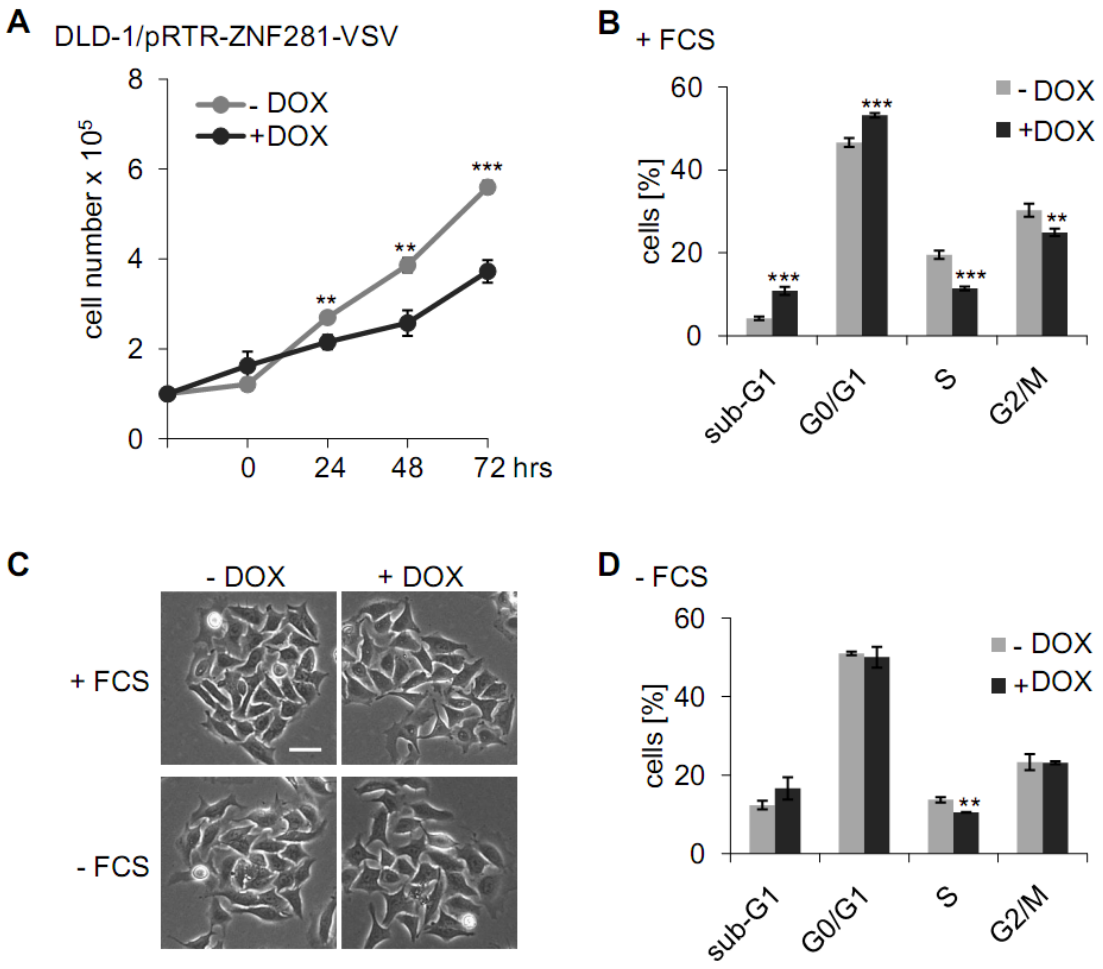

Figure 25: ZNF281 induction leads to a diminished proliferation capacity of the cells. Analyses of DLD-1/pRTR-ZNF281-VSV cells. (A) Cell numbers were determined after induction of ectopic ZNF281 expression by addition of DOX for the indicated periods. (B) Analysis of cell cycle distribution by flow cytometric determination of DNA content of cells treated with DOX for 48 hours or left untreated. (C) Phase-contrast pictures after DOX addition for 48 hours or left untreated. Cells were kept in normal medium supplemented with 10% FCS (+ FCS) or in medium supplemented with 0.1% FCS (- FCS). The scale bar represents 25 µm. (D) Cell cycle analysis by flow cytometry as in (B) after addition of DOX for 48 hours in medium with 0.1% serum.
In (A), (B) and (D) error bars represent +/- SD (n=3). A Student's t-test was applied. **: $p<0.01$ and ***: $p<0.001$.

5.1.5 Transcriptional regulation of EMT markers by ZNF281

Next, it was determined whether ZNF281 also induces changes in the expression of genes previously implicated in the transcriptional program of EMT. After activation of ectopic ZNF281 expression in DLD-1 cells an up-regulation of SNAIL was observed at the protein and mRNA level (Figure 26A-B). In addition, the mesenchymal markers *SLUG, ZEB-1* and *Fibronectin-1* were induced after ectopic ZNF281 expression in the DLD-1 CRC cells (Figure 26B). In line with the indirect immunofluorescence results as shown above in Figure 22 (upper panel) E-cadherin/*CDH-1* was repressed at the protein level after induction of ZNF281 (Figure 26A), whereas expression of *CDH-1* mRNA was not significantly affected by ZNF281 (Figure 27).

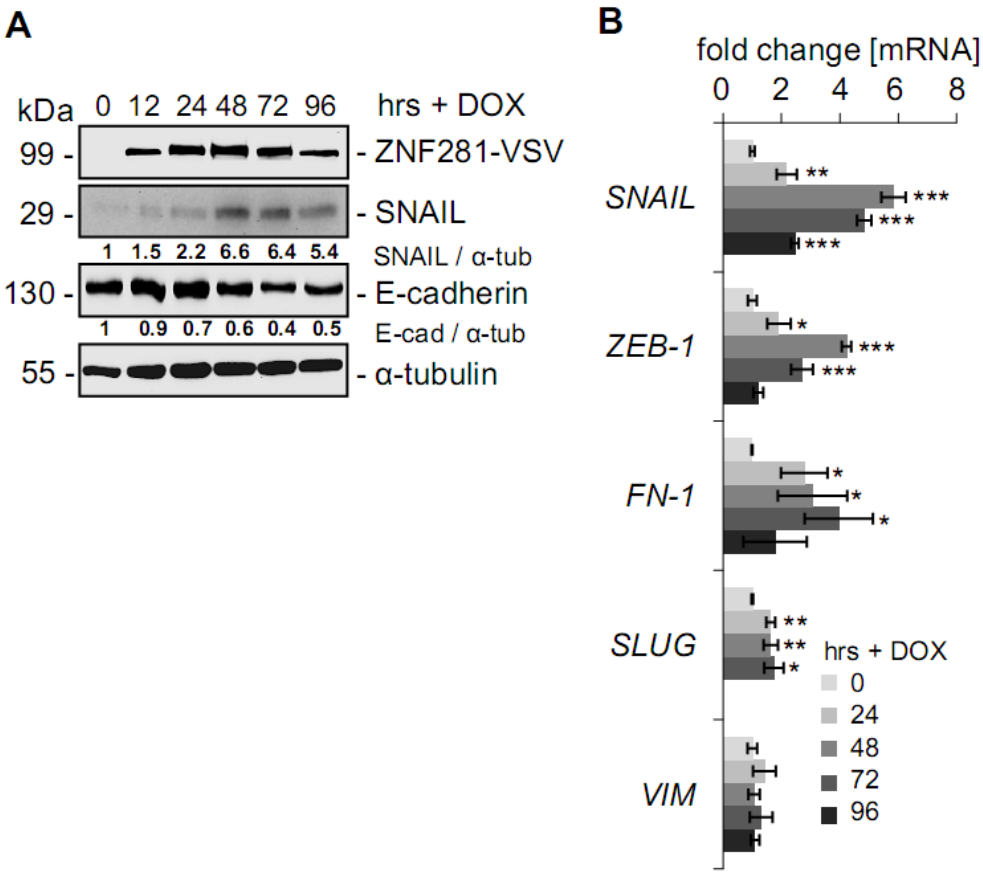

Figure 26: ZNF281 regulates genes implicated in the EMT process. DLD-1 cells harboring a pRTR-ZNF281-VSV vector treated with DOX or left untreated were analyzed. (A) Western blot detection of the indicated proteins after ectopic expression of ZNF281 for the indicated periods. Detection of α-tubulin served as a loading control and was used for relative densitometric quantifications. E-cad = E-cadherin, α-tub = α-tubulin. (B) Expression of the indicated mRNAs was determined by qPCR analyses. Results represent the mean +/- SD (n=3). A Student's t-test was used. *: $p<0.05$, **: $p<0.01$ and ***: $p<0.001$.

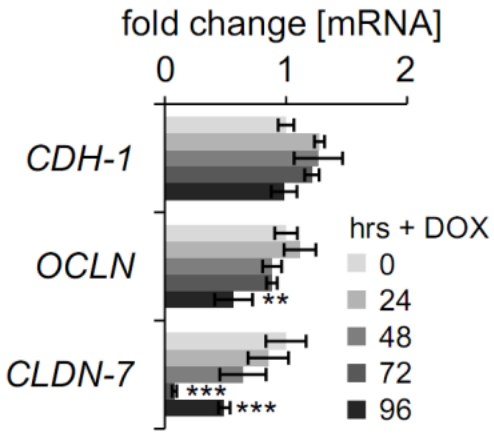

Figure 27: ZNF281 represses epithelial genes. DLD-1/pRTR-ZNF281-VSV cells treated with DOX for the indicated time-points or left untreated were analyzed. Expression of the indicated mRNAs was determined by qPCR analyses. Results represent the mean +/- SD (n=3). A Student's t-test was used. **: $p<0.01$ and ***: $p<0.001$.

However, when ZNF281 was expressed in HT29 CRC cells E-cadherin was repressed on both the protein and mRNA level (Figure 28A and C). Therefore, the regulation of EMT markers by ZNF281 is at least partially dependent on the cell line analyzed. Other epithelial markers such as *OCLN* and *CLDN-7* were repressed on the mRNA level in DLD-1 and HT29 cells (Figure 27 and Figure 28C), which is a characteristic of EMT (Ikenouchi et al, 2003; Martinez-Estrada et al, 2006), along with increased migratory and invasive capacities upon ectopic ZNF281 expression in HT29 cells (Figure 28D and E). Furthermore, ectopic ZNF281 expression resulted in the down-regulation of a number of additional epithelial marker genes, encoding components of tight junctions (*ZO-1*/*3*, *CLDN-1*), adherens junctions (*CDH-3*) as well as desmosomes (*PKP2*, *DSP*) (Figure 29), as previously shown for ZEB2 (Vandewalle et al, 2005). Since SNAIL is a potent inducer of EMT, we determined whether the up-regulation of SNAIL by ZNF281 is mediated by direct occupancy of the *SNAIL* promoter. ZNF281 is known to occupy GC-rich DNA sequences, as previously shown for the *ODC1* promoter (Law et al, 1999; Lisowsky et al, 1999). Similar GC-rich sequences are present in the *SNAIL* promoter (Figure 30A). When these regions were analyzed by a ZNF281-specific ChIP occupancy by ectopic and endogenous ZNF281 was detected in the vicinity of the *SNAIL* TSS (Figure 30B and C). The highest occupancy by ZNF281 protein was detected in a region encompassing the *SNAIL* TSS itself and ~600 bp upstream.

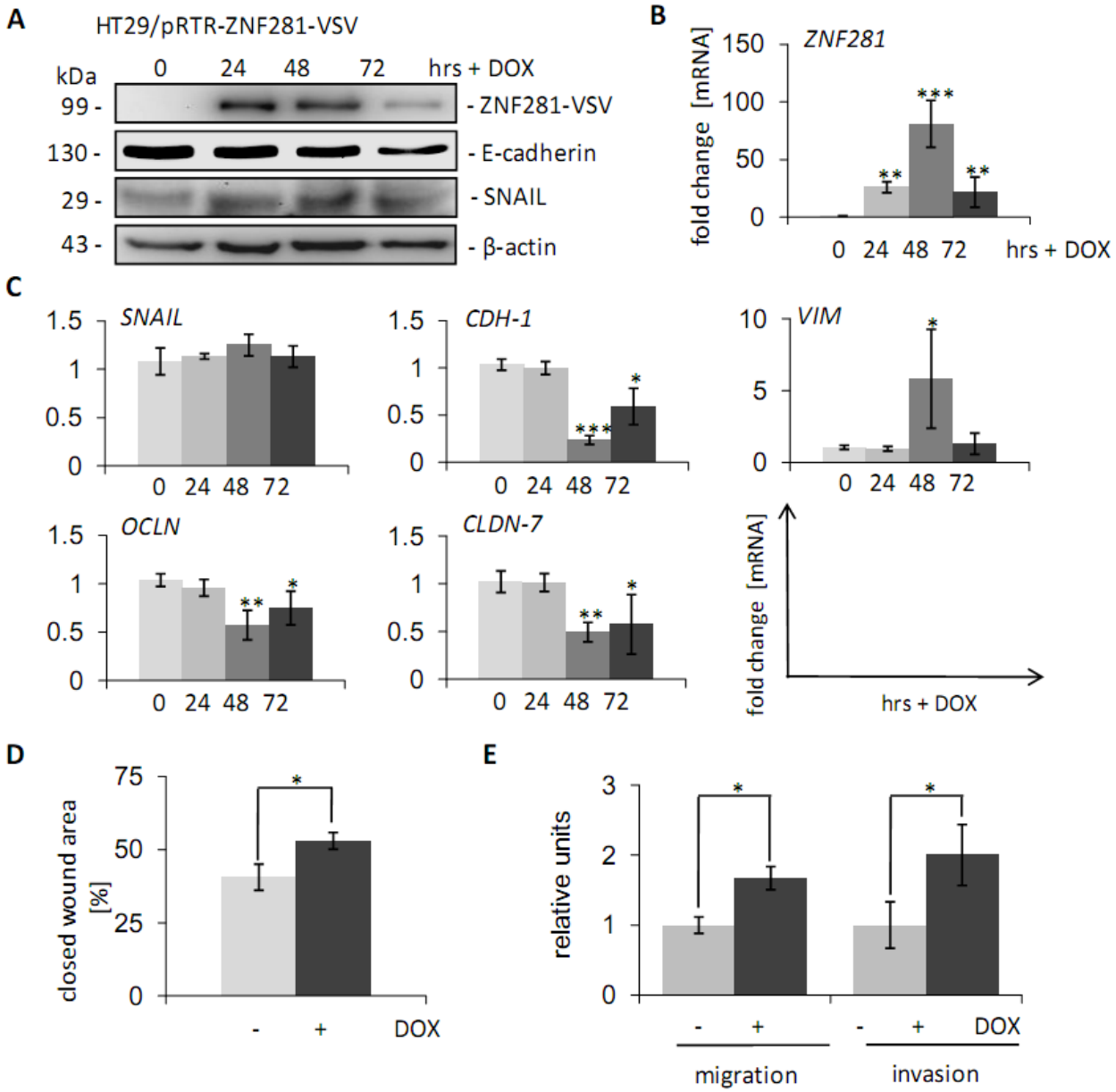

Figure 28: ZNF281 regulates epithelial and mesenchymal genes and influences motility in HT29 cells. HT29/pRTR-ZNF281-VSV cells were treated with DOX or left untreated for the indicated periods to activate ZNF281-VSV expression. (A) Western blot analysis of the indicated proteins. Detection of β-actin served as a loading control. (B) qPCR analysis of the *ZNF281* mRNA. The results represent the mean +/- SD (n=3). (C) qPCR analysis of the indicated mRNAs after ectopic expression of ZNF281 for the indicated periods. The results represent the mean +/- SD (n=3). (D) Cells were subjected to a wound healing assay. The cells were treated with DOX or left untreated for 72 hours before the scratch was applied. Wound healing was monitored at 0 and 48 hours. Results represent the mean percentage of the closed wound area in three independent wells +/- SD (n=3). (E) Boyden chamber-assays of cellular migration and invasion. Cells were cultivated in the presence or absence of DOX for 72 hours with serum starvation for the last 48 hours. For analysis of invasion the Boyden chambers were coated with Matrigel. After 48 hours cells were fixed and stained with DAPI. The average number of cells per well was counted in three different inserts. Relative migration and invasion is expressed as the ratio of treated cells to control cells with control set as one.
In (B-E) a Student's t-test was used. *: $p<0.05$, **: $p<0.01$ and ***: $p<0.001$.

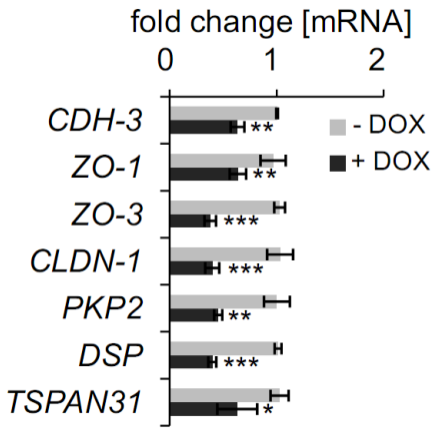

Figure 29: ZNF281 represses epithelial genes in DLD-1 cells. DLD-1 cells harboring a pRTR-ZNF281-VSV vector treated with DOX or left untreated were analyzed. Expression of the indicated mRNAs was determined by qPCR analyses. Results represent the mean +/- SD (n=3). A Student's t-test was used. *: p<0.05, **: p<0.01 and ***: p<0.001.

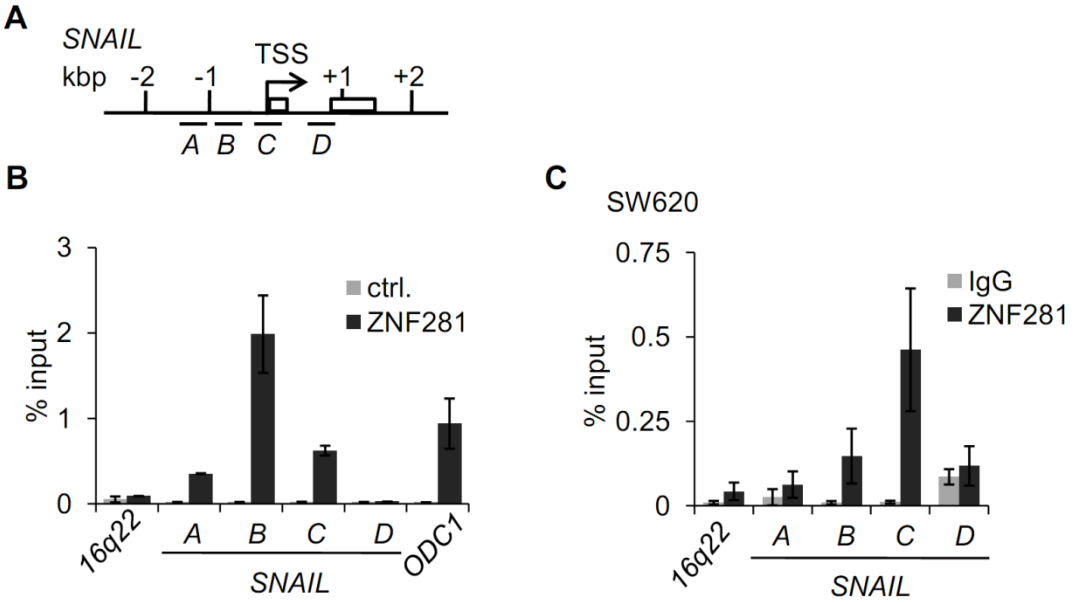

Figure 30: ZNF281 occupies the *SNAIL* promoter. (A) Schematic depiction of the *SNAIL* promoter. Amplicons (black bars) used for ChIP analysis, exons (black rectangles) and the TSS (transcription start site) are indicated. (B) ChIP assay of DLD-1/pRTR (ctrl.) or DLD-1/pRTR-ZNF281-VSV (ZNF281) cells 24 hours after addition of DOX using anti-VSV and anti-rabbit-IgG antibodies. The previously described ZNF281 occupancy at the *ODC1* promoter served as positive control. Results represent the percentage of input chromatin of induced versus control cells +/- SE (n=2). (C) ChIP assay in SW620 cells using an antibody against the endogenous ZNF281 protein (ZNF281) and the respective IgG control (IgG). Results represent the mean +/- SD (n=3).

A set of deletion constructs of the human *SNAIL* promoter (Barbera et al, 2004) was used to determine the regions mediating the regulation by ZNF281 in a reporter assay. The activation of the *SNAIL* promoter was most dominant for the -869/+59 bp reporter (Figure 31), which was in line with the dominant binding of ectopic ZNF281 to a region ~ 600 bp upstream of the TSS in the ChIP assay (Figure 30B). Unexpectedly, the longer -1558/+92 bp construct resulted in a weaker response to ZNF281, which may be due to repressive elements or binding sites for other transcription- or co-factors in the region between -869 and -1558 bp. Also the decreasing activity of further truncations indicates that the predominant region of ZNF281 binding is located between 514 bp and 869 bp upstream of the *SNAIL* TSS. Another, but less effective, binding region is presumably located closer to the TSS as also suggested by the ChIP results (Figure 30B and Figure 31). Occupancy by endogenous and ectopic ZNF281 was also detected in the promoter regions of *CDH-1*, *OCLN* and *CLDN-7* (Figure 32A and B).

When SNAIL was down-regulated by RNA interference in DLD-1 cells ectopically expressing ZNF281 morphological changes associated with EMT were not observed (Figure 33A and B). Moreover, E-cadherin persisted at the cell-membrane, whereas co-transfection of a control siRNA did not prevent its relocalization (Figure 33B). Therefore, ZNF281-induced EMT is mediated, at least in part, by SNAIL. In summary, these analyses show that ZNF281 directly regulates the expression of a subset of EMT regulators and effectors. The requirement of SNAIL for ZNF281-induced EMT suggests that at least some of these regulations are mediated and/or enhanced via the induction of SNAIL. Furthermore, ZNF281 directly induces SNAIL, which itself activates ZNF281 expression, thereby forming a positive feedback loop, which may enforce and stabilize the process of EMT.

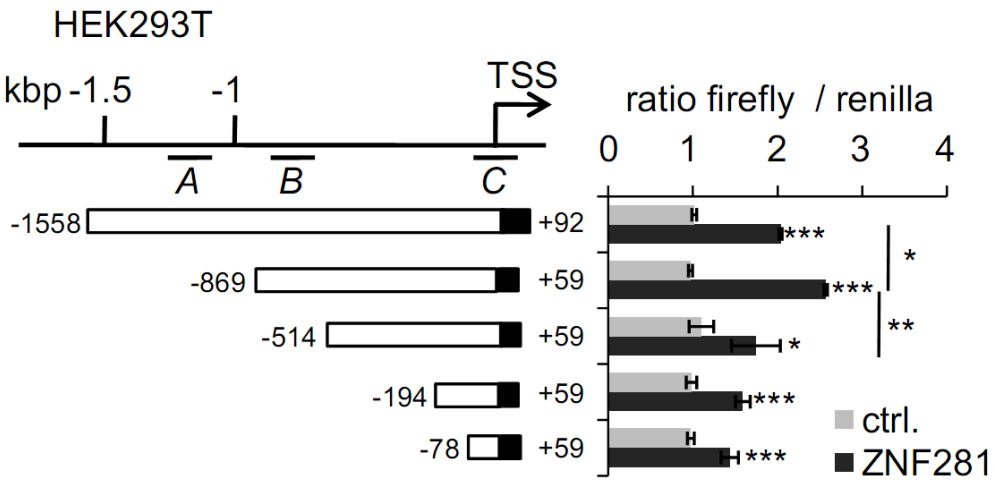

Figure 31: ZNF281 regulates the activity of *SNAIL* promoter reporters. The indicated pGL3-*SNAIL* promoter plasmids were co-transfected with pcDNA3-VSV (ctrl.) or pcDNA3-ZNF281-VSV (ZNF281) plasmids into HEK293T cells, which were subjected to a luciferase reporter assay after 48 hours. A Student's t-test was used. *: p<0.05, **: p<0.01 and ***: p<0.001.

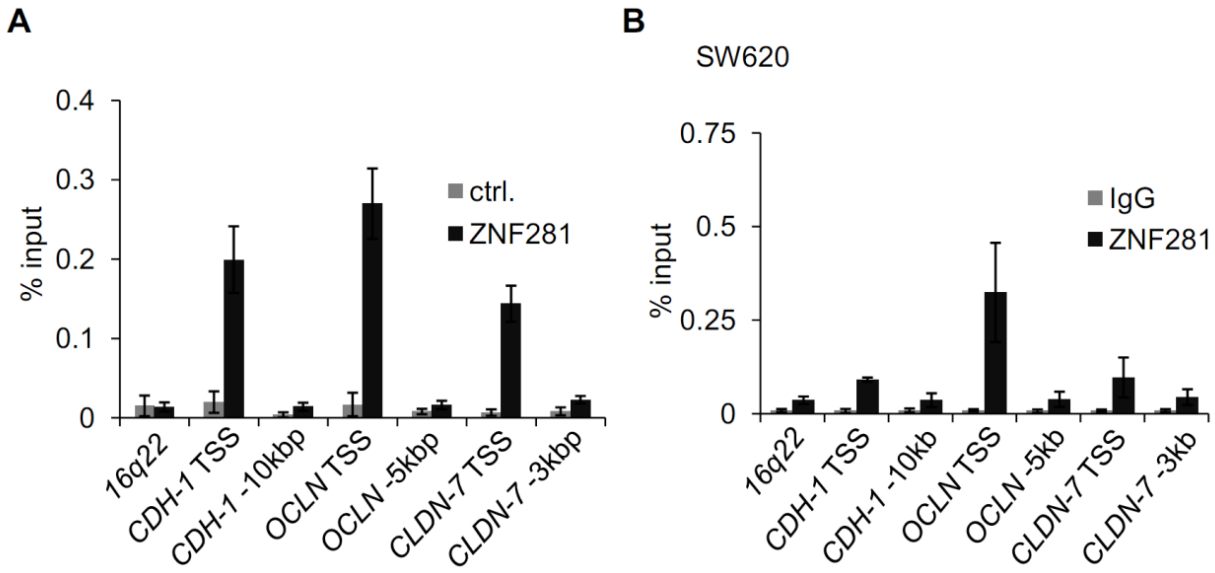

Figure 32: ZNF281 occupies promoters of epithelial genes. (A) ChIP assay of DLD-1/pRTR (ctrl.) or DLD-1/pRTR-ZNF281-VSV (ZNF281) cells 24 hours after addition of DOX using anti-VSV and anti-rabbit-IgG antibodies. (B) ChIP assay in SW620 cells using an antibody against the endogenous ZNF281 protein (ZNF281) and the respective IgG control (IgG). ZNF281 occupancy is shown at the indicated promoters or chromosomal region *16q22*, which served as negative control.
In (A) and (B) results represent the mean +/- SD (n=3).

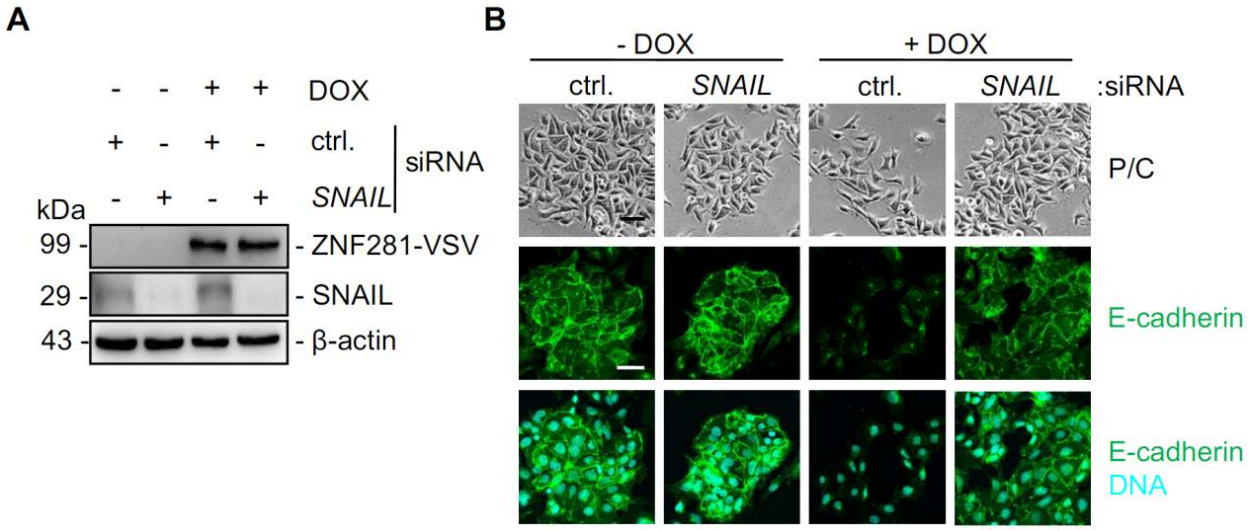

Figure 33: SNAIL mediates ZNF281-induced EMT. (A) DLD-1/pRTR-ZNF281-VSV cells were transfected with a *SNAIL*-specific siRNA or the respective control (ctrl.) for 96 hours and treated with DOX or left untreated for 72 hours. Analysis of the indicated proteins by Western blot. Detection of β-actin served as a loading control. (B) Representative phase-contrast (P/C) images of cells analyzed in (A). 200 x magnification. Lower two panels: Detection of E-cadherin by indirect immunofluorescence 96 hours after transfection of the indicated siRNAs and treatment of DOX or left untreated as in (A) using confocal laser-scanning microscopy. Nuclear DNA was visualized by DAPI staining. 200 x magnification. Scale bars represent 25 µm.

5.1.6 ZNF281 regulates β-catenin localization and activity as well as stemness

Interestingly, ectopic expression of ZNF281 in DLD-1 cells resulted in the translocation of β-catenin from the outer cell membrane to the nucleus (Figure 34), which is another characteristic of EMT (Brabletz et al, 2005b). Although, β-catenin mRNA and protein levels changed only slightly upon ZNF281 expression (Figure 35A and B), a significant increase in the transcriptional activity of β-catenin/TCF4 was observed after ZNF281 expression in DLD-1 and SW480 cells in a reporter assay (Figure 35C).

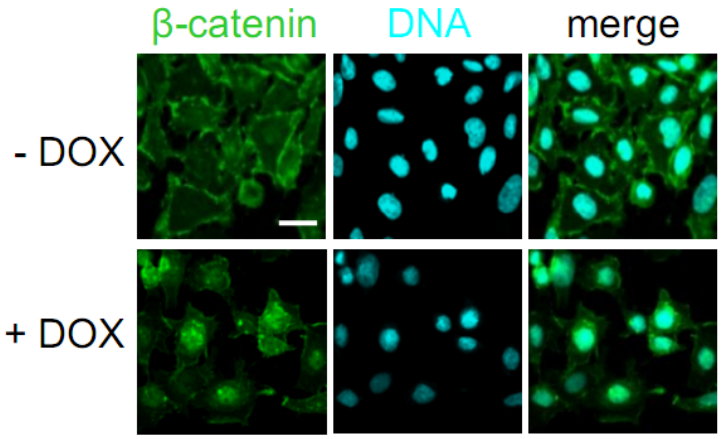

Figure 34: ZNF281 regulates β-catenin localization. DLD-1 cells harboring a pRTR-ZNF281-VSV vector were treated with DOX for 96 hours to activate ZNF281-VSV expression or left untreated. Detection of β-catenin by indirect immunofluorescence and confocal microscopy. Nuclear DNA was visualized by DAPI staining. 200 x magnification. The scale bar represents 25 µm.

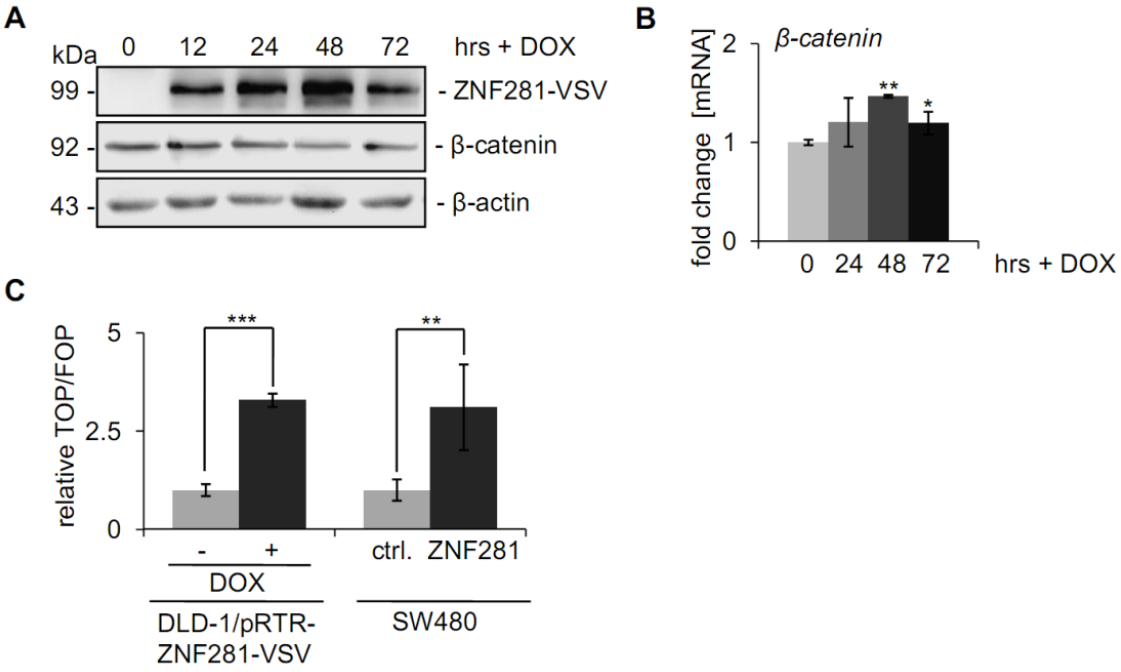

Figure 35: ZNF281 increases β-catenin activity. DLD-1/pRTR-ZNF281-VSV cells were treated with DOX for the indicated time-periods to activate ZNF281-VSV expression or left untreated. (A) Western blot analysis of the indicated proteins. Detection of β-actin served as a loading control. (B) qPCR analyses with results represented as mean values +/- SD (n=3) (C) Left: TOPflash reporter assay in the indicated cell line after addition of DOX for 48 hours and concomitant transfection with TOP/FOP vectors. Right: TOPflash reporter assay of SW480 cells transfected with TOP/FOP vectors and control vector (ctrl.) or pcDNA3-ZNF281-VSV vector (ZNF281; as indicated) for 48 hours. Results represent the mean +/- SD (n=3).
In (B) and (C) a Student's t-test was used. *: $p<0.05$, **: $p< 0.01$ and ***: $p<0.001$.

Axin2 negatively regulates the WNT/β-catenin/TCF4 signaling pathway by promoting phosphorylation and degradation of β-catenin/TCF4 via a multi-protein complex including APC and GSK3β (Lustig et al, 2002). Therefore, decreased levels of inhibitory Axin2 might result in the translocation of β-catenin to the nucleus. Indeed, *Axin2* mRNA was repressed upon ectopic expression of ZNF281 (Figure 36A). Furthermore, we detected increased binding of ZNF281 at the *Axin2* promoter, which harbors GC-rich regions representing potential binding sites for ZNF281 (Figure 36B and C). It is conceivable that a direct repression of *Axin2* by ZNF281 may contribute to the increased activity of β-catenin/TCF4. In addition, the loss of E-cadherin from the cell-membrane may contribute to the activation of β-catenin/TCF4 after ZNF281 activation. In line with the increase of β-catenin/TCF4 activity *LGR5* and *CD133,* which are known β-catenin target genes (Carmon et al, 2012; Fan et al, 2010; Glinka et al, 2011; Katoh & Katoh, 2007), were induced after ectopic expression of ZNF281 in DLD-1 cells (Figure 36A). qChIP analysis revealed ZNF281 occupancy at the *LGR5* promoter, but not at the *CD133* promoter (Figure 36B and C). Since *LGR5* and *CD133* represent markers for putative cancer stem cells (Barker et al, 2007; Munoz et al, 2012; Zhu et al, 2009) the activation of ZNF281 may be accompanied by the acquisition of stem cell traits. Indeed, ectopic ZNF281 expression significantly enhanced the formation of colono-spheres of non-adherent DLD-1 cells (Figure 37A and B). Taken together, ZNF281 enhances β-catenin activity and stemness of tumor cells. Both effects may contribute to metastases formation.

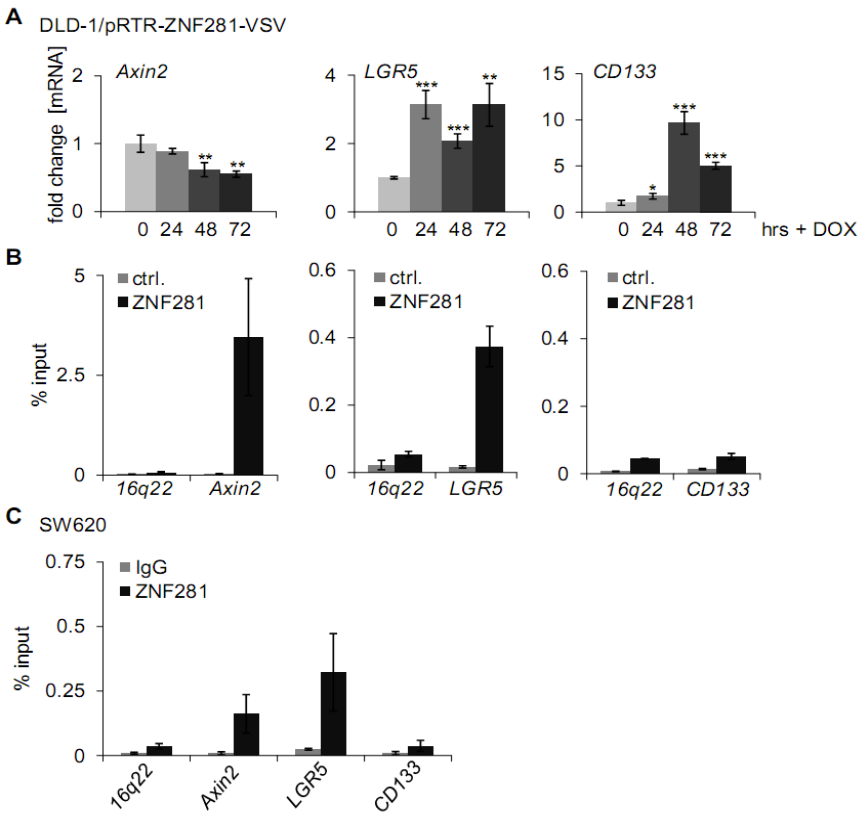

Figure 36: ZNF281 regulates β-catenin targets. (A) qPCR analyses of DLD-1 pRTR-ZNF281-VSV cells with results depicted as the mean +/- SD (n=3). A Student's t-test was used. *: p<0.05, **: p<0.01 and ***: p<0.001. (B) qChIP assay in DLD1/pRTR and DLD-1/pRTR-ZNF281-VSV cells 24 hours after addition of DOX using anti-VSV and anti-rabbit-IgG antibodies for ChIP. qChIP values are represented as percentage of input chromatin and qChIP amplicons are indicated. Error bars represent +/- SE (n=2). (C) ChIP assay in SW620 cells using an antibody against the endogenous ZNF281 protein. Results represent the mean +/- SD (n=3).
In (B) and (C) ZNF281 occupancy at the indicated promoters or chromosomal region *16q22*, which served as negative control, is shown.

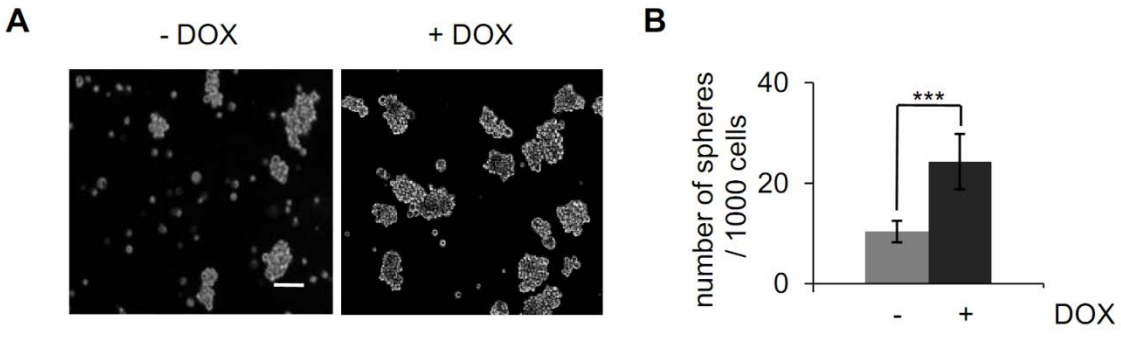

Figure 37: The ectopic expression of ZNF281 in DLD-1 cells increases the ability of the cells to form colono-spheres. DLD-1/pRTR-ZNF281-VSV cells were analyzed. (A) Representative phase-contrast images of spheres grown on low adherence plates seven days after addition of DOX. The scale bar represents 50 µm. (B) Quantification of the sphere number per 1000 cells. Results represent the mean +/- SD (n=3). A Student's t-test was used. ***: p<0.001.

5.1.7 Requirement of ZNF281 for EMT, migration and invasion

Next, it was thought to determine whether ZNF281 is not only sufficient for the induction of EMT, but also necessary for the maintenance of an EMT-like state in the CRC cell line SW480, which displays mesenchymal features such as low E-cadherin and high SNAIL expression (Figure 11) as well as enhanced migration, invasion and metastasis. In line with our previous findings SW480 cells displayed high levels of endogenous ZNF281 when compared to the more epithelial cell lines DLD-1 and HT29 (Figure 11). Therefore, we generated SW480 cell pools with DOX-inducible expression of a *ZNF281*-specific-miRNA or the respective control driven by an episomal pRTS vector. These cell pools showed ectopic expression of an inducible, co-expressed mRFP marker in ~90% of the cells after addition of DOX (Figure 38).

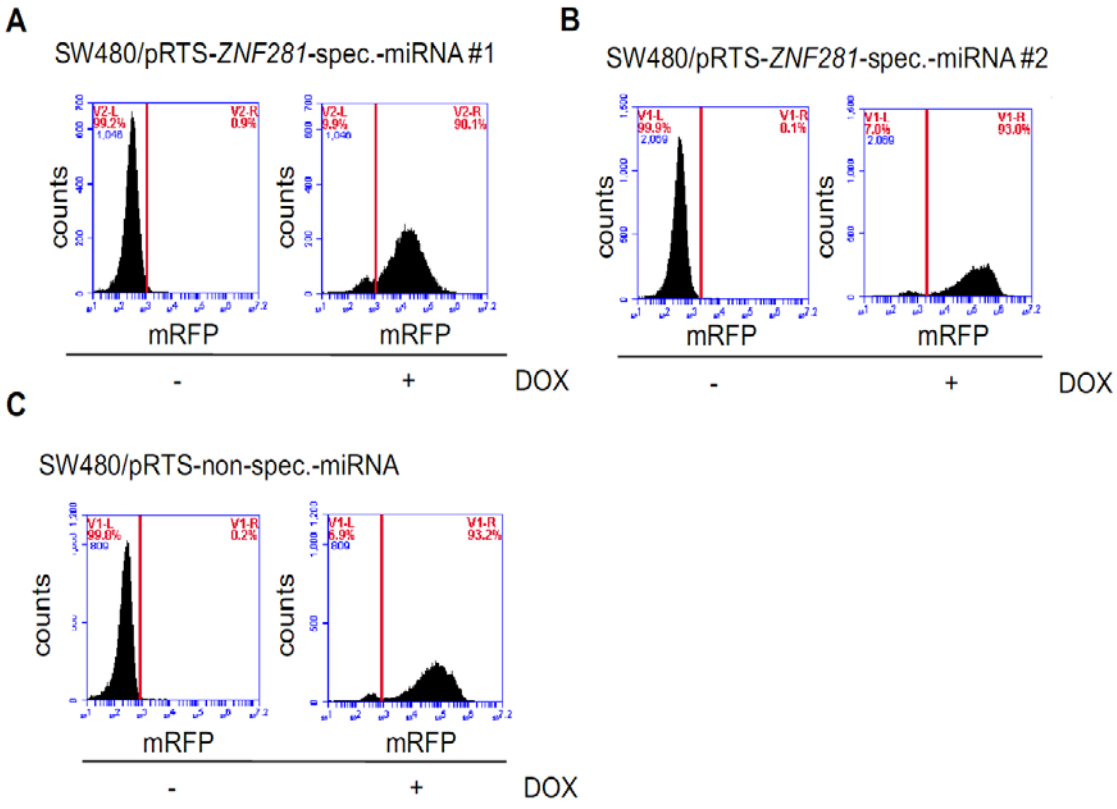

Figure 38: Determination of mRFP positivity of the cells used. Flow cytometric analysis of mRFP positivity 48 hours after addition of DOX. (A) and (B) SW480/pRTS-*ZNF281*-spec.-miRNA #1/2 cells were analyzed. (C) Flow cytometric analysis of SW480/pRTS-non-spec.-miRNA cells.

After induction of the *ZNF281*-specific miRNAs endogenous ZNF281 was repressed at the mRNA and protein level (Figure 39A and B). Simultaneously, mesenchymal markers such as SNAIL and Vimentin were repressed, whereas E-cadherin as epithelial marker was induced at the protein level (Figure 39B). Furthermore, SW480 cells lost their mesenchymal morphology upon ZNF281 knock-down and gained epithelial phenotypes with an increase in cell-cell contacts (Figure 40) and diminished expression of Vimentin (Figure 39B and Figure 40). Moreover, down-regulation of *ZNF281* in SW480 cells resulted in decreased migration in a scratch and a Boyden-chamber assay (Figure 41A and C and Figure 41B and D respectively) as well as diminished invasion in a Matrigel-transwell assay (Figure 41B and D). The down-regulation of *ZNF281* in SW480 cells had no significant effect on cell proliferation, cell cycle distribution and apoptosis (Figure 42). In addition, ZNF281 down-regulation resulted in a decrease in colony formation in soft agar (Figure 43A) and a reduction in sphere formation (Figure 43B). Similar effects were observed after expression of the other *ZNF281*-specific-miRNA (Figure 43C and D), whereas induction of a non-specific control miRNA did not result in significant effects in any of the assays described above (Figure 44A-D). Taken together, down-regulation of *ZNF281* induces MET in SW480 cells, which is associated with the loss of migratory and invasive capacities as well as reduced stemness. Therefore, expression of ZNF281 is not only sufficient for the induction of EMT, but presumably required to maintain a mesenchymal state in colorectal cancer cell lines. Furthermore, ZNF281 is not only sufficient to induce SNAIL, but also necessary for its continued expression.

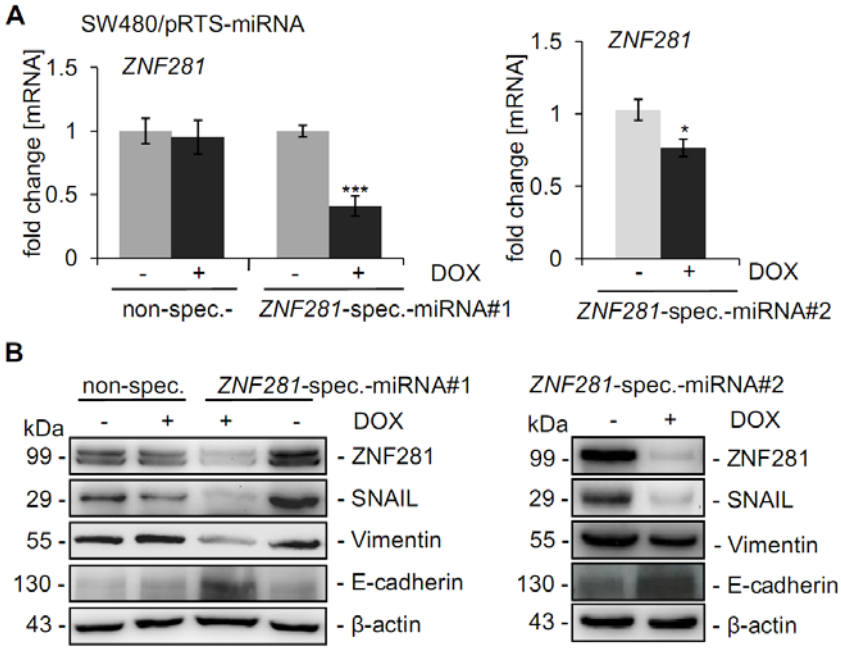

Figure 39: miRNA-mediated repression of *ZNF281*. SW480 cells harboring a pRTS vector encoding a miRNA directed against endogenous *ZNF281* (*ZNF281*-specific-miRNA (*ZNF281*-spec.-miRNA#1/2)) or pRTS non-specific control miRNA (non-spec.-miRNA) were analyzed. (A) qPCR analysis of the *ZNF281* mRNA expression 96 hours after addition of DOX. Results represent the mean +/- SD (n=3). (B) Western blot analysis of the indicated proteins 96 hours after addition of DOX. β-actin served as a loading control.

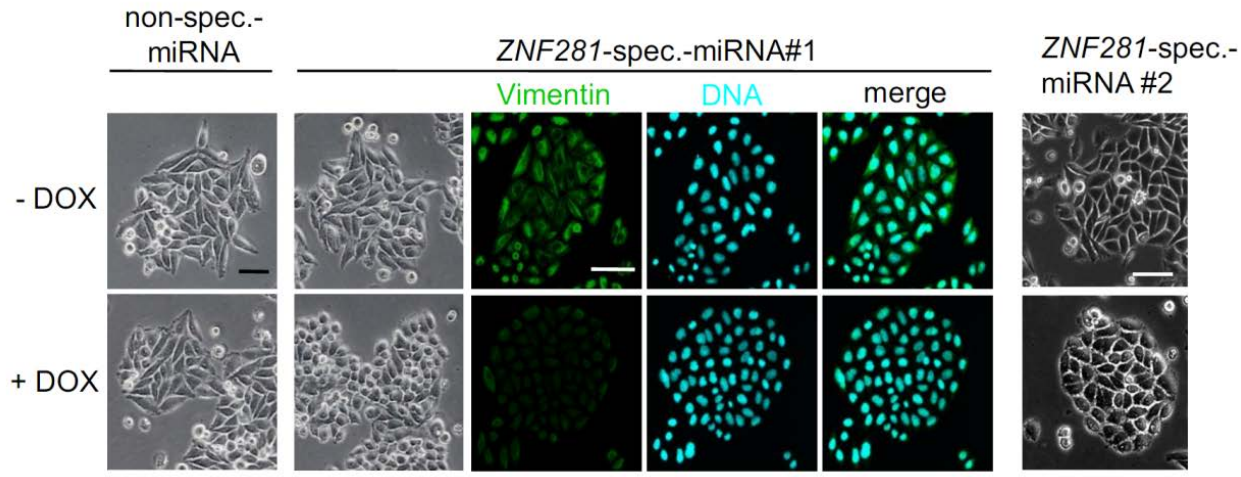

Figure 40: miRNA-mediated repression of *ZNF281* influences the cell morphology. SW480 cells harboring a pRTS vector encoding a miRNA directed against endogenous *ZNF281* (*ZNF281*-specific-miRNA (*ZNF281*-spec.-miRNA#1/2)) or pRTS non-specific control miRNA (non-spec.-miRNA) were analyzed. Representative phase contrast pictures 96 hours after addition of DOX. 200 x magnification. Middle part: confocal microscopy to detect Vimentin protein by indirect immunofluorescence staining. Nuclear DNA was visualized by DAPI staining. 200 x magnification. Scale bars represent 25 µm.

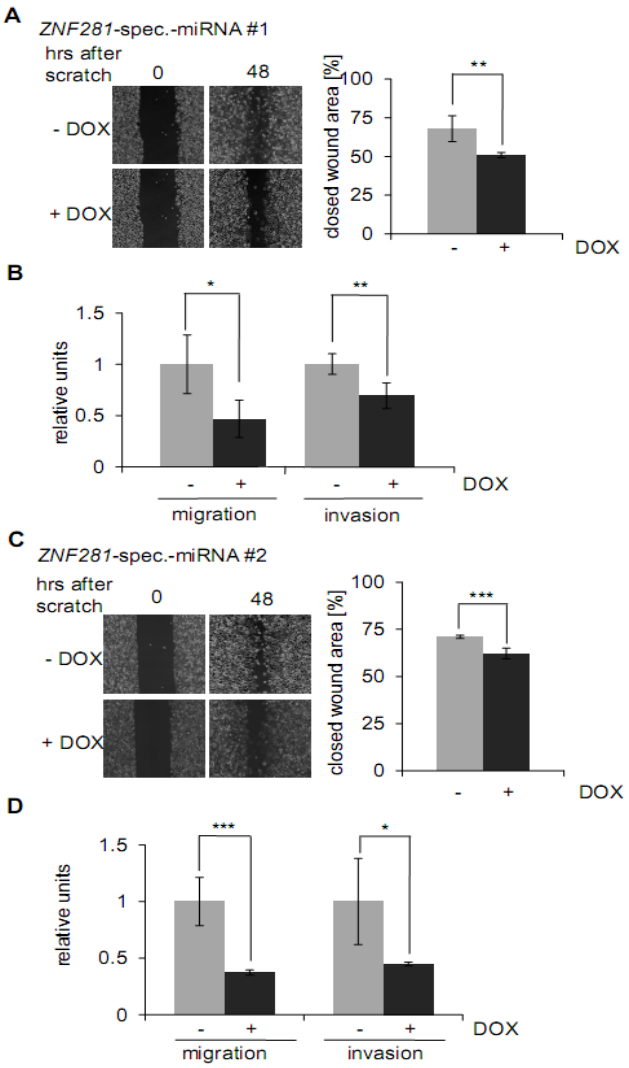

Figure 41: Repression of *ZNF281* diminishes the migratory and invasive capacities of SW480 cells. SW480 cells harboring a pRTS vector encoding a miRNA directed against endogenous *ZNF281* (*ZNF281*-spec.-miRNA#1/2) were analyzed as indicated. (A) Wound healing assay: SW480/pRTS-*ZNF281*-spec.-miRNA#1 cells were treated with DOX or left untreated 72 hours prior to scratching. Representative pictures of the wounding areas are shown. 100 x magnification. Results represent the mean average (%) +/- SD of wound closure determined by the final width of the scratch in three independent wells (n=3). (B) Boyden-chamber assay. Left panel: migration after treatment with DOX or left untreated for 72 hours, serum starvation for the last 48 hours and migration through the Boyden-chamber filter for 48 hours. Right panel: invasion through a Matrigel-coated filter for 48 hours. Results represent the relative change of cells detected in five fields in the Boyden-chamber with untreated cells set as one +/- SD (n=3). (C) Wound healing assay: SW480/pRTS-*ZNF281*-spec.-miRNA#2 cells were treated with DOX or left untreated 72 hours prior to application of a scratch. Wound healing was monitored at 0 and 48 hours. Representative pictures of the wounding areas are shown (left panel). 100 x magnification. Right panel: results represent the mean percentage of the closed wound area +/- SD (n=3). (D) In a Boyden-chamber migration assay cells according to (C) were treated with DOX or left untreated for 72 hours with serum starvation for the last 48 hours and allowed to migrate through the filter for 48 hours. In a Boyden-chamber invasion assay the cells were allowed to invade through a Matrigel-coated filter for 48 hours. Results represent the mean with untreated cells set to one +/- SD (n=3).
A Student's t-test was used in (A-D). *: $p<0.05$, **: $p<0.01$ and ***: $p<0.001$.

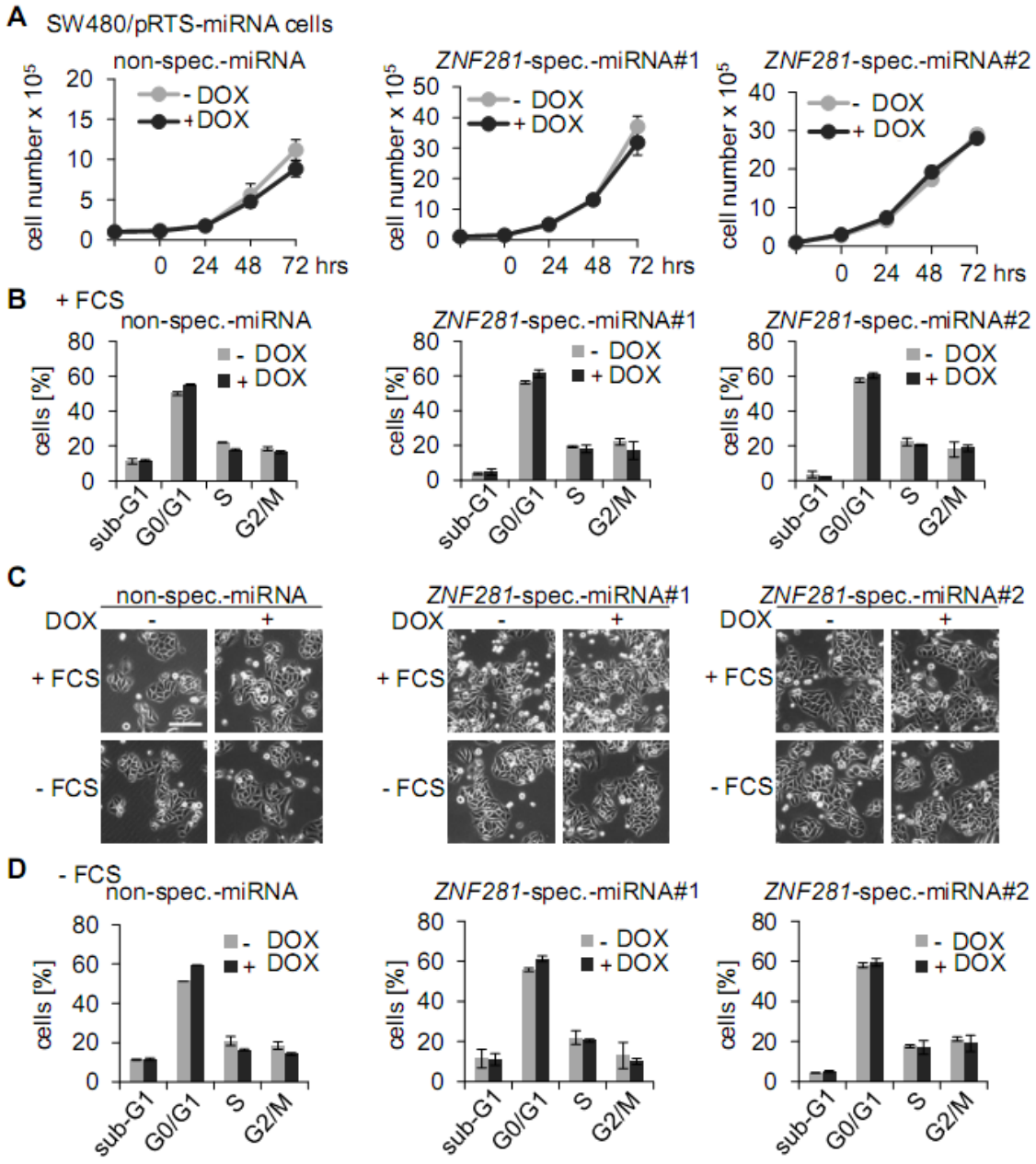

Figure 42: Repression of *ZNF281* does not impact cell proliferation. SW480 cells harboring a bicistronic pRTS-*ZNF281*-specific-miRNA#1/2 or non-specific-miRNA vector were treated with DOX for the indicated periods to activate expression of the respective miRNA or left untreated. (A) Proliferation assay after addition of DOX for the indicated periods to activate the particular miRNAs. (B) Cell cycle analysis of the indicated cells 48 hours after addition of DOX. (C) Representative phase-contrast pictures of the indicated cells. Cells were grown in medium with 10% (+) or 0.1% (-) FCS as indicated. 200 x magnification, scale bar represents 50 µm. (D) Cells treated with DOX for 48 hours or left untreated in medium with 0.1% FCS (-FCS) were subjected to cell cycle analysis.
In (A), (B) and (D) results represent the mean +/- SD (n=3).

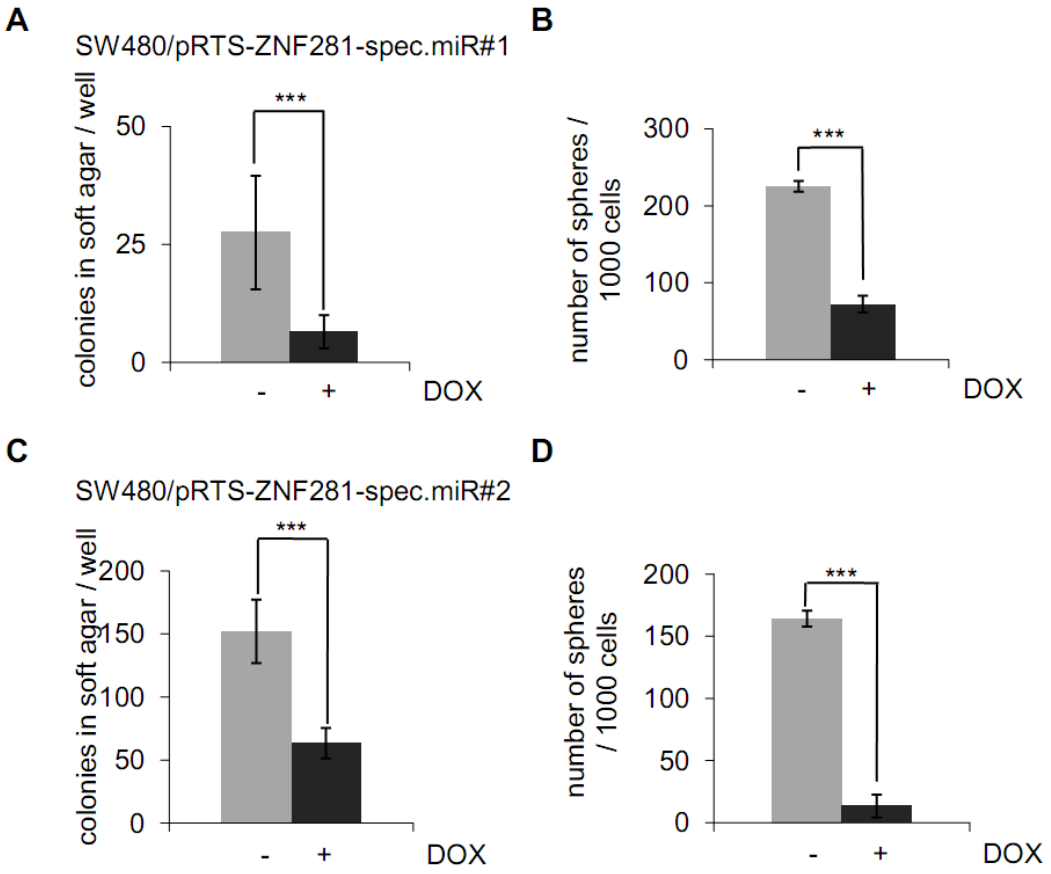

Figure 43: Down-regulation of *ZNF281* via specific miRNAs influences colony and sphere formation. SW480 cells harboring a bicistronic pRTS-*ZNF281*-specific-miRNA#1/2 were treated with DOX for the indicated periods to activate expression of the respective miRNA or left untreated. (A and C) Cells were subjected to a soft-agar assay and treated with DOX or left untreated during the experiment. Three weeks after seeding the resulting colonies were stained with crystal violet. Results represent the mean number of colonies in soft agar per well +/- SD (n=3). (B and D) Quantification of colono-spheres formed. The results are provided as the mean number of spheres formed per 1000 cells seeded +/- SD (n=3).
A Student's t-test was used in (A-D). ***: $p<0.001$.

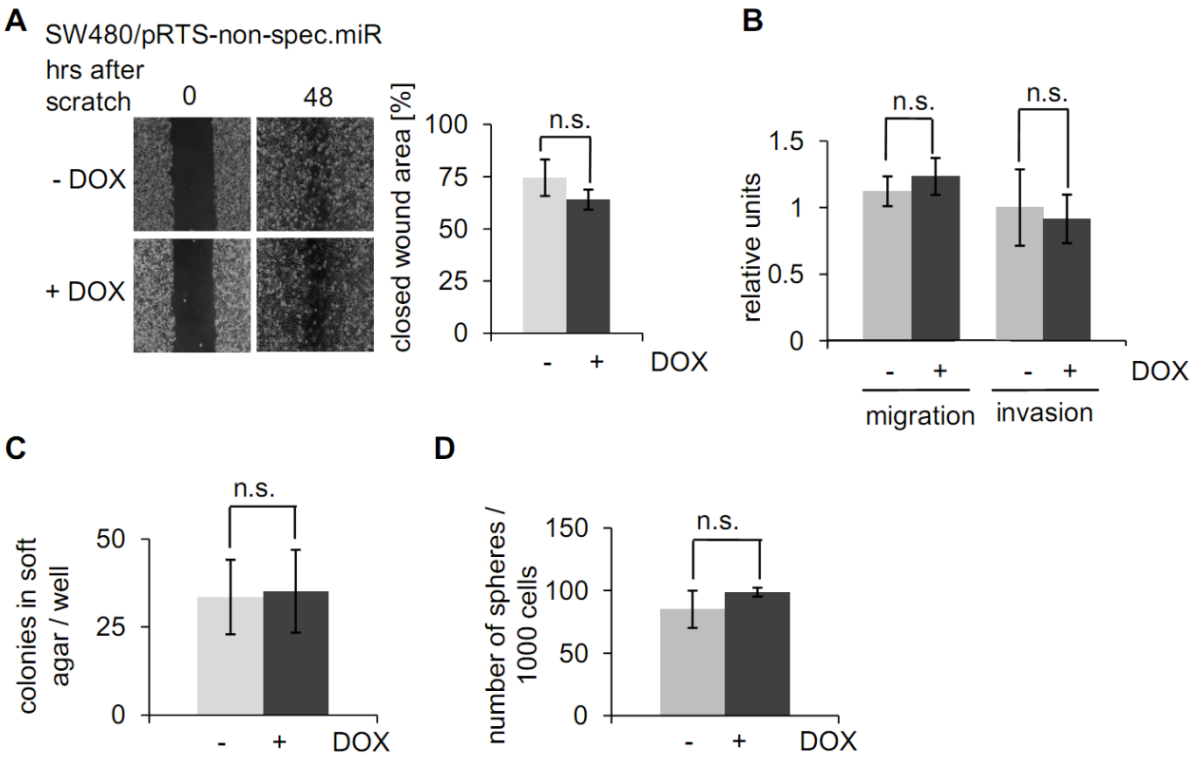

Figure 44: Expression of a non-specific miRNA does not have any impact on SW480 cells. SW480/pRTS-non-spec.-miRNA cells were analyzed. (A) Wound healing assay: the cells were treated with DOX or left untreated 72 hours prior to scratching. Wound healing was monitored immediately and 48 hours after scratching and representative pictures of the wounding areas are shown (left panel). 100 x magnification. Right panel: results represent the mean percentage of the closed wound area +/- SD (n=3). (B) In a Boyden-chamber migration assay the cells were treated with DOX or left untreated for 72 hours with serum starvation for the last 48 hours and allowed to migrate through the filter for 48 hours. In a Boyden-chamber invasion assay the cells were allowed to migrate through a Matrigel-coated filter for 48 hours. Results represent the mean with untreated cells set to one +/- SD (n=3). (C) The cells were subjected to a colony formation assay in soft-agar and treated with DOX or left untreated. Three weeks after seeding the resulting colonies were stained with crystal violet. Results are provided as the mean +/- SD (n=3). (D) Quantification of colono-spheres. The results are provided as the mean number of spheres formed per 1000 cells seeded +/- SD (n=3).
In (A-D) a Student's t-test was applied with $p>0.05$ being considered non-significant (n.s.).

5.1.8 Requirement of ZNF281 for c-MYC-induced EMT

Recently, it has been observed that ectopic c-MYC expression effectively induces EMT in DLD-1 cells, which was accompanied by an activation of SNAIL expression mediated to a large extend by AP4 (Jackstadt et al, 2013). Since an interaction between c-MYC and ZNF281 had also been detected before (Koch et al, 2007), the question was addressed whether ZNF281 is required for c-MYC-induced EMT. c-MYC activation resulted in an induction of ZNF281 expression at the protein and mRNA level (Figure 45A and B). This was presumably indirect since MYC binding sites (E-boxes) were not identified in the *ZNF281* promoter region. Interestingly, ectopic c-MYC expression and concomitant transfection of a *SNAIL*-specific siRNA diminished the induction of ZNF281 (Figure 46). When c-MYC was ectopically expressed in DLD-1 cells in the presence of siRNAs directed against *ZNF281*, the repression of E-cadherin and also the induction of SNAIL was less pronounced than with co-transfection of a control siRNA (Figure 47A). In addition, siRNA-mediated down-regulation of ZNF281 prevented the adoption of a mesenchymal phenotype after activation of c-MYC in colorectal DLD-1 cells (Figure 47B). After activation of ectopic c-MYC and concomitant transfection of the *ZNF281*-specific siRNAs E-cadherin remained at the membrane, whereas co-transfection of a control siRNA did not interfere with the c-MYC-induced loss of membranous E-cadherin (Figure 47B). Taken together, these results show that c-MYC-induced EMT is mediated by ZNF281.

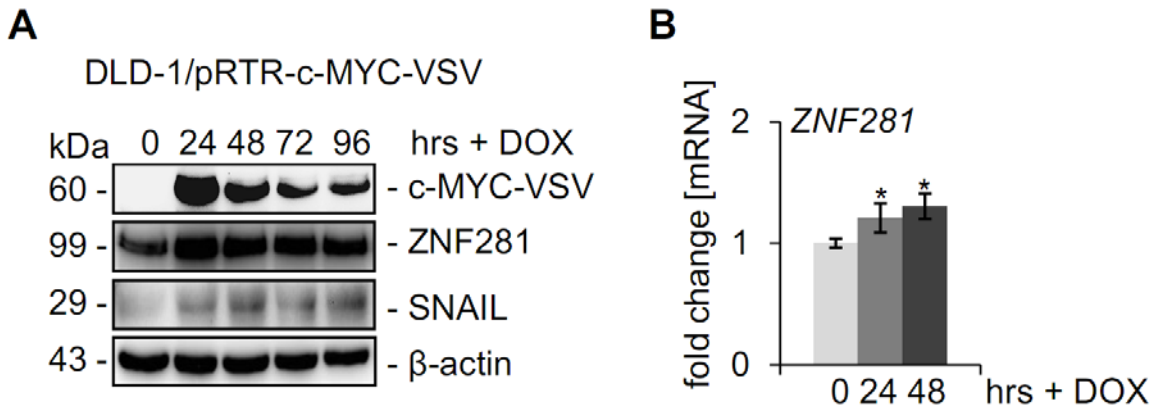

Figure 45: The expression of ZNF281 is induced by c-MYC. DLD-1/pRTR-c-MYC-VSV cells were analyzed. (A) Cells were treated with DOX for the indicated periods and subjected to Western blot analysis of the indicated proteins. Detection of β-actin served as loading control. (B) qPCR analyses of *ZNF281* mRNA expression at the indicated time-points. Results represent mean values +/- SD (n=3). A Student's t-test was used. *: $p<0.05$. The DLD-1/pRTR-c-MYC-VSV cells were generated by Rene Jackstadt and further the respective cDNA samples were kindly provided by Rene Jackstadt.

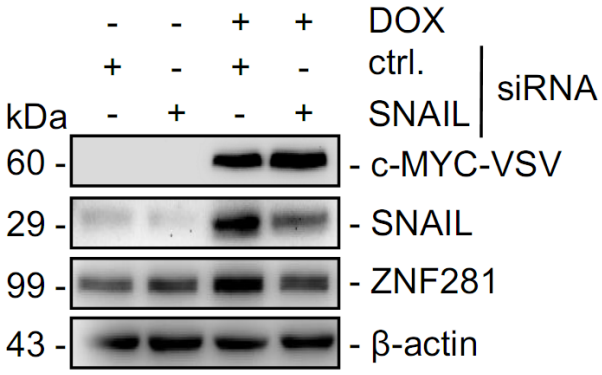

Figure 46: siRNA-mediated knock-down of *SNAIL* prevents the c-MYC-mediated induction of ZNF281. DLD-1/pRTR-c-MYC-VSV cells were transfected with the indicated siRNAs for 72 hours and DOX (indicated by +) was added for the last 24 hours. Subsequently, the indicated proteins were detected by Western blot analysis. Detection of β-actin served as loading control.

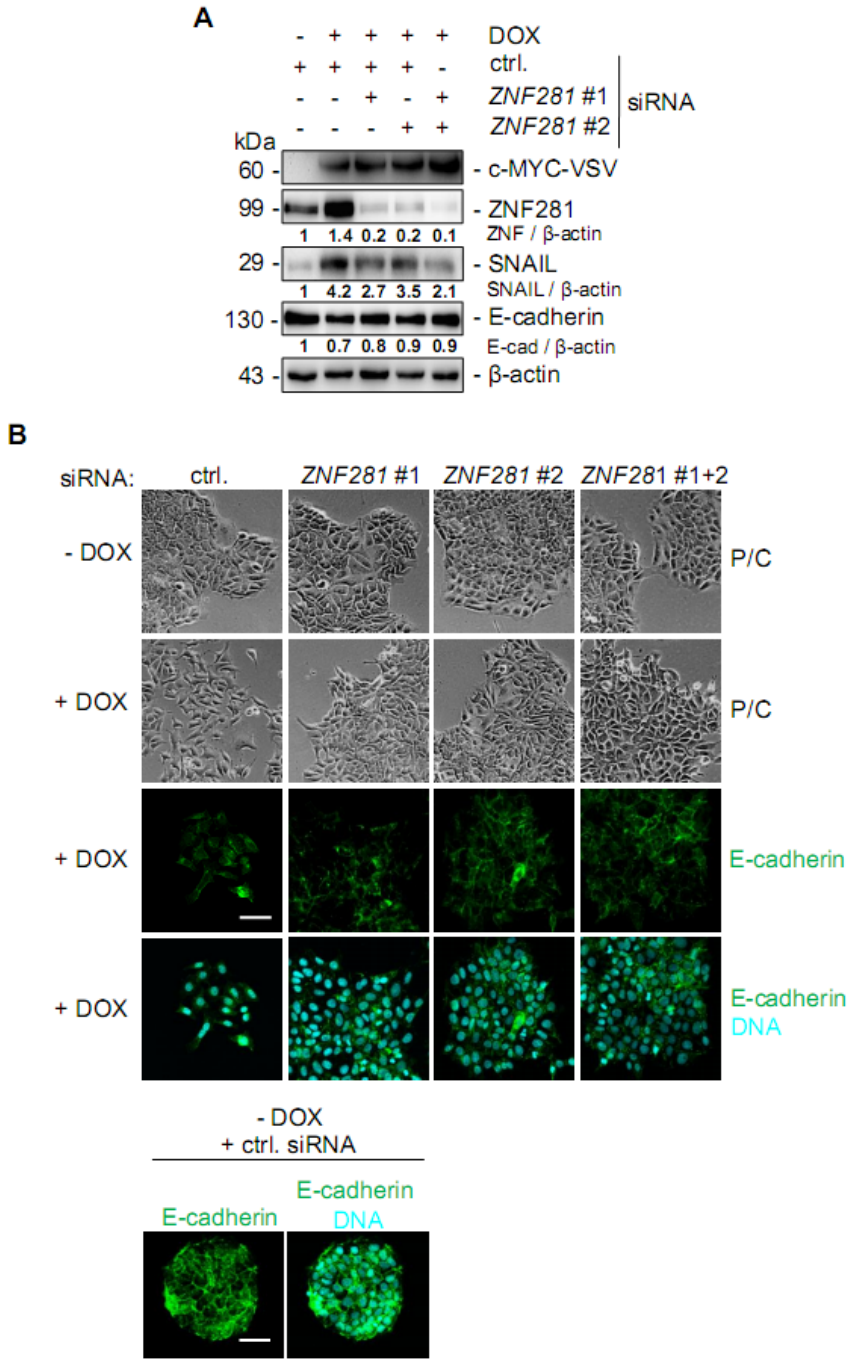

Figure 47: siRNA-mediated knock-down of ZNF281 prevents the c-MYC-induced EMT. (A) DLD-1/pRTR-c-MYC-VSV cells were transfected with two different *ZNF281*-specific (*ZNF281* #1 and *ZNF281* #2) siRNAs or the respective control (ctrl.) for 96 hours. For the last 24 hours DOX was added. Subsequently, the indicated proteins were detected by Western blot analysis. Detection of β-actin served as loading control. Relative densitometric quantifications are indicated. ZNF = ZNF281, E-cad = E-cadherin. (B) Representative phase-contrast (P/C) images of the cells analyzed in (A). 200 x magnification. Detection of E-cadherin was done by indirect immunofluorescence using confocal laser-scanning microscopy. Nuclear DNA was visualized by DAPI staining. 200 x magnification. siRNA control had no effect on these cells in the absence of DOX (lower panel). The scale bars represent 25 µm.

5.1.9 Role of ZNF281 in metastasis formation

Since EMT and the resulting cellular properties have been implicated in the metastatic process (Valastyan & Weinberg, 2011) it was asked whether inactivation of ZNF281 in the highly metastatic CRC cell line SW620 would influence metastases formation in a xenograph mouse model. Therefore, SW620 cells stably expressing luciferase2 were generated to monitor the development of metastases over time in a non-invasive manner (Figure 48A-C). Transfection of SW620-Luc2 cells with two different *ZNF281*-specific siRNAs resulted in a pronounced down-regulation of ZNF281 expression, which was accompanied by a decrease in Vimentin and SNAIL protein (Figure 49) in line with *SNAIL* being a direct target gene of ZNF281 (Figure 26A and B).

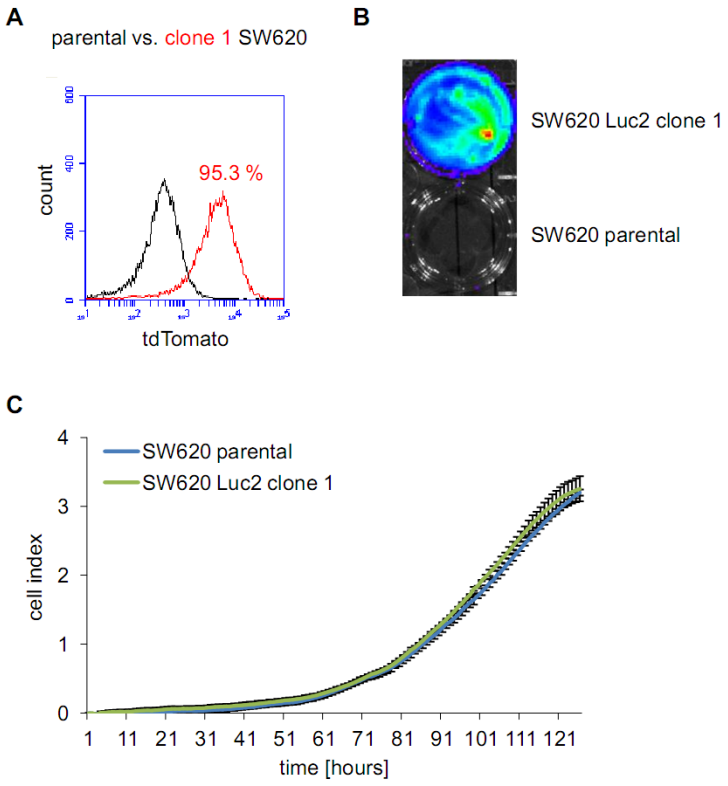

Figure 48: Characterization of SW620 Luc2 cells. Characterization of SW620 cells constitutively expressing Luc2 and tdTomato from a retroviral vector. (A) Flow cytometric detection of tdTomato expression of parental (black) and clone 1 (red) SW620 cells. (B) Measurement of the luciferase activity in the indicated cells 30 minutes after the addition of D-luciferin (150 µg/ml final concentration). (C) Cell proliferation was determined by impedance measurement in medium containing 10% serum. The cell index generally corresponded to the relative cell number.
These analyses were performed by Rene Jackstadt. The figure was also generated by Rene Jackstadt.

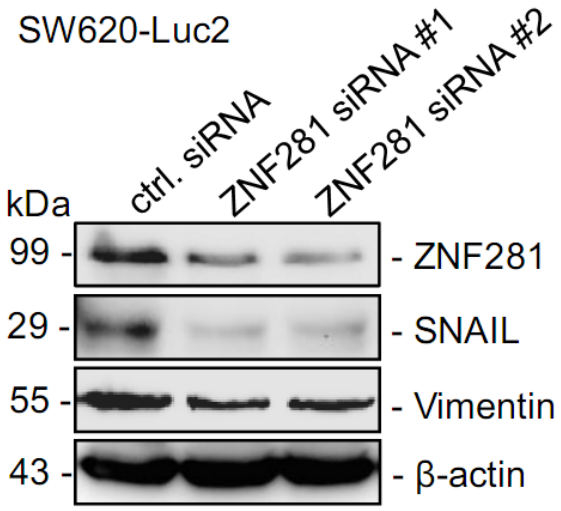

Figure 49: siRNA-mediated repression of *ZNF281* results in decreased SNAIL and Vimentin protein expression. SW620 cells stably expressing a pLXSN-Luc2-tdTomato vector were transfected with the respective siRNAs. After 72 hours Western blot analysis was performed to detect the indicated proteins. Detection of β-actin served as a loading control. The cell lysates were provided by Rene Jackstadt.

Subsequently, these cells were injected into the tail vein of NOD/SCID mice. Within four weeks mice injected with control siRNA transfected cells gave rise to luminescence signals in the lung indicating metastases, whereas mice injected with cells transfected with *ZNF281*-specific siRNAs did not show luminescence signals until seven to eight weeks after injection (Figure 50). Nine weeks after injection luminescent metastases were easily detectable in mice, which had received control siRNA treated cells, whereas cells treated with *ZNF281*-specific siRNAs only rarely gave rise to small metastases as evidenced by weak luminescence signals (Figure 50 and 51A). At this time-point lungs displayed macroscopically visible metastases in the control group, while lungs from mice injected with cells transfected with *ZNF281*-specific siRNAs were devoid of macroscopically visible metastases (Figure 51A). Haematoxylin and eosin (H&E) staining revealed the presence of metastases in the lungs of the control siRNA group, whereas the knock-down of ZNF281 largely prevented the colonization of SW620 cells in the lung (Figure 51A). Histological examination of the lungs revealed a significant decrease in the total number of metastatic nodules upon inhibition of ZNF281 (Figure 51B). In conclusion, ZNF281 is necessary for metastatic colonization of CRC cells in this *in vivo* model.

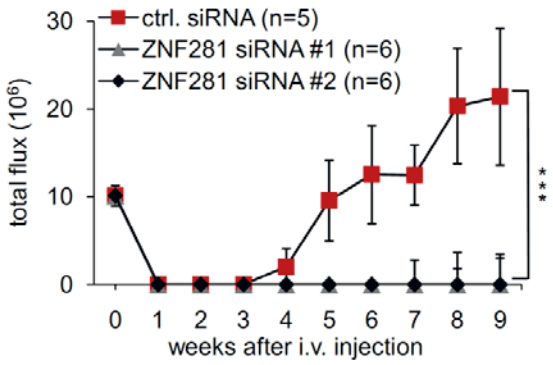

Figure 50: siRNA-mediated repression of *ZNF281* in SW620 cells results in the failure to develop lung metastases. Cells transfected with two different *ZNF281*-specific siRNAs or the respective control were injected into the tail vein of six- to eight-week-old immuno-compromised NOD/SCID mice and bioluminescence signals presented as "total flux" per mouse were recorded at the indicated time-points. Data are represented as mean +/- SD (n=5-6). A Student's t-test was used with: ***: p<0.001.
These analyses were performed by Rene Jackstadt. The figure was also generated by Rene Jackstadt.

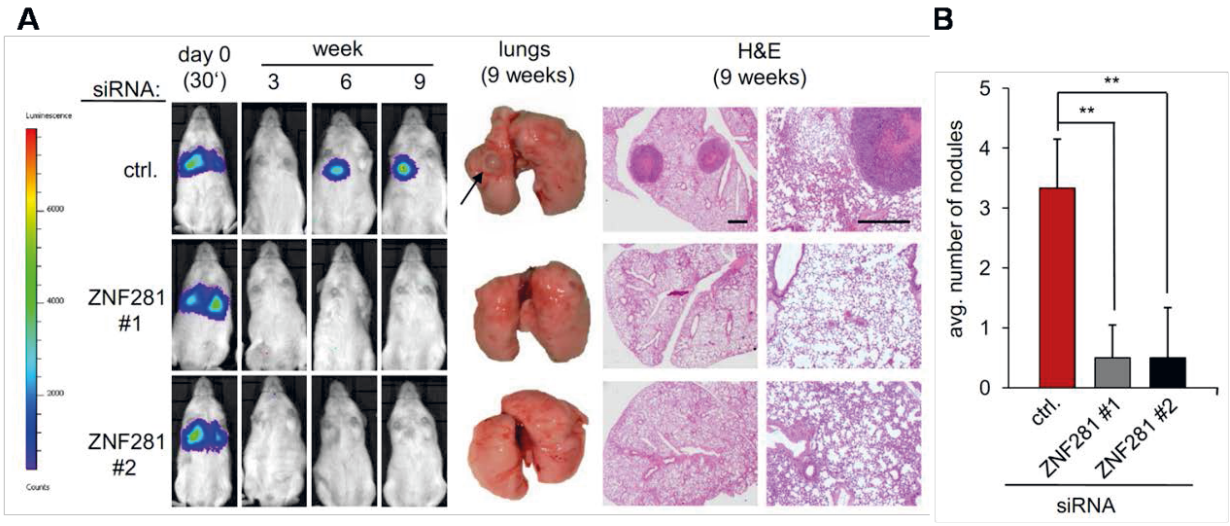

Figure 51: ZNF281 expression is required for the development of lung metastases in mice. Cells with siRNA-mediated knock-down of *ZNF281* or the respective control were injected into the tail vein of six- to eight-week-old immuno-compromised NOD/SCID mice. (A) Left panel: representative images show bioluminescence signals 30 minutes and three, six and nine weeks after the intra-venous injection of the siRNA transfected SW620 cells. Middle panel: representative examples of the resected lungs per group. The arrow indicates a macroscopically visible metastatic tumor nodule in the control group. Right panel: representative example of the haematoxylin and eosin (H&E) staining of the resected lungs nine weeks upon tail vein injection of SW620 cells transfected with the respective siRNAs. Scale bars represent 200 µm. (B) Quantification of detectable metastatic tumor nodules in the lung per mouse nine weeks after the intra-venous injection of SW620 cells transfected with the indicated siRNA. Data are represented as mean +/- SD (n=5-6). A Student's t-test was used with: **: p<0.01.
These analyses were performed by Rene Jackstadt. The figure was also generated by Rene Jackstadt.

5.1.10 ZNF281 is up-regulated in human colon and breast cancer

In order to evaluate whether the pro-metastatic functions of ZNF281 are reflected in enhanced expression of ZNF281 during progression of CRC and other carcinomas the Oncomine database was used for analyses (Rhodes et al, 2004). In eleven out of twelve tumor entities ZNF281 expression was found to be up-regulated in tumor versus normal tissue (Figure 52). In primary tumor samples of two colorectal and two breast cancer cohorts cancer-specific up-regulation of ZNF281 was consistently found (Figure 53A-D). In addition, an increased ZNF281 expression in the primary tumor of colorectal cancer patients was associated with recurrence, and therefore presumably metastasis, three years after removal of the primary tumor (Figure 53E).

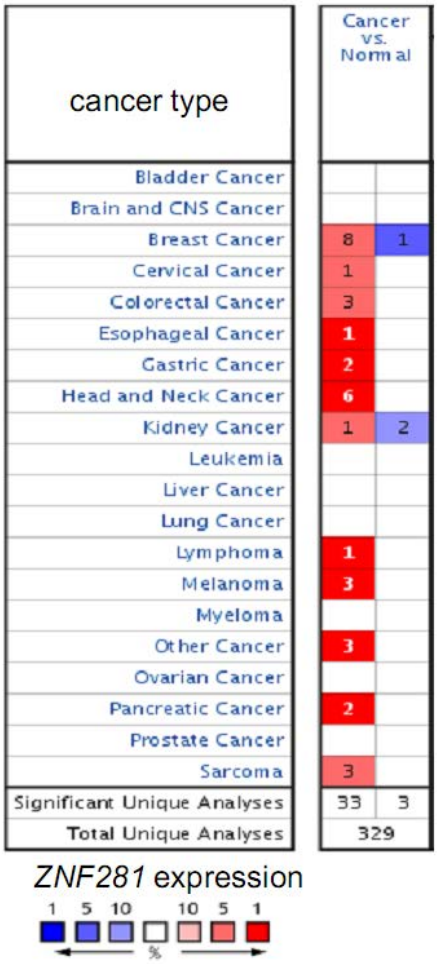

Figure 52: Comparison of *ZNF281* expression levels in multiple human cancers. Analysis of *ZNF281* mRNA expression in human Oncomine datasets (datasets updated as of November 2011). Summary of *ZNF281* mRNA expression in various human cancer types compared to the respective normal tissue. Indications of the colors used: red: up-regulated in cancer; blue: down-regulated in cancer.

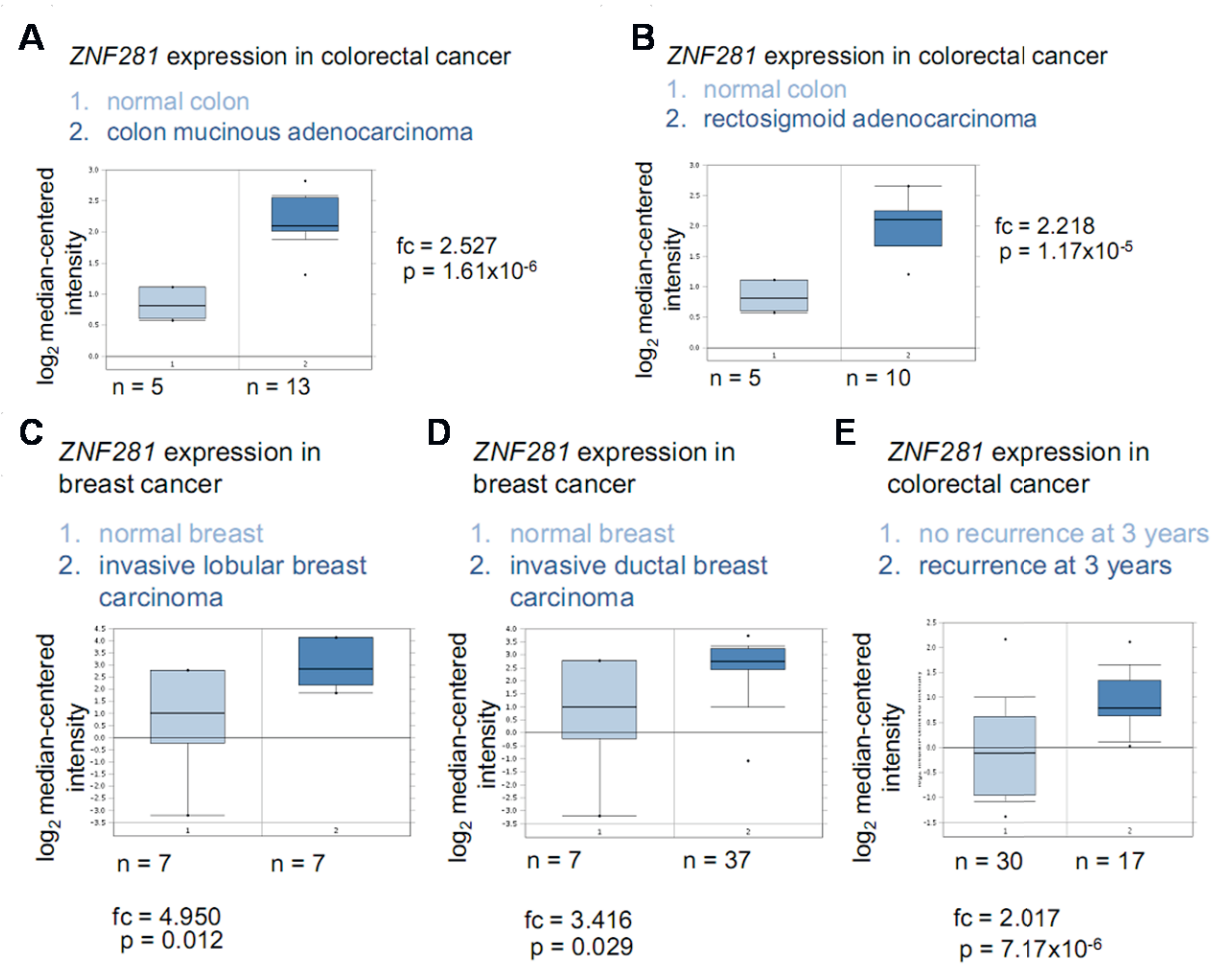

Figure 53: Analysis of *ZNF281* mRNA expression in human colon and breast Oncomine datasets. Oncomine datasets updated as of November 2011 were analyzed for *ZNF281* expression levels. Comparison of normal colon tissue with (A) colon mucinous adenocarcinoma and (B) rectosigmoid adenocarcinoma using the Kaiser dataset. Comparison of normal breast tissue with (C) invasive lobular breast carcinoma and (D) invasive ductal breast carcinoma using the Radvanyi dataset. (E) Comparison of the *ZNF281* expression levels of recurrent and non-recurrent colorectal cancer after three years using the Smith dataset. In all graphs y-axes are provided in $\log_2$ scale.

6. DISCUSSION

The results obtained in this thesis show that ZNF281 is an integral part of the regulatory network controlling the transition between epithelial and mesenchymal states in colorectal cancer cells (see schematic model in Figure 54). The results further demonstrate a coherent feed-forward loop consisting of SNAIL and miR-34a which induces ZNF281 expression. Furthermore, the sufficiency of ZNF281 expression for induction of EMT and its requirement to maintain a mesenchymal state in CRC cell lines was shown. This effect is mediated by the direct activation of SNAIL and repression of epithelial marker genes and effectors. Additionally, it could be shown that ZNF281 regulates stemness. By these mechanisms ZNF281 presumably contributes to metastases formation.

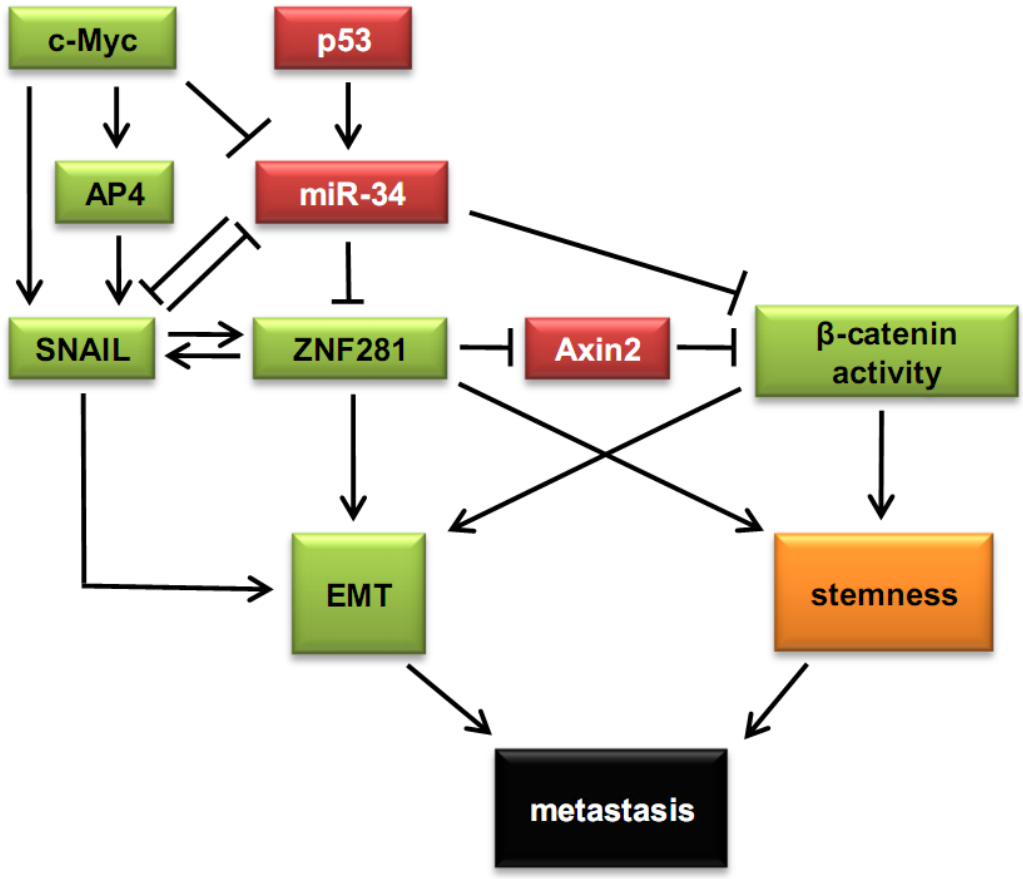

Figure 54: ZNF281 as a regulator of EMT and stemness. Schematic model integrating the results of this study with previous findings. Green rectangles represent factors that promote and red rectangles represent factors that inhibit EMT and stemness. EMT in combination with increased cancer cell stemness promotes the formation of metastases (Hahn et al, 2013).

As depicted in Figure 54, a coherent feed-forward loop involving the EMT-TF SNAIL regulates ZNF281 expression in CRC cells, where SNAIL directly binds to the *ZNF281* promoter and induces its transcription. Although SNAIL is mainly known as a transcriptional repressor direct induction of target genes by SNAIL has been shown (De Craene et al, 2005; Guaita et al, 2002; Rembold et al, 2014; Vetter et al, 2010). This regulatory loop also involves miR-34a, which in turn is repressed by SNAIL in a negative feedback loop (Kim et al, 2011; Siemens et al, 2011) and itself could be shown to target *ZNF281.* Additional evidence could be provided that ZNF281 is induced by SNAIL also in other types of carcinomas such as pancreatic and breast carcinomas. Furthermore, miR-34a repressed ZNF281 in a pancreatic cancer cell line. Therefore, the regulations described here may also be important for the regulation of EMT and metastasis in other types of carcinomas besides CRC. Recently, increased SNAIL expression was demonstrated to inversely correlate with *miR-34a* expression in a cohort of 94 colon cancer patients and associate with liver metastasis (Siemens et al, 2013). Therefore, the increased expression of *ZNF281* identified in public datasets of colorectal and other tumor types may be caused by down-regulation of miR-34a expression due to cancer-specific CpG methylation and/or p53 inactivation. Ectopic ZNF281 expression directly induced *SNAIL* transcription. However, this resulted in varying degrees of EMT effector regulations in the two different CRC cell lines DLD-1 and HT29, especially with regard to the effects on *CDH-1* mRNA. In DLD-1 cells rather the E-cadherin protein expression was decreased upon ectopic ZNF281 expression, but not the *CDH-1* mRNA expression level. In contrast, in the colorectal cell line HT29 the E-cadherin/*CDH-1* was negatively regulated on transcriptional and protein level, displaying cell type specific differences with regard to the transcriptional influence on *CDH-1*. This raises the question as to whether loss of *CDH-1* is necessary for the loss of cellular adhesions. Indeed, in human breast cancer cells loss of E-cadherin expression is not required for EMT (Hollestelle et al, 2013) as some breast cancer cell lines gained a spindle like cell morphology and revealed increased mesenchymal markers, but failed to repress E-cadherin expression during induction of EMT. Further, it has been shown that E-cadherin reconstitution in E-cadherin negative cell lines that had undergone EMT failed to revert the mesenchymal phenotype back to an epithelial phenotype (Hollestelle et al, 2013). This may indicate cell type-specific differences in various colorectal cancer cell lines during EMT and E-cadherin regulation. Nonetheless,

ZNF281 expression consistently resulted in the loss of intercellular adhesions and enhanced migration and invasion in HT29 and DLD-1 CRC cells. The subtle differences in the transcriptional response of different CRC cell lines to ZNF281 activation may be due to variations in related signaling pathways and therefore varying degrees of permissiveness for EMT or plasticity of the respective cells. Moreover, a number of additional epithelial marker genes encoding components of tight junctions (*ZO-1/3*, *CLDN-1*) and adherens junctions (*CDH-3*) as well as desmosomes (*PKP2*, *DSP*) were repressed upon ectopic expression of ZNF281 in DLD-1 cells, which may further contribute to the loss of cell-cell contacts, as previously shown for ZEB2 (Vandewalle et al, 2005). The ZNF281 paralog ZBP89 has been demonstrated to repress the mesenchymal marker Vimentin via the interaction with Sp1 in *Drosophila* Schneider cells (S2) (Zhang et al, 2003). Moreover, a similar repressive effect of ZNF281 on a *Vimentin* minimal promoter reporter has been shown in S2 cells (Zhang et al, 2003). In contrast, evidence has been provided here that in human CRC cells Vimentin expression is enhanced upon ectopic ZNF281 expression, whereas knock-down of *ZNF281* resulted in a repression of Vimentin. Presumably, species-specific differences might account for these different observations as well as variations in the experimental settings. For example artificial protein-protein-interactions in the minimal promoter reporter system might occur compared to the natural settings of the investigation of endogenous expression levels. Nevertheless, further experiments might reveal more similarities and differences between the two paralogs since the homology primarily concerns the zinc finger regions whereas several other domains differ as e.g. the acidic domain, which is not present in ZNF281 and might be responsible for ZBP-89 mediated protein-protein-interactions (Lisowsky et al, 1999). The results demonstrate that ZNF281 represents a new EMT-promoting transcription factor. Notably, ZNF281 is structurally related to the zinc-finger transcription factor family like SNAIL, SLUG and ZEB1/2 (as indicated in Figure 55). However, there is a major difference between ZNF281 and the core EMT-transcription factors (EMT-TFs) SNAIL, SLUG and ZEB concerning the recognition site in target promoters. Whereas the above mentioned core EMT-TFs bind to a non-canonical E-Box motif (CACCTG), ZNF281 so far just has been shown to bind to GC-rich regions in the promoter of e.g. *ODC* (Law et al, 1999; Lisowsky et al, 1999). This might lead to differences in the set of genes being regulated during the process of EMT and requires further investigation in order to understand the

role of ZNF281 in this process. Moreover, additional information should be gained on ZNF281 and the specificity, redundancy and/or cooperation within the network of EMT-inducing factors. Furthermore, it might be possible that ZNF281 can actively be recruited to specific promoters as a co-factor. Alternatively, direct functional interactions with other EMT-TFs are possible.

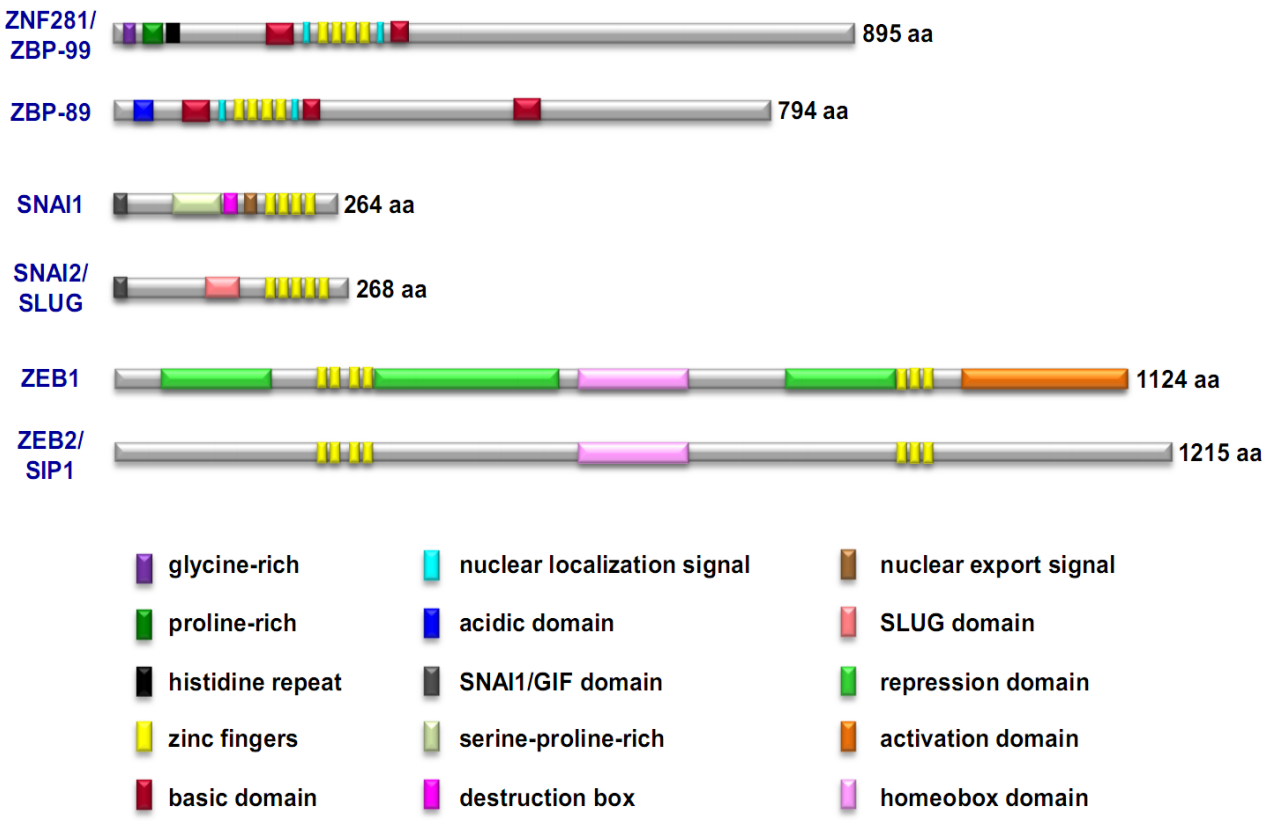

Figure 55: Comparison of ZNF281/ZBP-99, ZBP-89 and other EMT-inducing transcription factors (EMT-TFs). Numbers represent amino acids (aa). Colored boxes represent the indicated domains (Hahn & Hermeking, 2014, *revised version submitted*).

It is well documented that EMT is regulated by several regulatory networks (as described in chapter 1.3.1.1), presumably to confer robustness to the process. The most prominent network is built by the core EMT-transcription factors SNAIL, SLUG, ZEB and TWIST. However, there are additional networks existing in parallel. miRNAs, differential splicing and translational and post-translational control represent additional regulatory layers (De Craene & Berx, 2013). ZNF281 was integrated within some of

those regulatory networks due to the feed-forward regulation by SNAIL and miR-34a. Since *miR-34a/b/c* genes are directly repressed by SNAIL (Siemens et al, 2011), the induction of ZNF281 by SNAIL represents a feed-forward regulation, which is mediated by at least two mechanisms: transcriptional activation of *ZNF281* and suppression of a *ZNF281*-specific miRNA. Therefore, it seems to be worth to further investigate other potential aspects of ZNF281-mediated EMT regulation with regard to post-translational events or the possible impact of ZNF281 on the chromatin structure of certain EMT-relevant genes with regard to the induction and maintenance of an EMT. Epigenetic changes play an important role for the regulation of EMT (Tam & Weinberg, 2013) and the epigenetic regulation of the *CDH-1* promoter represents the most extensively studied example. SNAIL expression has been associated with *CDH-1* promoter methylation by introducing repressive histone modifications through the recruitment of the histone deacetylases 1/2 (HDAC 1/2) (Peinado et al, 2004). Furthermore, SNAIL may recruit histone modifying enzymes such as the demethylase LSD1, the methyltransferases EZH2, SUZ12, SUV39H1 as well as G9a to the promoters of its target genes (Dong et al, 2013; Dong et al, 2012; Herranz et al, 2008; Lin et al, 2010). Also ZEB1 has been shown to modify the histone marks of histone H3 at the *CDH-1* promoter via recruitment of the sirtuin1 (SIRT1) deacetylase resulting in a diminished binding capacity of RNA polymerase II (Byles et al, 2012). Since genome-wide epigenetic reprogramming is involved in EMT (Tam & Weinberg, 2013) it is necessary to carry out further studies on how ZNF281 might influence genome-wide changes in gene expression by interacting with different epigenetic modifiers as shown for other EMT-transcription factors. The current literature further suggests an extensive crosstalk between EMT-inducing transcription factors and miRNAs during the establishment and maintenance of the mesenchymal phenotype of cells (reviewed in (De Craene & Berx, 2013; Sanchez-Tillo et al, 2012)). The list of directly or indirectly EMT-influencing miRNAs increased extensively during the past years. However, mainly two miRNA families are associated with EMT: the miR-200 and miR-34 families (De Craene & Berx, 2013; Lu et al, 2013a; Tian et al, 2013). Interestingly, both miRNA families are under the positive control of the tumor suppressor p53 (Chang et al, 2011; Hermeking, 2012; Siemens et al, 2011). The miR-34 family has an impact on the regulation of the EMT-process towards epithelial differentiation by directly controlling SNAIL and ZEB expression (Kim et al, 2011; Siemens et al, 2011). The presented results now further

extend this network by adding reciprocal connections between SNAIL, ZNF281 and miR-34a. Epithelial differentiation further has been associated with the expression of the miR-200 family. Both EMT and MET are tightly controlled via a reciprocal feedback loop consisting of the miR-200 family and ZEB1/2 (Gregory et al, 2008; Korpal et al, 2008; Park et al, 2008). Besides targeting ZEB1/2 miR-200 further mediates differentiation by down-regulation of epigenetic modifiers such as BMI1 and SUZ12 (Iliopoulos et al, 2010; Wellner et al, 2009). The epithelial and mesenchymal phenotypes of cells as well as cells with mixed characteristics seem to be regulated by an interconnected circuit consisting of the miR-34/SNAIL and the miR-200/ZEB1/2 mutual-inhibition feedback circuits (Lu et al, 2013a). Lu et.al tested modeled predictions of dynamic gene expression to closer define changes in gene expression during complete and partial epithelial and mesenchymal transitions with regard to the miR-34/SNAIL and the miR-200/ZEB1/2 circuits. They proposed that the miR-200/ZEB1/2 loop acts as ternary switch between epithelial, mesenchymal and hybrid phenotypes, which is driven by miR-34/SNAIL as integrator of internal and external signals (Lu et al, 2013a). Besides SNAIL and ZEB1/2, which are targeted by miR-34 and miR-200 respectively, it was recently shown that the c-MYC-induced EMT-TF AP4 is negatively regulated by miR-15a/16-1 (Shi et al, 2014). Therefore, multiple axes of mutual miRNA and EMT-TF regulations mediate the suppression of the mesenchymal state by p53, which ultimately leads to inhibition of invasion, stemness and metastasis (Figure 56). Thereby, p53 may achieve a more effective and robust tumor suppression, which is presumably more resistant to the loss of single down-stream components than a single linear signaling pathway would be.

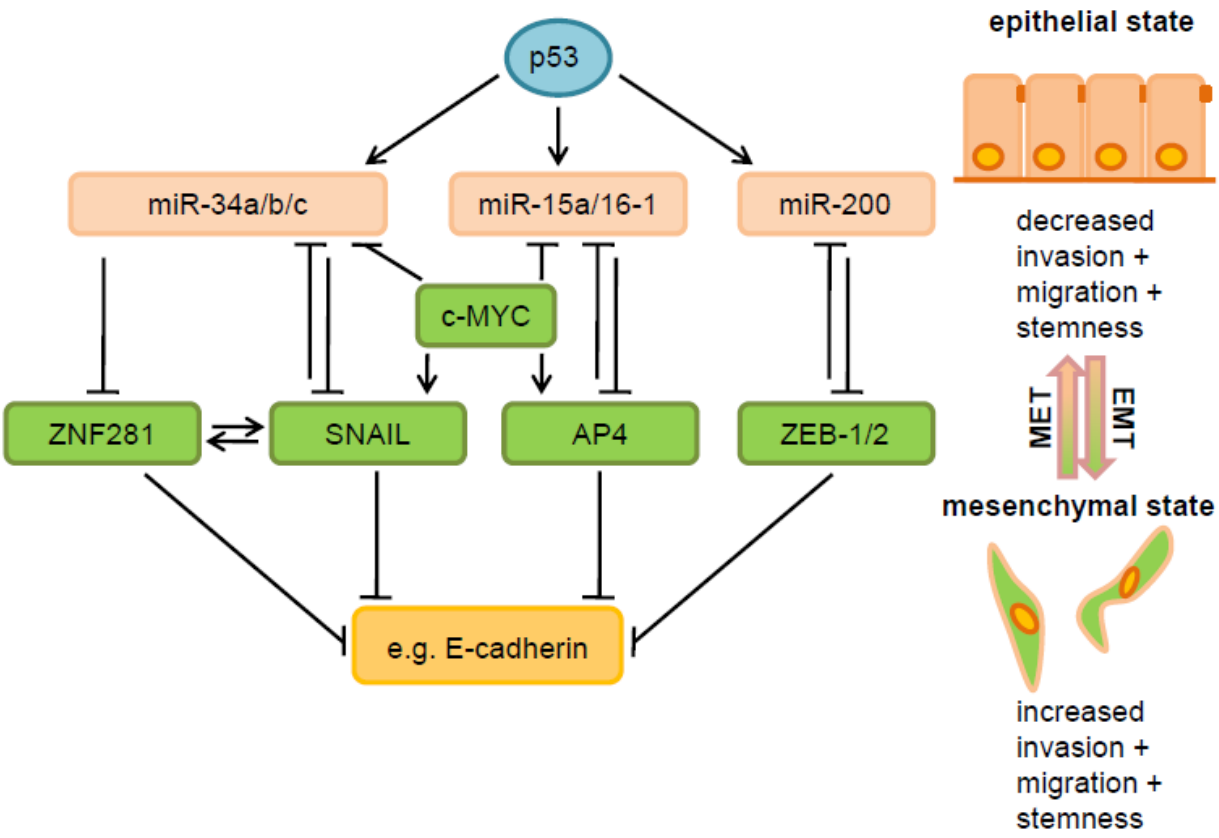

Figure 56: The regulation of EMT/MET by miRNAs and EMT-TFs. Model summarizing the regulatory loops connecting p53-induced MET-promoting miRNAs (beige) and EMT-TFs (green) (Hahn & Hermeking, 2014, *revised version submitted*).

The opposite mode of regulation of ZNF281 by SNAIL and miR-34a already implies that the correct concentration of ZNF281 is important for the regulation of EMT. In order to disseminate from the tumor mass and to intravasate into and extravasate from the bloodstream tumor cells have to undergo EMT. They gain a mesenchymal phenotype along with the capacities to migrate, invade and survive in adverse environments. Nevertheless, cancer cells in the invasion-metastasis-cascade are further dependent on the reverse program of MET in order to restart proliferation after settling down in distant organs (Nieto, 2013). The reversibility of epithelial and mesenchymal phenotypic changes is important for cancer cells in order to form micro- and macro-metastases (Scheel & Weinberg, 2012; Thiery, 2002; Thiery et al, 2009). Expression of EMT-inducing factors such as SNAIL resulted in diminished proliferation (Peinado et al, 2007) being counterproductive for the outgrowth of a metastasis. It has been shown that carcinoma metastases adopt a differentiated epithelial phenotype resembling the pathological histology of the primary tumor (Brabletz et al, 2001). This reflects the

epithelial plasticity implicated in tumor progression and the importance of MET. The repression of ZNF281 by miR-34a may be part of the MET-process and experimental down-regulation of ZNF281 resulted in an epithelial phenotype. These findings integrate the new EMT-TF ZNF281 in the regulatory system including EMT-TFs and MET-promoting miRNAs. Therefore, *in vivo* mechanisms down-regulating ZNF281 at distant sites are an interesting object for future analyses.

Previously, it has been shown that c-MYC binds to ZNF281 (Koch et al, 2007). Here, it has been found that ectopic expression of c-MYC increased ZNF281 expression. The absence of c-MYC binding sites in the promoter region of *ZNF281* implies the existence of alternative regulatory mechanisms. Here, it was shown that c-MYC-mediated induction of SNAIL led to the enhanced expression of ZNF281. In addition, c-MYC has been shown to directly down-regulate *miR-34a* in human and mouse B cell lymphoma models, which contributes to tumorigenesis (Chang et al, 2008). However, c-MYC-induced SNAIL could additionally repress *miR-34*, which would further contribute to increased ZNF281 expression. Alternatively, the association of c-MYC protein with ZNF281 may inhibit the turn-over of ZNF281. Moreover, ZNF281 represents a necessary mediator of SNAIL- and c-MYC-induced EMT. Therefore, ZNF281 might be an important mediator of tumor progression in tumor entities with deregulation of the oncoprotein c-MYC. EMT-TFs are known to regulate each other (Hugo et al, 2011; Taube et al, 2010). It could be demonstrated that in different cell lines with concomitant expression of multiple EMT-inducers the knock-down of even a single EMT-TF was sufficient enough to partially or completely block EMT and metastases formation (Casas et al, 2011; Olmeda et al, 2008; Spaderna et al, 2008). Recently, core microRNA- as well as core gene-signatures associated with various inducers of EMT were defined (Diaz-Martin et al, 2014; Hugo et al, 2011; Moreno-Bueno et al, 2006; Taube et al, 2010). Nevertheless, additional EMT-TF-specific alterations of the regulated genetic programs were shown, which support also differential roles of the different EMT-TFs for tumor progression and invasion (Diaz-Martin et al, 2014; Hugo et al, 2011; Moreno-Bueno et al, 2006; Taube et al, 2010). Therefore, it seems to be necessary to determine the similarities and differences of ZNF281-induced EMT compared to EMT induced by other EMT-inducing factors as well as the mode of interaction within the EMT network.

It has been shown before that the EMT process yields cells with properties of stem cells (Polyak & Weinberg, 2009; Valastyan & Weinberg, 2011). For example, activation

of the EMT-inducers SNAIL and ZEB1 promotes the formation of tumor initiating cells with stem cell properties (Dang et al, 2011; Hwang et al, 2011; Mani et al, 2008; Wellner et al, 2009). Recently, an enrichment of ZNF281 has been demonstrated in basal epidermal stem cells (Yi et al, 2008), which suggests a stemness-related function of ZNF281. In addition, a chromatin immunoprecipitation (ChIP) analysis of mouse embryonic stem cells (ESCs) ectopically expressing ZNF281 revealed more than 2,000 direct ZNF281 targets including several known regulators of pluripotency (Wang et al, 2008). Additionally, global analysis of gene expression after knock-down of ZNF281 in murine cells revealed numerous activated and repressed genes indicating a bifunctional role of ZNF281 within diverse molecular networks (Wang et al, 2008). Moreover, ZNF281 seems to be involved in the regulation of pluripotency by interacting with the core transcriptional regulatory network factors controlling stemness, including NANOG, OCT4 and SOX2 (Wang et al, 2006; Wang et al, 2008). Notably, ZNF281 was also shown to bind to c-MYC (Koch et al, 2007), another factor implicated in the regulation of pluripotency and induced pluripotent stem cell (iPSC) formation. RNA-interference mediated down-regulation of ZNF281 in murine ESC clones led to the differentiation of ESCs, whereas enforced ZNF281 expression resulted in the suppression of ESC differentiation, which occurs after LIF deprivation (Wang et al, 2006; Wang et al, 2008). Taken together, these results show that appropriate expression of ZNF281 is not only required for the maintenance of pluripotency, but also that its repression is necessary for induction of differentiation. However, in another study ZNF281 expression seemed to be dispensable for survival and proliferation of ESCs (Fidalgo et al, 2011). Moreover, ESCs with deletion of *ZNF281* displayed a slightly enhanced self-renewal capacity (Fidalgo et al, 2011). Additionally, it has been shown that the depletion of *ZNF281* enhances the reprogramming of pre-induced pluripotent stem cells (pre-iPSCs) to iPSCs (Fidalgo et al, 2012). Several studies demonstrated that ZNF281 directly regulates *NANOG* expression in concert with OCT4 and SOX2 (Fidalgo et al, 2012; Fidalgo et al, 2011; Wang et al, 2008). ZNF281 recruits the NuRD repressor complex to the *NANOG* locus and contributes to the NANOG auto-regulation in mouse ESCs (Fidalgo et al, 2012; Fidalgo et al, 2011). Interestingly, Wang and colleagues identified potential binding sites for NANOG, SOX2 and OCT4 in the *ZNF281* locus (Wang et al, 2008), which implies the existence of regulatory feedback loops. In *Medaka* fish *ZNF281* is preferentially expressed in gonads similar to *SALL4*, another pluripotency

factor (Wang et al, 2011). Additionally, elevated *ZNF281* expression was shown during early embryonic development due to maternally supplied mRNA followed by a dramatic decrease during gastrulation (Wang et al, 2011). Notably, the elevated expression of *ZNF281* in pluripotent cells is conserved between mammals and lower vertebrates (Wang et al, 2011). A growing body of evidence indicates that cancer stem cells exhibit characteristics similar to embryonic stem cells, since these often express genes, which are typically expressed in normal stem cells. As indicated above ZNF281 seems to be involved in the regulation of pluripotency and stemness by interacting with NANOG, OCT4 and SOX2 (Wang et al, 2006; Wang et al, 2008). Elevated expression of the pluripotency factors NANOG, OCT4 and SOX2 has been implicated in gastric, colorectal, lung, prostate, bladder, esophageal and breast cancer (Amsterdam et al, 2013; Bornschein et al, 2013; Chen et al, 2012; Ibrahim et al, 2012; Lengerke et al, 2011; Lu et al, 2013b; Lu et al, 2010; Raghoebir et al, 2012; Tsukamoto et al, 2005; Yasuda et al, 2011; Zhang et al, 2013; Zhang et al, 2010). Moreover, enhanced NANOG, OCT4 and SOX2 expression is associated with elevated tumorigenic potential (Chen et al, 2012; Chen et al, 2009; Ibrahim et al, 2012; Lu et al, 2013b; Xiang et al, 2011) and metastases formation (Han et al, 2012; Liu et al, 2013; Lu et al, 2013b; Meng et al, 2010; Noh et al, 2012; Zhang et al, 2013). Furthermore, NANOG, OCT4 and SOX2 correlated with the differentiation status of tumors (Amsterdam et al, 2013; Chen et al, 2009; Liu et al, 2013; Raghoebir et al, 2012) and NANOG and OCT4 correlated with poor patient prognosis (Li et al, 2012; Matsuoka et al, 2012; Meng et al, 2010). Furthermore, down-regulation of SOX2 in breast cancer cells inhibited tumor growth in a mouse model (Stolzenburg et al, 2012). Over-expression of OCT4 has been detected in CRC samples and the induced pluripotent stem cell (iPS cell) signature (OCT4, NANOG and LIN28) correlated with tumor site, lymph node status and Dukes classification of CRC patients (Liu et al, 2013). Liu et al. further demonstrated increased sphere formation, proliferation, colony formation, migration and tumor growth of CRC cells upon mixed iPS gene expression consisting of the factors SOX2, c-MYC, OCT4 and KLF4 (Liu et al, 2013), whereas the underlying mechanism lacks explanation and might point towards the influence of ZNF281 in cell colony formation and migration. Recent studies demonstrated that pluripotent stem cells derived from differentiated somatic cells (iPS cells) display similar properties as ESCs (Takahashi & Yamanaka, 2006). The generation of those iPS cells can be achieved by retroviral transduction of the four

transcription factors OCT4, SOX2, KLF4 and c-MYC (reviewed in (Yamanaka & Blau, 2010)). Since ZNF281 interacts with the oncoprotein c-MYC (Koch et al, 2007) and has been shown to influence OCT4 and SOX2 (Wang et al, 2006; Wang et al, 2008), three out of four of the so called “Yamanaka” factors (Yamanaka & Blau, 2010) are functionally connected to ZNF281. However, so far it is unclear how important ZNF281 is for the generation of the iPS cells. Due to the interaction of ZNF281 with NANOG, OCT4 and SOX2 and the enhanced expression of ZNF281 in breast and colorectal cancer it is conceivable that ZNF281 also contributes to the activity of NANOG, OCT4 and SOX2 in tumors. However, whether this is the case may be the subject of future studies. Recently, a bimodal switch consisting of miR-34a and its target Notch1, which determines whether colorectal cancer stem cells (CCSCs) undergo symmetric or asymmetric divisions and therefore whether CCSCs differentiate, has been described (Bu et al, 2013). Decreased miR-34a and increased Notch1 expression are hallmarks of CCSCs, whereas the reverse expression pattern is found in differentiated cells. It seems to be likely that ZNF281, which was recently identified as a direct target of miR-34a (Hahn et al, 2013), may also play a role in the miR-34a-mediated fate determination and suppression of stemness. In line with this assumption, ZNF281 is a direct target of miR-203 (Yi et al, 2008), which is known to suppress stem cell associated traits. *ZNF281* expression was down-regulated in transgenic K14-*miR-203* mice as well as in miR-203 transduced primary mouse keratinocytes (Yi et al, 2008). The *miR-203* gene is repressed by the EMT-TF ZEB1 (Wellner et al, 2009) and its epigenetic silencing is required for EMT and various other properties of cancer stem cells (Taube et al, 2013). Furthermore, miR-203 and SNAIL form a double negative feedback loop (Moes et al, 2012). Therefore, it is likely that SNAIL concomitantly with miR-203 form another feed-forward ZNF281-regulating circuit similar to the newly identified SNAIL and miR-34a feed-forward regulation presented in this thesis.

Moreover, the ZNF281-induced re-localization of β-catenin to the nucleus and the concomitant enhancement of β-catenin activity might contribute to ZNF281-mediated stemness, since WNT signaling is necessary to maintain stem cells in the intestinal crypts (Brabletz et al, 2005b; Pinto & Clevers, 2005; Scoville et al, 2008). Interestingly, Seo et al. found that knock-down of *ZNF281* resulted in decreased proliferation and diminished β-catenin expression in human multipotent stem cells (hMSCs) (Seo et al, 2013). Conversely, ectopic ZNF281 expression led to increased β-catenin expression,

which was accompanied by direct binding of ZNF281 to the *β-catenin* promoter (Seo et al, 2013). The occupation of the *β-catenin* promoter by ZNF281 may also contribute to the enhanced expression of *β-catenin* that was observed after ectopic ZNF281 expression in colorectal cancer cells (Hahn et al, 2013). Moreover, the study by Seo et al. showed that *ZNF281* knock-down in umbilical cord blood-derived mesenchymal stem cells (hUCB-MSCs) inhibits the adipogenic differentiation ability probably due to the resulting decrease in β-catenin, an important factor for early events in the adipogenesis of MSCs (Seo et al, 2013). In contrast, the osteogenic potential of hUCB-MSCs was enhanced after ZNF281 knock-down (Seo et al, 2013). The latter was verified by subcutaneous implantation of hUCB-MSCs with silenced *ZNF281* into mice, where the *ZNF281*-depleted hUCB-MSCs converted into osteoblasts more rapidly than the control cells (Seo et al, 2013). Furthermore, here it was demonstrated that ZNF281 directly represses *Axin2*, a negative regulator of the WNT pathway (Lustig et al, 2002). Thereby, ZNF281 presumably interrupts the negative feedback regulation of β-catenin by Axin2 and allows β-catenin to accumulate in the nucleus and activate target genes. However, ZNF281 might also promote β-catenin/TCF4 activity by mediating the loss of E-cadherin expression. E-cadherin is capable to prevent the nuclear localization and therefore activation of β-catenin by recruiting it to the cell-membrane (Orsulic et al, 1999; Sadot et al, 1998). Here, it could be further demonstrated that ZNF281 induces the expression of the stem cell markers *CD133* and *LGR5*. Additionally, ectopic ZNF281 expression increased sphere formation of colorectal cancer cells, which is an indicator of stemness, whereas ZNF281 knock-down decreased sphere formation (Hahn et al, 2013). Therefore, ZNF281 seems to be a regulator of tumor cell stemness similar to SNAIL, TWIST and ZEB1 which mediate increased stemness as well as EMT (Mani et al, 2008; Wellner et al, 2009). Colon tumors were shown to contain a subpopulation of CD133-positive cells with the ability to initiate tumor growth (Horst et al, 2008). In addition, high CD133 expression was associated with poor survival of colorectal cancer patients. Moreover, the combination of CD133 and the nuclear localization of β-catenin identified cases of low stage colorectal cancer with a high risk for tumor progression (Horst et al, 2009). In the future, the localization of ZNF281 in diverse stem cell compartments besides basal epidermal cells (Yi et al, 2008) has to be defined with respect to co-expression with stem cell markers and the expression pattern of other EMT-TFs. The expression of SNAIL und SLUG has already been observed in several

stem cell compartments such as those of melanocytes, hematopoietic cells as well as in the epithelial compartment of the gut (Horvay et al, 2011; Perez-Losada et al, 2002; Sanchez-Martin et al, 2003).

Since down-regulation of ZNF281 prevented the formation of lung metastases of a CRC cell line in a xenograft mouse model, it seems likely that enhancement of EMT and/or stemness by ZNF281 are important functions of ZNF281 during CRC progression. The inhibition of metastases formation after experimental down-regulation of SNAIL has been observed in a similar assay (Jackstadt et al, 2013). Therefore, the effect of ZNF281 down-regulation might be mediated, at least in part, by decreased expression of SNAIL and the concomitant loss of mesenchymal properties. Furthermore, the down-regulation of ZNF281 by p53 via miR-34a indicates that limiting ZNF281 function is critical for tumor suppression by p53. The increased expression of *ZNF281* mRNA in primary colorectal and breast carcinomas also points towards cancer promoting effects of ZNF281. Enhanced ZNF281 expression correlated with recurrence three years after removal of the primary colorectal tumor, suggesting that detection of elevated ZNF281 expression in primary tumors may have prognostic value. The ZNF281 paralog ZBP-89 already has been demonstrated to be up-regulated in various tumors such as gastric, colorectal and breast cancer (Zhang et al, 2012a). Moreover, enhanced ZBP-89 expression has been shown to correlate with the increased formation of distant metastases and poor survival of clear cell renal cell cancer patients (Cai et al, 2012). This underlines the necessity of closer investigations of ZNF281 expression levels in tumor tissues besides colon and breast cancer. In normal tissue enhanced ZNF281 expression levels were detected in the placenta, kidney, brain, heart, liver and lymphocytes (Law et al, 1999). Moreover, the detection of ZNF281 for the clinical characterization of tumor samples seems to be important to define the clinical patient outcome and the probability for recurrence.

More efforts are necessary to identify new upstream regulators of ZNF281 to better incorporate the newly defined EMT-inducer ZNF281 into the existing network of EMT-inducing transcription factors particularly with regard to potential regulatory signaling pathways. It should be interrogated whether well-known EMT-triggering pathways such as TGF-ß, WNT/β-catenin or HIF-1α signaling affect ZNF281 expression in order to induce EMT. Therefore, it seems to be important to precisely understand the role of ZNF281 within this process and to clearly define how ZNF281 and associated control

mechanisms influence tumor progression. The observations that systemic knock-out of *ZNF281* is embryonically lethal (Fidalgo et al, 2011) and that EMT plays a major role in embryonic development emphasize the importance of further studies on ZNF281. Similar to the deletion of *ZNF281*, the germ-line deletion of the EMT-TF *SNAIL* resulted in early embryonic lethality around day E8 due to gastrulation defects (Carver et al, 2001). To circumvent embryonic lethality Murray et al. generated mice with a floxed *SNAIL* allele, which allows the temporally controlled, Cre-mediated deletion of *SNAIL* and thereby the functional analysis of SNAIL in late embryogenesis and adult mice (Murray et al, 2006). Since systemic knock-out of *ZNF281* is embryonically lethal this implies that organismal studies on ZNF281 using conditional, somatic knock-out strategies should be performed in order to determine the *in vivo* relevance of ZNF281 during later stages of embryogenesis and postnatal development as well as in tumor progression and metastasis in more detail.

Tumor-suppressive miRNAs represent an interesting starting point for new therapeutical investigations with regard to cancer therapy as they are often down-regulated during cancer progression. The repression of ZNF281 by miR-34a may be an important component of the MET-process and experimental down-regulation of ZNF281 in a mesenchymal CRC cell line resulted in an epithelial phenotype. miR-34a might represent an attractive therapeutic starting point for ZNF281-mediated carcinogenesis. Kasinski and Slack demonstrated the therapeutic importance of miR-34a treatment by analyzing a Kras (LSL-G12D) (-/+) – Trp53 (LSL-R172H) (-/+) mouse lung cancer model. *In vivo* treatment by lentiviral infection with miR-34a prevented tumor formation and progression in those mice (Kasinski & Slack, 2012). This indicates the potential of miR-34 as a lung tumor-preventative and tumor–static agent (Kasinski & Slack, 2012), supposedly working via inhibition of SNAIL and ZNF281 as well as other miR-34a targets. Hence, a combined analysis of the status of miR-34a methylation, EMT-inducer expression (potentially ZNF281) and the following treatment with miR-34a mimicking molecules could represent a potential diagnostic and therapeutic approach in the clinic. Specific miRNA-replacement therapy seems to bear increasing potential for cancer treatment. Interestingly, a liposome-based miR-34 mimetic, MRX34, is the first cancer-targeting miRNA-based drug in Phase I clinical trials in patients with advanced or metastatic liver cancer (Ling et al, 2013). In orthotropic hepatocellular carcinoma mouse models MRX34 injection into the tail-vein resulted in reduced tumor growth and

increased survival rates (Bader, 2012). This supports the importance of miR-34-mediated target regulation in the carcinogenesis and may be, at least in part, due to the direct inhibition of ZNF281 by miR-34a. However, whether ZNF281 down-regulation is necessary for these effects remains to be shown.

In summary, ZNF281 was shown to represent an EMT-inducing transcription factor and that it presumably participates in the regulation of stemness and pluripotency by interaction with the transcription factors NANOG, OCT4, SOX2 and c-MYC in untransformed cells. Furthermore, there is evidence that ZNF281 also contributes to stemness in tumor stem cells (Figure 57). Nevertheless, the functional and organismal analysis of ZNF281 is still in its beginnings and many aspects still require more analyses. For example, the functional consequences of the direct interaction between the oncoprotein c-MYC and ZNF281 are still unknown (Koch et al, 2007). Potentially, ZNF281 could be used as both a disease marker of (c-MYC-driven) tumors and as a potential drug target. The identification of small molecules specifically preventing the DNA-binding of the ZNF281 transcription factor could also be part of future investigations towards cancer therapy. The results described here suggest that ZNF281 may be an interesting therapeutic target to inhibit metastasis. In the future it will be important to further illuminate the role and regulation of ZNF281 in diverse physiological and pathological processes in more detail. This knowledge will potentially serve as a basis for novel cancer diagnostic and therapeutic approaches in the future.

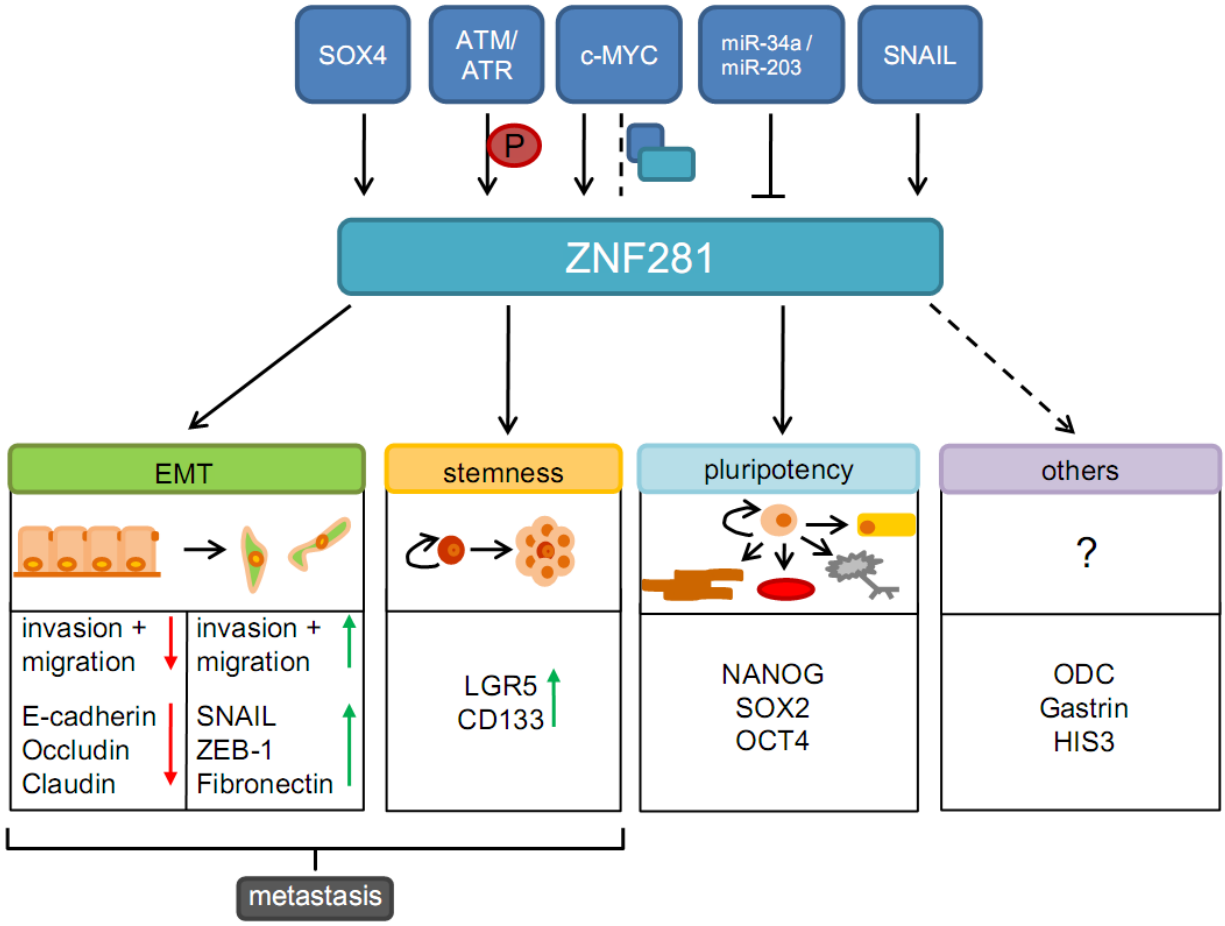

Figure 57: Model summarizing the regulation and function of ZNF281 presented in this thesis and in previous studies. Summary of regulations affecting ZNF281 expression/function and processes/factors regulated by ZNF281. Dashed lines indicate connections (protein interactions, gene regulations) for which the functional consequences still have to be determined. Red arrows symbolize inhibitions and green arrows indicate inductions (Hahn & Hermeking, 2014, *revised version submitted*).

7. SUMMARY

The vast majority of colorectal cancer (CRC)-related deaths is caused by the metastatic spread of tumor cells to distant organs rather than by the growth of the primary tumor. However, until today the mechanisms involved in CRC metastasis are not completely understood. For cancer cells the epithelial-mesenchymal transition (EMT) is thought to represent a prerequisite to invade adjacent tissue and form metastases at distant sites. Transcription factors, cytokines or oncogenic signaling pathways play an important role in the regulation of the EMT program. Recently, the oncoprotein c-MYC was shown to induce EMT, e.g. by enhancing SNAIL expression. Previously an interaction between c-MYC and the transcription factor ZNF281/ZBP-99 has been described. However, so far it remained elusive which upstream signals regulate ZNF281 levels or activity and furthermore, what functions are mediated by ZNF281, which may contribute to the c-MYC-mediated tumor progression. Here, it could be shown that SNAIL and miR-34a/b/c control the expression of ZNF281 in a coherent feed-forward-loop: the EMT-transcription factor SNAIL directly induced *ZNF281* transcription and repressed miR-34a/b/c, thereby alleviating ZNF281 from direct down-regulation by miR-34. Moreover, p53 activation led to a miR-34a-dependent down-regulation of ZNF281 expression. Additionally, in CRC cells it could be demonstrated, that ectopic ZNF281 expression induces EMT. This process was mediated by and dependent on the direct induction of SNAIL. Furthermore, ectopic ZNF281 increased migration/invasion, and enhanced β-catenin activity. Expression of the stemness markers *LGR5* was directly and *CD133* indirectly induced by ectopic ZNF281 expression, which also increased sphere formation. Conversely, in CRC cells the experimental down-regulation of ZNF281 resulted in a mesenchymal-epithelial transition (MET), inhibited migration/invasion and decreased sphere formation. Additionally, repression of ZNF281 led to decreased formation of lung metastases by CRC cells in a xenograft mouse tumor model. Furthermore, ZNF281 protein expression was indirectly elevated by ectopic c-MYC expression. Inactivation of ZNF281 prevented the induction of EMT by c-MYC or SNAIL. The analysis of tumor samples revealed that *ZNF281* expression increases during CRC progression and correlates with tumor recurrence.

Taken together, the results identify ZNF281 as a new EMT-promoting transcription factor, which contributes to metastasis formation in CRC. In the future, this knowledge may be exploited for therapeutic and diagnostic purposes in cancer therapy.

8. ZUSAMMENFASSUNG

Die überwiegende Mehrheit der durch das Kolorektalkarzinom (KRK) bedingten Todesfälle wird durch das metastatische Ausbreiten von Tumorzellen in von dem Primärtumor entferntere Organe verursacht, anstatt durch das lokale Wachstum des Primärtumors. Die für die Metastasierung von KRK verantwortlichen Mechanismen sind jedoch bis heute noch nicht vollständig aufgeklärt. Die epithelial-mesenchymale Transition (EMT) wird als Voraussetzung dafür angesehen, dass Krebszellen in angrenzendes Gewebe und die Blutbahn eindringen und so in entfernten Organen Metastasen bilden können. Transkriptionsfaktoren, Zytokine oder onkogen-wirkende Signalwege spielen eine wichtige Rolle in der Regulation des EMT-Programmes. Vor Kurzem konnte gezeigt werden, dass das c-MYC Onkoprotein, beispielsweise durch die Induktion von SNAIL, EMT regulieren kann. Weiterhin konnte zuvor die Interaktion zwischen c-MYC und dem Transkriptionsfaktor ZNF281/ZBP-99 beschrieben werden. Jedoch war bisher kaum oder nicht bekannt, welche übergeordneten Signale die Expression oder Aktivität von ZNF281 regulieren und des Weiteren, welche Funktionen durch ZNF281 ausgeübt werden, die zu der c-MYC-vermittelten Tumorprogression beitragen können. In dieser Arbeit konnte gezeigt werden, dass die Expression von ZNF281 durch SNAIL und miR-34a/b/c in einer kohärent vorwärts-gerichteten Regulationsschleife kontrolliert wird: der EMT-hervorrufende Transkriptionsfaktor SNAIL induzierte direkt die *ZNF281* Transkription und reprimierte miR-34a/b/c, wodurch die direkte Repression von ZNF281 durch miR-34 abgeschwächt wird. Darüber hinaus resultierte die Aktivierung des Tumorsupressors p53 in der miR-34a-abhängigen Unterdrückung der ZNF281 Expression. Außerdem konnte gezeigt werden, dass die ektopische ZNF281 Expression in KRK-Zellen EMT induziert. Dieser Prozess wird durch die direkte Induktion von SNAIL vermittelt. Zudem erhöhte die ektopische Expression von ZNF281 die Migration/Invasion und verstärkte die β-Catenin Aktivität. Durch ektopische ZNF281 Expression wurde die Expression der Stammzellmarker *LGR5* direkt und *CD133* indirekt gesteigert. Hierdurch wurde zusätzlich die Fähigkeit von KRK-Zellen Sphären zu bilden verstärkt. Im Gegensatz dazu resultierte die experimentelle Repression von ZNF281 in KRK-Zellen in einer mesenchymal-epithelialen Transition (MET), einer verminderten Migration und Invasion sowie einer verringerten Zellsphärenbildung. Zusätzlich führte die Verminderung von ZNF281 zu einer geringeren Bildung von Lungenmetastasen durch KRK-Zellen in einem Xenograft-

Maustumormodell. Außerdem konnte die ZNF281 Expression durch ektopisches c-MYC gesteigert werden. Die Inaktivierung von ZNF281 verhinderte die Induktion einer EMT durch c-MYC oder SNAIL. Die Analyse von Patientenproben ergab, dass die *ZNF281* Expression mit fortschreitendem Verlauf bei KRK ansteigt und mit dem Wiederauftreten des Tumors nach Therapie korreliert.

Zusammenfassend konnte der Transkriptionsfaktor ZNF281 als ein EMT-fördernder Faktor identifiziert werden, welcher zur Bildung von Metastasen bei KRK beiträgt. In der Zukunft könnte dieses Wissen für therapeutische und diagnostische Zwecke in der Krebstherapie genutzt werden.

9. REFERENCES

Amati B, Frank SR, Donjerkovic D, Taubert S (2001) Function of the c-Myc oncoprotein in chromatin remodeling and transcription. *Biochim Biophys Acta* **1471:** M135-145

Amsterdam A, Raanan C, Schreiber L, Freyhan O, Fabrikant Y, Melzer E, Givol D (2013) Differential localization of LGR5 and Nanog in clusters of colon cancer stem cells. *Acta Histochem* **115:** 320-329

Antonini D, Russo MT, De Rosa L, Gorrese M, Del Vecchio L, Missero C (2010) Transcriptional repression of miR-34 family contributes to p63-mediated cell cycle progression in epidermal cells. *J Invest Dermatol* **130:** 1249-1257

Bader AG (2012) miR-34 - a microRNA replacement therapy is headed to the clinic. *Front Genet* **3:** 120

Bai L, Kao JY, Law DJ, Merchant JL (2006) Recruitment of ataxia-telangiectasia mutated to the p21(waf1) promoter by ZBP-89 plays a role in mucosal protection. *Gastroenterology* **131:** 841-852

Bai L, Merchant JL (2001) ZBP-89 promotes growth arrest through stabilization of p53. *Mol Cell Biol* **21:** 4670-4683

Bai L, Merchant JL (2007) ATM phosphorylates ZBP-89 at Ser202 to potentiate p21waf1 induction by butyrate. *Biochem Biophys Res Commun* **359:** 817-821

Bai L, Yoon SO, King PD, Merchant JL (2004) ZBP-89-induced apoptosis is p53-independent and requires JNK. *Cell Death Differ* **11:** 663-673

Barbera MJ, Puig I, Dominguez D, Julien-Grille S, Guaita-Esteruelas S, Peiro S, Baulida J, Franci C, Dedhar S, Larue L, Garcia de Herreros A (2004) Regulation of Snail transcription during epithelial to mesenchymal transition of tumor cells. *Oncogene* **23:** 7345-7354

Barker N, van Es JH, Kuipers J, Kujala P, van den Born M, Cozijnsen M, Haegebarth A, Korving J, Begthel H, Peters PJ, Clevers H (2007) Identification of stem cells in small intestine and colon by marker gene Lgr5. *Nature* **449:** 1003-1007

Bartel DP (2004) MicroRNAs: genomics, biogenesis, mechanism, and function. *Cell* **116:** 281-297

Bartel DP (2009) MicroRNAs: target recognition and regulatory functions. *Cell* **136:** 215-233

Batlle E, Sancho E, Franci C, Dominguez D, Monfar M, Baulida J, Garcia De Herreros A (2000) The transcription factor snail is a repressor of E-cadherin gene expression in epithelial tumour cells. *Nat Cell Biol* **2:** 84-89

Baudino TA, McKay C, Pendeville-Samain H, Nilsson JA, Maclean KH, White EL, Davis AC, Ihle JN, Cleveland JL (2002) c-Myc is essential for vasculogenesis and angiogenesis during development and tumor progression. *Genes Dev* **16:** 2530-2543

Baum B, Settleman J, Quinlan MP (2008) Transitions between epithelial and mesenchymal states in development and disease. *Semin Cell Dev Biol* **19:** 294-308

Beauchemin N (2011) The colorectal tumor microenvironment: the next decade. *Cancer Microenviron* **4:** 181-185

Beroukhim R, Mermel CH, Porter D, Wei G, Raychaudhuri S, Donovan J, Barretina J, Boehm JS, Dobson J, Urashima M, Mc Henry KT, Pinchback RM, Ligon AH, Cho YJ, Haery L, Greulich H, Reich M, Winckler W, Lawrence MS, Weir BA, Tanaka KE, Chiang DY, Bass AJ, Loo A, Hoffman C, Prensner J, Liefeld T, Gao Q, Yecies D, Signoretti S, Maher E, Kaye FJ, Sasaki H, Tepper JE, Fletcher JA, Tabernero J, Baselga J, Tsao MS, Demichelis F, Rubin MA, Janne PA, Daly MJ, Nucera C, Levine RL, Ebert BL, Gabriel S, Rustgi AK, Antonescu CR, Ladanyi M, Letai A, Garraway LA, Loda M, Beer DG, True LD, Okamoto A, Pomeroy SL, Singer S, Golub TR, Lander ES, Getz G, Sellers WR, Meyerson M (2010) The landscape of somatic copy-number alteration across human cancers. *Nature* **463:** 899-905

Birchmeier W, Brinkmann V, Niemann C, Meiners S, DiCesare S, Naundorf H, Sachs M (1997) Role of HGF/SF and c-Met in morphogenesis and metastasis of epithelial cells. *Ciba Found Symp* **212:** 230-240; discussion 240-236

Black AR, Black JD, Azizkhan-Clifford J (2001) Sp1 and kruppel-like factor family of transcription factors in cell growth regulation and cancer. *J Cell Physiol* **188:** 143-160

Bommer GT, Gerin I, Feng Y, Kaczorowski AJ, Kuick R, Love RE, Zhai Y, Giordano TJ, Qin ZS, Moore BB, MacDougald OA, Cho KR, Fearon ER (2007) p53-mediated activation of miRNA34 candidate tumor-suppressor genes. *Curr Biol* **17:** 1298-1307

Boominathan L (2010) The guardians of the genome (p53, TA-p73, and TA-p63) are regulators of tumor suppressor miRNAs network. *Cancer Metastasis Rev* **29:** 613-639

Bornkamm GW, Berens C, Kuklik-Roos C, Bechet JM, Laux G, Bachl J, Korndoerfer M, Schlee M, Holzel M, Malamoussi A, Chapman RD, Nimmerjahn F, Mautner J, Hillen W, Bujard H, Feuillard J (2005) Stringent doxycycline-dependent control of gene activities using an episomal one-vector system. *Nucleic Acids Res* **33:** e137

Bornschein J, Toth K, Selgrad M, Kuester D, Wex T, Molnar B, Tulassay Z, Malfertheiner P (2013) Dysregulation of CDX1, CDX2 and SOX2 in patients with gastric cancer also affects the non-malignant mucosa. *J Clin Pathol* **66:** 819-822

Boyer B, Roche S, Denoyelle M, Thiery JP (1997) Src and Ras are involved in separate pathways in epithelial cell scattering. *EMBO J* **16:** 5904-5913

Boyer B, Thiery JP (1993) Epithelium-mesenchyme interconversion as example of epithelial plasticity. *APMIS* **101:** 257-268

Brabletz T (2012) MiR-34 and SNAIL: another double-negative feedback loop controlling cellular plasticity/EMT governed by p53. *Cell Cycle* **11:** 215-216

Brabletz T, Hlubek F, Spaderna S, Schmalhofer O, Hiendlmeyer E, Jung A, Kirchner T (2005a) Invasion and metastasis in colorectal cancer: epithelial-mesenchymal transition, mesenchymal-epithelial transition, stem cells and beta-catenin. *Cells Tissues Organs* **179:** 56-65

Brabletz T, Jung A, Reu S, Porzner M, Hlubek F, Kunz-Schughart LA, Knuechel R, Kirchner T (2001) Variable beta-catenin expression in colorectal cancers indicates tumor progression driven by the tumor environment. *Proc Natl Acad Sci U S A* **98:** 10356-10361

Brabletz T, Jung A, Spaderna S, Hlubek F, Kirchner T (2005b) Opinion: migrating cancer stem cells - an integrated concept of malignant tumour progression. *Nat Rev Cancer* **5:** 744-749

Brownawell AM, Macara IG (2002) Exportin-5, a novel karyopherin, mediates nuclear export of double-stranded RNA binding proteins. *J Cell Biol* **156:** 53-64

Bu P, Chen KY, Chen JH, Wang L, Walters J, Shin YJ, Goerger JP, Sun J, Witherspoon M, Rakhilin N, Li J, Yang H, Milsom J, Lee S, Zipfel W, Jin MM, Gumus ZH, Lipkin SM, Shen X (2013) A microRNA miR-34a-regulated bimodal switch targets notch in colon cancer stem cells. *Cell Stem Cell* **12:** 602-615

Bubendorf L, Kononen J, Koivisto P, Schraml P, Moch H, Gasser TC, Willi N, Mihatsch MJ, Sauter G, Kallioniemi OP (1999) Survey of gene amplifications during prostate

cancer progression by high-throughout fluorescence in situ hybridization on tissue microarrays. *Cancer Res* **59:** 803-806

Buttyan R, Sawczuk IS, Benson MC, Siegal JD, Olsson CA (1987) Enhanced expression of the c-myc protooncogene in high-grade human prostate cancers. *Prostate* **11:** 327-337

Byles V, Zhu L, Lovaas JD, Chmilewski LK, Wang J, Faller DV, Dai Y (2012) SIRT1 induces EMT by cooperating with EMT transcription factors and enhances prostate cancer cell migration and metastasis. *Oncogene* **31:** 4619-4629

Cai MY, Luo RZ, Li YH, Dong P, Zhang ZL, Zhou FJ, Chen JW, Yun JP, Zhang CZ, Cao Y (2012) High-expression of ZBP-89 correlates with distal metastasis and poor prognosis of patients in clear cell renal cell carcinoma. *Biochem Biophys Res Commun* **426:** 636-642

Cannito S, Novo E, Compagnone A, Valfre di Bonzo L, Busletta C, Zamara E, Paternostro C, Povero D, Bandino A, Bozzo F, Cravanzola C, Bravoco V, Colombatto S, Parola M (2008) Redox mechanisms switch on hypoxia-dependent epithelial-mesenchymal transition in cancer cells. *Carcinogenesis* **29:** 2267-2278

Cano A, Perez-Moreno MA, Rodrigo I, Locascio A, Blanco MJ, del Barrio MG, Portillo F, Nieto MA (2000) The transcription factor snail controls epithelial-mesenchymal transitions by repressing E-cadherin expression. *Nat Cell Biol* **2:** 76-83

Carmon KS, Lin Q, Gong X, Thomas A, Liu Q (2012) LGR5 interacts and cointernalizes with Wnt receptors to modulate Wnt/beta-catenin signaling. *Mol Cell Biol* **32:** 2054-2064

Carver EA, Jiang R, Lan Y, Oram KF, Gridley T (2001) The mouse snail gene encodes a key regulator of the epithelial-mesenchymal transition. *Mol Cell Biol* **21:** 8184-8188

Casas E, Kim J, Bendesky A, Ohno-Machado L, Wolfe CJ, Yang J (2011) Snail2 is an essential mediator of Twist1-induced epithelial mesenchymal transition and metastasis. *Cancer Res* **71:** 245-254

Chang CJ, Chao CH, Xia W, Yang JY, Xiong Y, Li CW, Yu WH, Rehman SK, Hsu JL, Lee HH, Liu M, Chen CT, Yu D, Hung MC (2011) p53 regulates epithelial-mesenchymal transition and stem cell properties through modulating miRNAs. *Nat Cell Biol* **13:** 317-323

Chang TC, Wentzel EA, Kent OA, Ramachandran K, Mullendore M, Lee KH, Feldmann G, Yamakuchi M, Ferlito M, Lowenstein CJ, Arking DE, Beer MA, Maitra A, Mendell JT

(2007) Transactivation of miR-34a by p53 broadly influences gene expression and promotes apoptosis. *Mol Cell* **26:** 745-752

Chang TC, Yu D, Lee YS, Wentzel EA, Arking DE, West KM, Dang CV, Thomas-Tikhonenko A, Mendell JT (2008) Widespread microRNA repression by Myc contributes to tumorigenesis. *Nat Genet* **40:** 43-50

Chen S, Xu Y, Chen Y, Li X, Mou W, Wang L, Liu Y, Reisfeld RA, Xiang R, Lv D, Li N (2012) SOX2 gene regulates the transcriptional network of oncogenes and affects tumorigenesis of human lung cancer cells. *PLoS One* **7:** e36326

Chen Z, Xu WR, Qian H, Zhu W, Bu XF, Wang S, Yan YM, Mao F, Gu HB, Cao HL, Xu XJ (2009) Oct4, a novel marker for human gastric cancer. *J Surg Oncol* **99:** 414-419

Cheng CY, Hwang CI, Corney DC, Flesken-Nikitin A, Jiang L, Oner GM, Munroe RJ, Schimenti JC, Hermeking H, Nikitin AY (2014) miR-34 Cooperates with p53 in Suppression of Prostate Cancer by Joint Regulation of Stem Cell Compartment. *Cell Rep* **6:** 1000-1007

Christiansen JJ, Rajasekaran AK (2006) Reassessing epithelial to mesenchymal transition as a prerequisite for carcinoma invasion and metastasis. *Cancer Res* **66:** 8319-8326

Christoffersen NR, Shalgi R, Frankel LB, Leucci E, Lees M, Klausen M, Pilpel Y, Nielsen FC, Oren M, Lund AH (2010) p53-independent upregulation of miR-34a during oncogene-induced senescence represses MYC. *Cell Death Differ* **17:** 236-245

Cowling VH, Cole MD (2006) Mechanism of transcriptional activation by the Myc oncoproteins. *Semin Cancer Biol* **16:** 242-252

Dang CV (2012) MYC on the path to cancer. *Cell* **149:** 22-35

Dang CV, Resar LM, Emison E, Kim S, Li Q, Prescott JE, Wonsey D, Zeller K (1999) Function of the c-Myc oncogenic transcription factor. *Exp Cell Res* **253:** 63-77

Dang H, Ding W, Emerson D, Rountree CB (2011) Snail1 induces epithelial-to-mesenchymal transition and tumor initiating stem cell characteristics. *BMC Cancer* **11:** 396

De Craene B, Berx G (2013) Regulatory networks defining EMT during cancer initiation and progression. *Nat Rev Cancer* **13:** 97-110

De Craene B, Gilbert B, Stove C, Bruyneel E, van Roy F, Berx G (2005) The transcription factor snail induces tumor cell invasion through modulation of the epithelial cell differentiation program. *Cancer Res* **65:** 6237-6244

de Herreros AG, Peiro S, Nassour M, Savagner P (2010) Snail family regulation and epithelial mesenchymal transitions in breast cancer progression. *J Mammary Gland Biol Neoplasia* **15:** 135-147

Diaz-Martin J, Diaz-Lopez A, Moreno-Bueno G, Castilla MA, Rosa-Rosa JM, Cano A, Palacios J (2014) A core microRNA signature associated with inducers of the epithelial-to-mesenchymal transition. *J Pathol* **232:** 319-329

Dong C, Wu Y, Wang Y, Wang C, Kang T, Rychahou PG, Chi YI, Evers BM, Zhou BP (2013) Interaction with Suv39H1 is critical for Snail-mediated E-cadherin repression in breast cancer. *Oncogene* **32:** 1351-1362

Dong C, Wu Y, Yao J, Wang Y, Yu Y, Rychahou PG, Evers BM, Zhou BP (2012) G9a interacts with Snail and is critical for Snail-mediated E-cadherin repression in human breast cancer. *J Clin Invest* **122:** 1469-1486

Duesberg PH, Vogt PK (1979) Avian acute leukemia viruses MC29 and MH2 share specific RNA sequences: evidence for a second class of transforming genes. *Proc Natl Acad Sci U S A* **76:** 1633-1637

Eilers M, Eisenman RN (2008) Myc's broad reach. *Genes Dev* **22:** 2755-2766

Epanchintsev A, Jung P, Menssen A, Hermeking H (2006) Inducible microRNA expression by an all-in-one episomal vector system. *Nucleic Acids Res* **34:** e119

Esquela-Kerscher A, Slack FJ (2006) Oncomirs - microRNAs with a role in cancer. *Nat Rev Cancer* **6:** 259-269

Essien BE, Grasberger H, Romain RD, Law DJ, Veniaminova NA, Saqui-Salces M, El-Zaatari M, Tessier A, Hayes MM, Yang AC, Merchant JL (2013) ZBP-89 regulates expression of tryptophan hydroxylase I and mucosal defense against Salmonella typhimurium in mice. *Gastroenterology* **144:** 1466-1477, 1477 e1461-1469

Fan XS, Wu HY, Yu HP, Zhou Q, Zhang YF, Huang Q (2010) Expression of Lgr5 in human colorectal carcinogenesis and its potential correlation with beta-catenin. *Int J Colorectal Dis* **25:** 583-590

Felsher DW, Bishop JM (1999) Transient excess of MYC activity can elicit genomic instability and tumorigenesis. *Proc Natl Acad Sci U S A* **96:** 3940-3944

Fidalgo M, Faiola F, Pereira CF, Ding J, Saunders A, Gingold J, Schaniel C, Lemischka IR, Silva JC, Wang J. (2012) Zfp281 mediates Nanog autorepression through recruitment of the NuRD complex and inhibits somatic cell reprogramming. *Proc Natl Acad Sci U S A*, Vol. 109, pp. 16202-16207.

Fidalgo M, Shekar PC, Ang YS, Fujiwara Y, Orkin SH, Wang J (2011) Zfp281 functions as a transcriptional repressor for pluripotency of mouse embryonic stem cells. *Stem Cells* **29:** 1705-1716

Fidler IJ (2003) The pathogenesis of cancer metastasis: the 'seed and soil' hypothesis revisited. *Nat Rev Cancer* **3:** 453-458

Fleming WH, Hamel A, MacDonald R, Ramsey E, Pettigrew NM, Johnston B, Dodd JG, Matusik RJ (1986) Expression of the c-myc protooncogene in human prostatic carcinoma and benign prostatic hyperplasia. *Cancer Res* **46:** 1535-1538

Franci C, Takkunen M, Dave N, Alameda F, Gomez S, Rodriguez R, Escriva M, Montserrat-Sentis B, Baro T, Garrido M, Bonilla F, Virtanen I, Garcia de Herreros A (2006) Expression of Snail protein in tumor-stroma interface. *Oncogene* **25:** 5134-5144

Friedl P, Alexander S (2011) Cancer invasion and the microenvironment: plasticity and reciprocity. *Cell* **147:** 992-1009

Friedman RC, Farh KK, Burge CB, Bartel DP (2009) Most mammalian mRNAs are conserved targets of microRNAs. *Genome Res* **19:** 92-105

Frost M, Newell J, Lones MA, Tripp SR, Cairo MS, Perkins SL (2004) Comparative immunohistochemical analysis of pediatric Burkitt lymphoma and diffuse large B-cell lymphoma. *Am J Clin Pathol* **121:** 384-392

Gavioli R, Frisan T, Vertuani S, Bornkamm GW, Masucci MG (2001) c-myc overexpression activates alternative pathways for intracellular proteolysis in lymphoma cells. *Nat Cell Biol* **3:** 283-288

Glinka A, Dolde C, Kirsch N, Huang YL, Kazanskaya O, Ingelfinger D, Boutros M, Cruciat CM, Niehrs C (2011) LGR4 and LGR5 are R-spondin receptors mediating Wnt/beta-catenin and Wnt/PCP signalling. *EMBO Rep* **12:** 1055-1061

Gort EH, Groot AJ, van der Wall E, van Diest PJ, Vooijs MA (2008) Hypoxic regulation of metastasis via hypoxia-inducible factors. *Curr Mol Med* **8:** 60-67

Gregory PA, Bert AG, Paterson EL, Barry SC, Tsykin A, Farshid G, Vadas MA, Khew-Goodall Y, Goodall GJ (2008) The miR-200 family and miR-205 regulate epithelial to mesenchymal transition by targeting ZEB1 and SIP1. *Nat Cell Biol* **10:** 593-601

Griffin JB, Rodriguez-Melendez R, Zempleni J (2003) The nuclear abundance of transcription factors Sp1 and Sp3 depends on biotin in Jurkat cells. *J Nutr* **133:** 3409-3415

Grimson A, Farh KK, Johnston WK, Garrett-Engele P, Lim LP, Bartel DP (2007) MicroRNA targeting specificity in mammals: determinants beyond seed pairing. *Mol Cell* **27:** 91-105

Grunert S, Jechlinger M, Beug H (2003) Diverse cellular and molecular mechanisms contribute to epithelial plasticity and metastasis. *Nat Rev Mol Cell Biol* **4:** 657-665

Guaita S, Puig I, Franci C, Garrido M, Dominguez D, Batlle E, Sancho E, Dedhar S, De Herreros AG, Baulida J (2002) Snail induction of epithelial to mesenchymal transition in tumor cells is accompanied by MUC1 repression and ZEB1 expression. *J Biol Chem* **277:** 39209-39216

Hahn S and Hermeking H (2014) ZNF281/ZBP-99: a new player in epithelial-mesenchymal-transition, stemness and cancer. *J Mol Med*, *revised version submitted*

Hahn S, Jackstadt R, Siemens H, Hunten S, Hermeking H (2013) SNAIL and miR-34a feed-forward regulation of ZNF281/ZBP99 promotes epithelial-mesenchymal transition. *EMBO J* **32:** 3079-3095

Han X, Fang X, Lou X, Hua D, Ding W, Foltz G, Hood L, Yuan Y, Lin B (2012) Silencing SOX2 induced mesenchymal-epithelial transition and its expression predicts liver and lymph node metastasis of CRC patients. *PLoS One* **7:** e41335

He L, He X, Lim LP, de Stanchina E, Xuan Z, Liang Y, Xue W, Zender L, Magnus J, Ridzon D, Jackson AL, Linsley PS, Chen C, Lowe SW, Cleary MA, Hannon GJ (2007) A microRNA component of the p53 tumour suppressor network. *Nature* **447:** 1130-1134

He TC, Chan TA, Vogelstein B, Kinzler KW (1999) PPARdelta is an APC-regulated target of nonsteroidal anti-inflammatory drugs. *Cell* **99:** 335-345

He TC, Sparks AB, Rago C, Hermeking H, Zawel L, da Costa LT, Morin PJ, Vogelstein B, Kinzler KW (1998) Identification of c-MYC as a target of the APC pathway. *Science* **281:** 1509-1512

Hermeking H (2010) The miR-34 family in cancer and apoptosis. *Cell Death Differ* **17:** 193-199

Hermeking H (2012) MicroRNAs in the p53 network: micromanagement of tumour suppression. *Nat Rev Cancer* **12:** 613-626

Herranz N, Pasini D, Diaz VM, Franci C, Gutierrez A, Dave N, Escriva M, Hernandez-Munoz I, Di Croce L, Helin K, Garcia de Herreros A, Peiro S (2008) Polycomb complex 2 is required for E-cadherin repression by the Snail1 transcription factor. *Mol Cell Biol* **28:** 4772-4781

Hollestelle A, Peeters JK, Smid M, Timmermans M, Verhoog LC, Westenend PJ, Heine AA, Chan A, Sieuwerts AM, Wiemer EA, Klijn JG, van der Spek PJ, Foekens JA, Schutte M, den Bakker MA, Martens JW (2013) Loss of E-cadherin is not a necessity for epithelial to mesenchymal transition in human breast cancer. *Breast Cancer Res Treat* **138:** 47-57

Horst D, Kriegl L, Engel J, Jung A, Kirchner T (2009) CD133 and nuclear beta-catenin: the marker combination to detect high risk cases of low stage colorectal cancer. *Eur J Cancer* **45:** 2034-2040

Horst D, Kriegl L, Engel J, Kirchner T, Jung A (2008) CD133 expression is an independent prognostic marker for low survival in colorectal cancer. *Br J Cancer* **99:** 1285-1289

Horvay K, Casagranda F, Gany A, Hime GR, Abud HE (2011) Wnt signaling regulates Snai1 expression and cellular localization in the mouse intestinal epithelial stem cell niche. *Stem Cells Dev* **20:** 737-745

Hu SS, Lai MM, Vogt PK (1979) Genome of avian myelocytomatosis virus MC29: analysis by heteroduplex mapping. *Proc Natl Acad Sci U S A* **76:** 1265-1268

Hugo H, Ackland ML, Blick T, Lawrence MG, Clements JA, Williams ED, Thompson EW (2007) Epithelial--mesenchymal and mesenchymal--epithelial transitions in carcinoma progression. *J Cell Physiol* **213:** 374-383

Hugo HJ, Kokkinos MI, Blick T, Ackland ML, Thompson EW, Newgreen DF (2011) Defining the E-cadherin repressor interactome in epithelial-mesenchymal transition: the PMC42 model as a case study. *Cells Tissues Organs* **193:** 23-40

Hutvagner G, McLachlan J, Pasquinelli AE, Balint E, Tuschl T, Zamore PD (2001) A cellular function for the RNA-interference enzyme Dicer in the maturation of the let-7 small temporal RNA. *Science* **293:** 834-838

Hwang WL, Yang MH, Tsai ML, Lan HY, Su SH, Chang SC, Teng HW, Yang SH, Lan YT, Chiou SH, Wang HW (2011) SNAIL regulates interleukin-8 expression, stem cell-like activity, and tumorigenicity of human colorectal carcinoma cells. *Gastroenterology* **141:** 279-291, 291 e271-275

Iacobuzio-Donahue CA (2009) Epigenetic changes in cancer. *Annu Rev Pathol* **4:** 229-249

Ibrahim EE, Babaei-Jadidi R, Saadeddin A, Spencer-Dene B, Hossaini S, Abuzinadah M, Li N, Fadhil W, Ilyas M, Bonnet D, Nateri AS (2012) Embryonic NANOG activity defines colorectal cancer stem cells and modulates through AP1- and TCF-dependent mechanisms. *Stem Cells* **30:** 2076-2087

Ikenouchi J, Matsuda M, Furuse M, Tsukita S (2003) Regulation of tight junctions during the epithelium-mesenchyme transition: direct repression of the gene expression of claudins/occludin by Snail. *J Cell Sci* **116:** 1959-1967

Iliopoulos D, Lindahl-Allen M, Polytarchou C, Hirsch HA, Tsichlis PN, Struhl K (2010) Loss of miR-200 inhibition of Suz12 leads to polycomb-mediated repression required for the formation and maintenance of cancer stem cells. *Mol Cell* **39:** 761-772

Jackstadt R, Roeh S, Neumann S, Jung P, Hoffmann R, Horst D, Berens C, Bornkamm GW, Kirchner T, Menssen A, Hermeking H (2013) AP4 is a mediator of epithelial-mesenchymal transition and metastasis in colorectal cancer. *J Exp Med* **210:** 1331-1350

James D, Levine AJ, Besser D, Hemmati-Brivanlou A (2005) TGFbeta/activin/nodal signaling is necessary for the maintenance of pluripotency in human embryonic stem cells. *Development* **132:** 1273-1282

Jechlinger M, Grunert S, Tamir IH, Janda E, Ludemann S, Waerner T, Seither P, Weith A, Beug H, Kraut N (2003) Expression profiling of epithelial plasticity in tumor progression. *Oncogene* **22:** 7155-7169

Jiang J, Tang YL, Liang XH (2011) EMT: a new vision of hypoxia promoting cancer progression. *Cancer Biol Ther* **11:** 714-723

John B, Enright AJ, Aravin A, Tuschl T, Sander C, Marks DS (2004) Human MicroRNA targets. *PLoS Biol* **2:** e363:1862-1879

Joyce JA, Pollard JW (2009) Microenvironmental regulation of metastasis. *Nat Rev Cancer* **9:** 239-252

Jung P, Hermeking H (2009) The c-MYC-AP4-p21 cascade. *Cell Cycle* **8:** 982-989

Kaller M, Liffers ST, Oeljeklaus S, Kuhlmann K, Roh S, Hoffmann R, Warscheid B, Hermeking H (2011) Genome-wide characterization of miR-34a induced changes in protein and mRNA expression by a combined pulsed SILAC and microarray analysis. *Mol Cell Proteomics* **10:** M111 010462

Kalluri R, Weinberg RA (2009) The basics of epithelial-mesenchymal transition. *J Clin Invest* **119:** 1420-1428

Kasinski AL, Slack FJ (2012) miRNA-34 prevents cancer initiation and progression in a therapeutically resistant K-ras and p53-induced mouse model of lung adenocarcinoma. *Cancer Res* **72:** 5576-5587

Katoh Y, Katoh M (2007) Comparative genomics on PROM1 gene encoding stem cell marker CD133. *Int J Mol Med* **19:** 967-970

Kim NH, Kim HS, Li XY, Lee I, Choi HS, Kang SE, Cha SY, Ryu JK, Yoon D, Fearon ER, Rowe RG, Lee S, Maher CA, Weiss SJ, Yook JI (2011) A p53/miRNA-34 axis regulates Snail1-dependent cancer cell epithelial-mesenchymal transition. *J Cell Biol* **195:** 417-433

Koch HB, Zhang R, Verdoodt B, Bailey A, Zhang CD, Yates JR, 3rd, Menssen A, Hermeking H (2007) Large-scale identification of c-MYC-associated proteins using a combined TAP/MudPIT approach. *Cell Cycle* **6:** 205-217

Korpal M, Lee ES, Hu G, Kang Y (2008) The miR-200 family inhibits epithelial-mesenchymal transition and cancer cell migration by direct targeting of E-cadherin transcriptional repressors ZEB1 and ZEB2. *J Biol Chem* **283:** 14910-14914

Kress TR, Cannell IG, Brenkman AB, Samans B, Gaestel M, Roepman P, Burgering BM, Bushell M, Rosenwald A, Eilers M (2011) The MK5/PRAK kinase and Myc form a

negative feedback loop that is disrupted during colorectal tumorigenesis. *Mol Cell* **41:** 445-457

Law DJ, Du M, Law GL, Merchant JL (1999) ZBP-99 defines a conserved family of transcription factors and regulates ornithine decarboxylase gene expression. *Biochem Biophys Res Commun* **262:** 113-120

Law DJ, Labut EM, Adams RD, Merchant JL (2006a) An isoform of ZBP-89 predisposes the colon to colitis. *Nucleic Acids Res* **34:** 1342-1350

Law DJ, Labut EM, Merchant JL (2006b) Intestinal overexpression of ZNF148 suppresses ApcMin/+ neoplasia. *Mamm Genome* **17:** 999-1004

Lee JM, Dedhar S, Kalluri R, Thompson EW (2006) The epithelial-mesenchymal transition: new insights in signaling, development, and disease. *J Cell Biol* **172:** 973-981

Lee SH, Hu LL, Gonzalez-Navajas J, Seo GS, Shen C, Brick J, Herdman S, Varki N, Corr M, Lee J, Raz E (2010) ERK activation drives intestinal tumorigenesis in Apc(min/+) mice. *Nat Med* **16:** 665-670

Lengerke C, Fehm T, Kurth R, Neubauer H, Scheble V, Muller F, Schneider F, Petersen K, Wallwiener D, Kanz L, Fend F, Perner S, Bareiss PM, Staebler A (2011) Expression of the embryonic stem cell marker SOX2 in early-stage breast carcinoma. *BMC Cancer* **11:** 42

Li C, Yan Y, Ji W, Bao L, Qian H, Chen L, Wu M, Chen H, Li Z, Su C (2012) OCT4 positively regulates Survivin expression to promote cancer cell proliferation and leads to poor prognosis in esophageal squamous cell carcinoma. *PLoS One* **7:** e49693

Li X, Xiong JW, Shelley CS, Park H, Arnaout MA (2006) The transcription factor ZBP-89 controls generation of the hematopoietic lineage in zebrafish and mouse embryonic stem cells. *Development* **133:** 3641-3650

Lim SO, Kim H, Jung G (2010) p53 inhibits tumor cell invasion via the degradation of snail protein in hepatocellular carcinoma. *FEBS Lett* **584:** 2231-2236

Lin T, Ponn A, Hu X, Law BK, Lu J (2010) Requirement of the histone demethylase LSD1 in Snai1-mediated transcriptional repression during epithelial-mesenchymal transition. *Oncogene* **29:** 4896-4904

Ling H, Fabbri M, Calin GA (2013) MicroRNAs and other non-coding RNAs as targets for anticancer drug development. *Nat Rev Drug Discov* **12:** 847-865

Lisowsky T, Polosa PL, Sagliano A, Roberti M, Gadaleta MN, Cantatore P (1999) Identification of human GC-box-binding zinc finger protein, a new Kruppel-like zinc finger protein, by the yeast one-hybrid screening with a GC-rich target sequence. *FEBS Lett* **453:** 369-374

Liu YH, Li Y, Liu XH, Sui HM, Liu YX, Xiao ZQ, Zheng P, Chen L, Yao S, Xing C, Zhou J, Li JM (2013) A signature for induced pluripotent stem cell-associated genes in colorectal cancer. *Med Oncol* **30:** 426

Livak KJ, Schmittgen TD (2001) Analysis of relative gene expression data using real-time quantitative PCR and the 2(-Delta Delta C(T)) Method. *Methods* **25:** 402-408

Lize M, Klimke A, Dobbelstein M (2011) MicroRNA-449 in cell fate determination. *Cell Cycle* **10:** 2874-2882

Lodygin D, Tarasov V, Epanchintsev A, Berking C, Knyazeva T, Korner H, Knyazev P, Diebold J, Hermeking H (2008) Inactivation of miR-34a by aberrant CpG methylation in multiple types of cancer. *Cell Cycle* **7:** 2591-2600

Lu M, Jolly MK, Levine H, Onuchic JN, Ben-Jacob E (2013a) MicroRNA-based regulation of epithelial-hybrid-mesenchymal fate determination. *Proc Natl Acad Sci U S A* **110:** 18144-18149

Lu X, Mazur SJ, Lin T, Appella E, Xu Y (2013b) The pluripotency factor nanog promotes breast cancer tumorigenesis and metastasis. *Oncogene***:** epub

Lu Y, Futtner C, Rock JR, Xu X, Whitworth W, Hogan BL, Onaitis MW (2010) Evidence that SOX2 overexpression is oncogenic in the lung. *PLoS One* **5:** e11022

Lustig B, Jerchow B, Sachs M, Weiler S, Pietsch T, Karsten U, van de Wetering M, Clevers H, Schlag PM, Birchmeier W, Behrens J (2002) Negative feedback loop of Wnt signaling through upregulation of conductin/axin2 in colorectal and liver tumors. *Mol Cell Biol* **22:** 1184-1193

Mani SA, Guo W, Liao MJ, Eaton EN, Ayyanan A, Zhou AY, Brooks M, Reinhard F, Zhang CC, Shipitsin M, Campbell LL, Polyak K, Brisken C, Yang J, Weinberg RA (2008) The epithelial-mesenchymal transition generates cells with properties of stem cells. *Cell* **133:** 704-715

Martinez-Estrada OM, Culleres A, Soriano FX, Peinado H, Bolos V, Martinez FO, Reina M, Cano A, Fabre M, Vilaro S (2006) The transcription factors Slug and Snail act as repressors of Claudin-1 expression in epithelial cells. *Biochem J* **394:** 449-457

Massague J (2008) TGFbeta in Cancer. *Cell* **134:** 215-230

Matsuoka J, Yashiro M, Sakurai K, Kubo N, Tanaka H, Muguruma K, Sawada T, Ohira M, Hirakawa K (2012) Role of the stemness factors sox2, oct3/4, and nanog in gastric carcinoma. *J Surg Res* **174:** 130-135

Matsuoka S, Ballif BA, Smogorzewska A, McDonald ER, 3rd, Hurov KE, Luo J, Bakalarski CE, Zhao Z, Solimini N, Lerenthal Y, Shiloh Y, Gygi SP, Elledge SJ (2007) ATM and ATR substrate analysis reveals extensive protein networks responsive to DNA damage. *Science* **316:** 1160-1166

Mauhin V, Lutz Y, Dennefeld C, Alberga A (1993) Definition of the DNA-binding site repertoire for the Drosophila transcription factor SNAIL. *Nucleic Acids Res* **21:** 3951-3957

Meng HM, Zheng P, Wang XY, Liu C, Sui HM, Wu SJ, Zhou J, Ding YQ, Li JM (2010) Overexpression of nanog predicts tumor progression and poor prognosis in colorectal cancer. *Cancer Biol Ther* **9:** 295-302

Menssen A, Epanchintsev A, Lodygin D, Rezaei N, Jung P, Verdoodt B, Diebold J, Hermeking H (2007) c-MYC delays prometaphase by direct transactivation of MAD2 and BubR1: identification of mechanisms underlying c-MYC-induced DNA damage and chromosomal instability. *Cell Cycle* **6:** 339-352

Menssen A, Hermeking H (2002) Characterization of the c-MYC-regulated transcriptome by SAGE: identification and analysis of c-MYC target genes. *Proc Natl Acad Sci U S A* **99:** 6274-6279

Meyer N, Penn LZ (2008) Reflecting on 25 years with MYC. *Nat Rev Cancer* **8:** 976-990

Moes M, Le Bechec A, Crespo I, Laurini C, Halavatyi A, Vetter G, Del Sol A, Friederich E (2012) A novel network integrating a miRNA-203/SNAI1 feedback loop which regulates epithelial to mesenchymal transition. *PLoS One* **7:** e35440

Morel AP, Lievre M, Thomas C, Hinkal G, Ansieau S, Puisieux A (2008) Generation of breast cancer stem cells through epithelial-mesenchymal transition. *PLoS One* **3:** e2888

Moreno-Bueno G, Cubillo E, Sarrio D, Peinado H, Rodriguez-Pinilla SM, Villa S, Bolos V, Jorda M, Fabra A, Portillo F, Palacios J, Cano A (2006) Genetic profiling of epithelial cells expressing E-cadherin repressors reveals a distinct role for Snail, Slug, and E47 factors in epithelial-mesenchymal transition. *Cancer Res* **66:** 9543-9556

Moreno-Bueno G, Peinado H, Molina P, Olmeda D, Cubillo E, Santos V, Palacios J, Portillo F, Cano A (2009) The morphological and molecular features of the epithelial-to-mesenchymal transition. *Nat Protoc* **4:** 1591-1613

Morgenstern JP, Land H (1990) Advanced mammalian gene transfer: high titre retroviral vectors with multiple drug selection markers and a complementary helper-free packaging cell line. *Nucleic Acids Res* **18:** 3587-3596

Munoz J, Stange DE, Schepers AG, van de Wetering M, Koo BK, Itzkovitz S, Volckmann R, Kung KS, Koster J, Radulescu S, Myant K, Versteeg R, Sansom OJ, van Es JH, Barker N, van Oudenaarden A, Mohammed S, Heck AJ, Clevers H (2012) The Lgr5 intestinal stem cell signature: robust expression of proposed quiescent '+4' cell markers. *EMBO J* **31:** 3079-3091

Murray SA, Carver EA, Gridley T (2006) Generation of a Snail1 (Snai1) conditional null allele. *Genesis* **44:** 7-11

Myant K, Sansom OJ (2011) Wnt/Myc interactions in intestinal cancer: partners in crime. *Exp Cell Res* **317:** 2725-2731

Nagaoka M, Shiraishi Y, Sugiura Y (2001) Selected base sequence outside the target binding site of zinc finger protein Sp1. *Nucleic Acids Res* **29:** 4920-4929

Naidu R, Wahab NA, Yadav M, Kutty MK (2002) Protein expression and molecular analysis of c-myc gene in primary breast carcinomas using immunohistochemistry and differential polymerase chain reaction. *Int J Mol Med* **9:** 189-196

Nguyen DX, Bos PD, Massague J (2009) Metastasis: from dissemination to organ-specific colonization. *Nat Rev Cancer* **9:** 274-284

Nieto MA (2002) The snail superfamily of zinc-finger transcription factors. *Nat Rev Mol Cell Biol* **3:** 155-166

Nieto MA (2013) Epithelial plasticity: a common theme in embryonic and cancer cells. *Science* **342:** 1234850

Niimi H, Pardali K, Vanlandewijck M, Heldin CH, Moustakas A (2007) Notch signaling is necessary for epithelial growth arrest by TGF-beta. *J Cell Biol* **176:** 695-707

Noh KH, Kim BW, Song KH, Cho H, Lee YH, Kim JH, Chung JY, Hewitt SM, Seong SY, Mao CP, Wu TC, Kim TW (2012) Nanog signaling in cancer promotes stem-like phenotype and immune evasion. *J Clin Invest* **122:** 4077-4093

Noseda M, McLean G, Niessen K, Chang L, Pollet I, Montpetit R, Shahidi R, Dorovini-Zis K, Li L, Beckstead B, Durand RE, Hoodless PA, Karsan A (2004) Notch activation results in phenotypic and functional changes consistent with endothelial-to-mesenchymal transformation. *Circ Res* **94:** 910-917

Okada N, Lin CP, Ribeiro MC, Biton A, Lai G, He X, Bu P, Vogel H, Jablons DM, Keller AC, Wilkinson JE, He B, Speed TP, He L (2014) A positive feedback between p53 and miR-34 miRNAs mediates tumor suppression. *Genes Dev* **28:** 438-450

Olmeda D, Montes A, Moreno-Bueno G, Flores JM, Portillo F, Cano A (2008) Snai1 and Snai2 collaborate on tumor growth and metastasis properties of mouse skin carcinoma cell lines. *Oncogene* **27:** 4690-4701

Orsulic S, Huber O, Aberle H, Arnold S, Kemler R (1999) E-cadherin binding prevents beta-catenin nuclear localization and beta-catenin/LEF-1-mediated transactivation. *J Cell Sci* **112 (Pt 8):** 1237-1245

Ozdamar B, Bose R, Barrios-Rodiles M, Wang HR, Zhang Y, Wrana JL (2005) Regulation of the polarity protein Par6 by TGFbeta receptors controls epithelial cell plasticity. *Science* **307:** 1603-1609

Park SM, Gaur AB, Lengyel E, Peter ME (2008) The miR-200 family determines the epithelial phenotype of cancer cells by targeting the E-cadherin repressors ZEB1 and ZEB2. *Genes Dev* **22:** 894-907

Patel MR, Chang YF, Chen IY, Bachmann MH, Yan X, Contag CH, Gambhir SS (2010) Longitudinal, noninvasive imaging of T-cell effector function and proliferation in living subjects. *Cancer Res* **70:** 10141-10149

Peinado H, Ballestar E, Esteller M, Cano A (2004) Snail mediates E-cadherin repression by the recruitment of the Sin3A/histone deacetylase 1 (HDAC1)/HDAC2 complex. *Mol Cell Biol* **24:** 306-319

Peinado H, Olmeda D, Cano A (2007) Snail, Zeb and bHLH factors in tumour progression: an alliance against the epithelial phenotype? *Nat Rev Cancer* **7:** 415-428

Peinado H, Quintanilla M, Cano A (2003) Transforming growth factor beta-1 induces snail transcription factor in epithelial cell lines: mechanisms for epithelial mesenchymal transitions. *J Biol Chem* **278:** 21113-21123

Pelengaris S, Khan M, Evan GI (2002) Suppression of Myc-induced apoptosis in beta cells exposes multiple oncogenic properties of Myc and triggers carcinogenic progression. *Cell* **109:** 321-334

Perez-Losada J, Sanchez-Martin M, Rodriguez-Garcia A, Sanchez ML, Orfao A, Flores T, Sanchez-Garcia I (2002) Zinc-finger transcription factor Slug contributes to the function of the stem cell factor c-kit signaling pathway. *Blood* **100:** 1274-1286

Pillai RS, Bhattacharyya SN, Artus CG, Zoller T, Cougot N, Basyuk E, Bertrand E, Filipowicz W (2005) Inhibition of translational initiation by Let-7 MicroRNA in human cells. *Science* **309:** 1573-1576

Pinto D, Clevers H (2005) Wnt, stem cells and cancer in the intestine. *Biol Cell* **97:** 185-196

Polyak K, Weinberg RA (2009) Transitions between epithelial and mesenchymal states: acquisition of malignant and stem cell traits. *Nat Rev Cancer* **9:** 265-273

Raghoebir L, Bakker ER, Mills JC, Swagemakers S, Kempen MB, Munck AB, Driegen S, Meijer D, Grosveld F, Tibboel D, Smits R, Rottier RJ (2012) SOX2 redirects the developmental fate of the intestinal epithelium toward a premature gastric phenotype. *J Mol Cell Biol* **4:** 377-385

Raver-Shapira N, Marciano E, Meiri E, Spector Y, Rosenfeld N, Moskovits N, Bentwich Z, Oren M (2007) Transcriptional activation of miR-34a contributes to p53-mediated apoptosis. *Mol Cell* **26:** 731-743

Rembold M, Ciglar L, Yanez-Cuna JO, Zinzen RP, Girardot C, Jain A, Welte MA, Stark A, Leptin M, Furlong EE (2014) A conserved role for Snail as a potentiator of active transcription. *Genes Dev* **28:** 167-181

Rhodes DR, Yu J, Shanker K, Deshpande N, Varambally R, Ghosh D, Barrette T, Pandey A, Chinnaiyan AM (2004) ONCOMINE: a cancer microarray database and integrated data-mining platform. *Neoplasia* **6:** 1-6

Robertson KD (2005) DNA methylation and human disease. *Nat Rev Genet* **6:** 597-610

Rokavec M, Oner MG, Li H, Jackstadt R, Jiang L, Lodygin D, Kaller M, Horst D, Ziegler PK, Schwitalla S, Slotta-Huspenina J, Bader FG, Greten FR, Hermeking H (2014) IL-6R/STAT3/miR-34a feedback loop promotes EMT-mediated colorectal cancer invasion and metastasis. *J Clin Invest* **124:** 1853-1867

Sadot E, Simcha I, Shtutman M, Ben-Ze'ev A, Geiger B (1998) Inhibition of beta-catenin-mediated transactivation by cadherin derivatives. *Proc Natl Acad Sci U S A* **95:** 15339-15344

Sahlgren C, Gustafsson MV, Jin S, Poellinger L, Lendahl U (2008) Notch signaling mediates hypoxia-induced tumor cell migration and invasion. *Proc Natl Acad Sci U S A* **105:** 6392-6397

Sanchez-Martin M, Perez-Losada J, Rodriguez-Garcia A, Gonzalez-Sanchez B, Korf BR, Kuster W, Moss C, Spritz RA, Sanchez-Garcia I (2003) Deletion of the SLUG (SNAI2) gene results in human piebaldism. *Am J Med Genet A* **122A:** 125-132

Sanchez-Tillo E, Liu Y, de Barrios O, Siles L, Fanlo L, Cuatrecasas M, Darling DS, Dean DC, Castells A, Postigo A (2012) EMT-activating transcription factors in cancer: beyond EMT and tumor invasiveness. *Cell Mol Life Sci* **69:** 3429-3456

Sansom OJ, Reed KR, Hayes AJ, Ireland H, Brinkmann H, Newton IP, Batlle E, Simon-Assmann P, Clevers H, Nathke IS, Clarke AR, Winton DJ (2004) Loss of Apc in vivo immediately perturbs Wnt signaling, differentiation, and migration. *Genes Dev* **18:** 1385-1390

Sayin VI, Nilton A, Ibrahim MX, Agren P, Larsson E, Petit MM, Hulten LM, Stahlman M, Johansson BR, Bergo MO, Lindahl P (2013) Zfp148 deficiency causes lung maturation defects and lethality in newborn mice that are rescued by deletion of p53 or antioxidant treatment. *PLoS One* **8:** e55720

Scharer CD, McCabe CD, Ali-Seyed M, Berger MF, Bulyk ML, Moreno CS (2009) Genome-wide promoter analysis of the SOX4 transcriptional network in prostate cancer cells. *Cancer Res* **69:** 709-717

Scheel C, Weinberg RA (2012) Cancer stem cells and epithelial-mesenchymal transition: concepts and molecular links. *Semin Cancer Biol* **22:** 396-403

Schneider CA, Rasband WS, Eliceiri KW (2012) NIH Image to ImageJ: 25 years of image analysis. *Nat Methods* **9:** 671-675

Scoville DH, Sato T, He XC, Li L (2008) Current view: intestinal stem cells and signaling. *Gastroenterology* **134:** 849-864

Seo KW, Roh KH, Bhandari DR, Park SB, Lee SK, Kang KS (2013) ZNF281 Knockdown Induced Osteogenic Differentiation of Human Multipotent Stem Cells In Vivo and In Vitro. *Cell Transplant* **22:** 29-40

Shchors K, Shchors E, Rostker F, Lawlor ER, Brown-Swigart L, Evan GI (2006) The Myc-dependent angiogenic switch in tumors is mediated by interleukin 1beta. *Genes Dev* **20:** 2527-2538

Sheiness D, Bishop JM (1979) DNA and RNA from uninfected vertebrate cells contain nucleotide sequences related to the putative transforming gene of avian myelocytomatosis virus. *J Virol* **31:** 514-521

Shi L, Jackstadt R, Siemens H, Li H, Kirchner T, Hermeking H (2014) p53-induced miR-15a/16-1 and AP4 form a double-negative feedback loop to regulate epithelial-mesenchymal transition and metastasis in colorectal cancer. *Cancer Res* **74:** 532-542

Shi Y, Massague J (2003) Mechanisms of TGF-beta signaling from cell membrane to the nucleus. *Cell* **113:** 685-700

Shoemaker RH (2006) The NCI60 human tumour cell line anticancer drug screen. *Nat Rev Cancer* **6:** 813-823

Siegel PM, Massague J (2003) Cytostatic and apoptotic actions of TGF-beta in homeostasis and cancer. *Nat Rev Cancer* **3:** 807-821

Siemens H, Jackstadt R, Hunten S, Kaller M, Menssen A, Gotz U, Hermeking H (2011) miR-34 and SNAIL form a double-negative feedback loop to regulate epithelial-mesenchymal transitions. *Cell Cycle* **10:** 4256-4271

Siemens H, Neumann J, Jackstadt R, Mansmann U, Horst D, Kirchner T, Hermeking H (2013) Detection of miR-34a promoter methylation in combination with elevated expression of c-Met and beta-catenin predicts distant metastasis of colon cancer. *Clin Cancer Res* **19:** 710-720

Sleeman J, Steeg PS (2010) Cancer metastasis as a therapeutic target. *Eur J Cancer* **46:** 1177-1180

Spaderna S, Schmalhofer O, Wahlbuhl M, Dimmler A, Bauer K, Sultan A, Hlubek F, Jung A, Strand D, Eger A, Kirchner T, Behrens J, Brabletz T (2008) The transcriptional repressor ZEB1 promotes metastasis and loss of cell polarity in cancer. *Cancer Res* **68:** 537-544

Stolzenburg S, Rots MG, Beltran AS, Rivenbark AG, Yuan X, Qian H, Strahl BD, Blancafort P (2012) Targeted silencing of the oncogenic transcription factor SOX2 in breast cancer. *Nucleic Acids Res* **40:** 6725-6740

Takahashi K, Yamanaka S (2006) Induction of pluripotent stem cells from mouse embryonic and adult fibroblast cultures by defined factors. *Cell* **126:** 663-676

Takeno S, Noguchi T, Fumoto S, Kimura Y, Shibata T, Kawahara K (2004) E-cadherin expression in patients with esophageal squamous cell carcinoma: promoter hypermethylation, Snail overexpression, and clinicopathologic implications. *Am J Clin Pathol* **122:** 78-84

Takeuchi A, Mishina Y, Miyaishi O, Kojima E, Hasegawa T, Isobe K (2003) Heterozygosity with respect to Zfp148 causes complete loss of fetal germ cells during mouse embryogenesis. *Nat Genet* **33:** 172-176

Tam WL, Weinberg RA (2013) The epigenetics of epithelial-mesenchymal plasticity in cancer. *Nat Med* **19:** 1438-1449

Tamura M, Uyama M, Sugiyama Y, Sato M (2013) Canonical Wnt signaling activates miR-34 expression during osteoblastic differentiation. *Mol Med Rep* **8:** 1807-1811

Tarasov V, Jung P, Verdoodt B, Lodygin D, Epanchintsev A, Menssen A, Meister G, Hermeking H (2007) Differential regulation of microRNAs by p53 revealed by massively parallel sequencing: miR-34a is a p53 target that induces apoptosis and G1-arrest. *Cell Cycle* **6:** 1586-1593

Taube JH, Herschkowitz JI, Komurov K, Zhou AY, Gupta S, Yang J, Hartwell K, Onder TT, Gupta PB, Evans KW, Hollier BG, Ram PT, Lander ES, Rosen JM, Weinberg RA, Mani SA (2010) Core epithelial-to-mesenchymal transition interactome gene-expression signature is associated with claudin-low and metaplastic breast cancer subtypes. *Proc Natl Acad Sci U S A* **107:** 15449-15454

Taube JH, Malouf GG, Lu E, Sphyris N, Vijay V, Ramachandran PP, Ueno KR, Gaur S, Nicoloso MS, Rossi S, Herschkowitz JI, Rosen JM, Issa JP, Calin GA, Chang JT, Mani SA (2013) Epigenetic silencing of microRNA-203 is required for EMT and cancer stem cell properties. *Sci Rep* **3:** 2687

Thiery JP (2002) Epithelial-mesenchymal transitions in tumour progression. *Nat Rev Cancer* **2:** 442-454

Thiery JP, Acloque H, Huang RY, Nieto MA (2009) Epithelial-mesenchymal transitions in development and disease. *Cell* **139:** 871-890

Thiery JP, Sleeman JP (2006) Complex networks orchestrate epithelial-mesenchymal transitions. *Nat Rev Mol Cell Biol* **7:** 131-142

Thompson EW, Williams ED (2008) EMT and MET in carcinoma--clinical observations, regulatory pathways and new models. *Clin Exp Metastasis* **25:** 591-592

Tian XJ, Zhang H, Xing J (2013) Coupled reversible and irreversible bistable switches underlying TGFbeta-induced epithelial to mesenchymal transition. *Biophys J* **105:** 1079-1089

Timmerman LA, Grego-Bessa J, Raya A, Bertran E, Perez-Pomares JM, Diez J, Aranda S, Palomo S, McCormick F, Izpisua-Belmonte JC, de la Pompa JL (2004) Notch promotes epithelial-mesenchymal transition during cardiac development and oncogenic transformation. *Genes Dev* **18:** 99-115

Tiwari N, Tiwari VK, Waldmeier L, Balwierz PJ, Arnold P, Pachkov M, Meyer-Schaller N, Schubeler D, van Nimwegen E, Christofori G (2013) Sox4 is a master regulator of epithelial-mesenchymal transition by controlling Ezh2 expression and epigenetic reprogramming. *Cancer Cell* **23:** 768-783

Toyota M, Suzuki H, Sasaki Y, Maruyama R, Imai K, Shinomura Y, Tokino T (2008) Epigenetic silencing of microRNA-34b/c and B-cell translocation gene 4 is associated with CpG island methylation in colorectal cancer. *Cancer Res* **68:** 4123-4132

Tsukamoto T, Mizoshita T, Mihara M, Tanaka H, Takenaka Y, Yamamura Y, Nakamura S, Ushijima T, Tatematsu M (2005) Sox2 expression in human stomach adenocarcinomas with gastric and gastric-and-intestinal-mixed phenotypes. *Histopathology* **46:** 649-658

Valastyan S, Weinberg RA (2011) Tumor metastasis: molecular insights and evolving paradigms. *Cell* **147:** 275-292

Vandewalle C, Comijn J, De Craene B, Vermassen P, Bruyneel E, Andersen H, Tulchinsky E, Van Roy F, Berx G (2005) SIP1/ZEB2 induces EMT by repressing genes of different epithelial cell-cell junctions. *Nucleic Acids Res* **33:** 6566-6578

Veeman MT, Slusarski DC, Kaykas A, Louie SH, Moon RT (2003) Zebrafish prickle, a modulator of noncanonical Wnt/Fz signaling, regulates gastrulation movements. *Curr Biol* **13:** 680-685

Vervoorts J, Luscher-Firzlaff J, Luscher B (2006) The ins and outs of MYC regulation by posttranslational mechanisms. *J Biol Chem* **281:** 34725-34729

Vetter G, Saumet A, Moes M, Vallar L, Le Bechec A, Laurini C, Sabbah M, Arar K, Theillet C, Lecellier CH, Friederich E (2010) miR-661 expression in SNAI1-induced epithelial to mesenchymal transition contributes to breast cancer cell invasion by targeting Nectin-1 and StarD10 messengers. *Oncogene* **29:** 4436-4448

Vincent T, Neve EP, Johnson JR, Kukalev A, Rojo F, Albanell J, Pietras K, Virtanen I, Philipson L, Leopold PL, Crystal RG, de Herreros AG, Moustakas A, Pettersson RF, Fuxe J (2009) A SNAIL1-SMAD3/4 transcriptional repressor complex promotes TGF-beta mediated epithelial-mesenchymal transition. *Nat Cell Biol* **11:** 943-950

Wang D, Manali D, Wang T, Bhat N, Hong N, Li Z, Wang L, Yan Y, Liu R, Hong Y (2011) Identification of pluripotency genes in the fish medaka. *Int J Biol Sci* **7:** 440-451

Wang J, Rao S, Chu J, Shen X, Levasseur DN, Theunissen TW, Orkin SH (2006) A protein interaction network for pluripotency of embryonic stem cells. *Nature* **444:** 364-368

Wang ZX, Teh CH, Chan CM, Chu C, Rossbach M, Kunarso G, Allapitchay TB, Wong KY, Stanton LW (2008) The transcription factor Zfp281 controls embryonic stem cell pluripotency by direct activation and repression of target genes. *Stem Cells* **26:** 2791-2799

Welch C, Chen Y, Stallings RL (2007) MicroRNA-34a functions as a potential tumor suppressor by inducing apoptosis in neuroblastoma cells. *Oncogene* **26:** 5017-5022

Wellner U, Schubert J, Burk UC, Schmalhofer O, Zhu F, Sonntag A, Waldvogel B, Vannier C, Darling D, zur Hausen A, Brunton VG, Morton J, Sansom O, Schuler J, Stemmler MP, Herzberger C, Hopt U, Keck T, Brabletz S, Brabletz T (2009) The EMT-activator ZEB1 promotes tumorigenicity by repressing stemness-inhibiting microRNAs. *Nat Cell Biol* **11:** 1487-1495

Winter J, Jung S, Keller S, Gregory RI, Diederichs S (2009) Many roads to maturity: microRNA biogenesis pathways and their regulation. *Nat Cell Biol* **11:** 228-234

Woo AJ, Moran TB, Schindler YL, Choe SK, Langer NB, Sullivan MR, Fujiwara Y, Paw BH, Cantor AB (2008) Identification of ZBP-89 as a novel GATA-1-associated transcription factor involved in megakaryocytic and erythroid development. *Mol Cell Biol* **28:** 2675-2689

Xiang R, Liao D, Cheng T, Zhou H, Shi Q, Chuang TS, Markowitz D, Reisfeld RA, Luo Y (2011) Downregulation of transcription factor SOX2 in cancer stem cells suppresses growth and metastasis of lung cancer. *Br J Cancer* **104:** 1410-1417

Yamanaka S, Blau HM (2010) Nuclear reprogramming to a pluripotent state by three approaches. *Nature* **465:** 704-712

Yang J, Weinberg RA (2008) Epithelial-mesenchymal transition: at the crossroads of development and tumor metastasis. *Dev Cell* **14:** 818-829

Yang MH, Hsu DS, Wang HW, Wang HJ, Lan HY, Yang WH, Huang CH, Kao SY, Tzeng CH, Tai SK, Chang SY, Lee OK, Wu KJ (2010) Bmi1 is essential in Twist1-induced epithelial-mesenchymal transition. *Nat Cell Biol* **12:** 982-992

Yang P, Li QJ, Feng Y, Zhang Y, Markowitz GJ, Ning S, Deng Y, Zhao J, Jiang S, Yuan Y, Wang HY, Cheng SQ, Xie D, Wang XF (2012) TGF-beta-miR-34a-CCL22 signaling-induced Treg cell recruitment promotes venous metastases of HBV-positive hepatocellular carcinoma. *Cancer Cell* **22:** 291-303

Yasuda H, Tanaka K, Okita Y, Araki T, Saigusa S, Toiyama Y, Yokoe T, Yoshiyama S, Kawamoto A, Inoue Y, Miki C, Kusunoki M (2011) CD133, OCT4, and NANOG in ulcerative colitis-associated colorectal cancer. *Oncol Lett* **2:** 1065-1071

Yi R, Poy MN, Stoffel M, Fuchs E (2008) A skin microRNA promotes differentiation by repressing 'stemness'. *Nature* **452:** 225-229

Yu F, Yao H, Zhu P, Zhang X, Pan Q, Gong C, Huang Y, Hu X, Su F, Lieberman J, Song E (2007) let-7 regulates self renewal and tumorigenicity of breast cancer cells. *Cell* **131:** 1109-1123

Zavadil J, Cermak L, Soto-Nieves N, Bottinger EP (2004) Integration of TGF-beta/Smad and Jagged1/Notch signalling in epithelial-to-mesenchymal transition. *EMBO J* **23:** 1155-1165

Zeisberg M, Neilson EG (2009) Biomarkers for epithelial-mesenchymal transitions. *J Clin Invest* **119:** 1429-1437

Zhang CZ, Cao Y, Yun JP, Chen GG, Lai PB (2012a) Increased expression of ZBP-89 and its prognostic significance in hepatocellular carcinoma. *Histopathology* **60:** 1114-1124

Zhang J, Espinoza LA, Kinders RJ, Lawrence SM, Pfister TD, Zhou M, Veenstra TD, Thorgeirsson SS, Jessup JM (2013) NANOG modulates stemness in human colorectal cancer. *Oncogene* **32:** 4397-4405

Zhang J, Liang Q, Lei Y, Yao M, Li L, Gao X, Feng J, Zhang Y, Gao H, Liu DX, Lu J, Huang B (2012b) SOX4 induces epithelial-mesenchymal transition and contributes to breast cancer progression. *Cancer Res* **72:** 4597-4608

Zhang J, Wang X, Chen B, Xiao Z, Li W, Lu Y, Dai J (2010) The human pluripotency gene NANOG/NANOGP8 is expressed in gastric cancer and associated with tumor development. *Oncol Lett* **1:** 457-463

Zhang X, Diab IH, Zehner ZE (2003) ZBP-89 represses vimentin gene transcription by interacting with the transcriptional activator, Sp1. *Nucleic Acids Res* **31:** 2900-2914

Zheng H, Kang Y (2013) Multilayer control of the EMT master regulators. *Oncogene*: epub

Zhu L, Gibson P, Currle DS, Tong Y, Richardson RJ, Bayazitov IT, Poppleton H, Zakharenko S, Ellison DW, Gilbertson RJ (2009) Prominin 1 marks intestinal stem cells that are susceptible to neoplastic transformation. *Nature* **457:** 603-607

10. ACKNOWLEDGEMENTS

It would not have been possible to write this doctoral thesis without the help and support of the kind people around me to which I would like to express my gratitude to.

Above all, I would like to thank my supervisor Prof. Dr. rer. nat. Heiko Hermeking, who I am sincerely grateful to for the opportunity to work on a fascinating project, for his continuous personal help and scientific interest, guidance as well as his support, advices, constant fruitful discussions and ideas, which have been invaluable for the ongoing of the project. Additionally, I would like to express my thanks for the patience and support I received from him throughout the years as his doctoral student.

Moreover, this thesis would not have been possible without the help, support and patience of many other people I would like to mention. I would like to acknowledge all the members of the group for helpfulness and valuable scientific support and discussions throughout the entire time. Particularly, I want to thank Rene Jackstadt for his continuous scientific support and discussions, the enthusiasm, for teaching me a variety of valuable methods and especially for kindly explaining the laser scanning microscope, for valuable samples and for the performance of the animal experiments reported in this thesis. In addition, I like to express my gratitude to Helge Siemens, Sabine Hünten and Dr. Markus Kaller not only for their great and constructive scientific help, interesting discussions and support, but also for providing important scientific samples. Thanks for promoting a stimulating academic and social environment by sharing the bench and office with me. Furthermore, I would like to thank Dr. Antje Menssen for experimental and scientific suggestions, technical explanations and sharing her knowledge. I would also like to acknowledge the reliable and valuable technical support by Ursula Götz regarding all the smaller and larger daily scientific challenges.

Additionally, I further would like to express my gratefulness to the external reviewers for taking the time and effort evaluating my work.

Last, but by no means least, thanks go to my family and friends, who have given me their unequivocal support and faith, for “just being there”, for never ending

encouragement on my scientific journey, motivation and great patience at all times as always, for which my mere expression of thanks likewise does not suffice.